Appendix A1

Abstract EGU I. Vertical profile and aerosol size distribution measurements in Iceland (LOAC)

Geophysical Research Abstracts
Vol. 16, EGU2014-8765, 2014
EGU General Assembly 2014

Vertical profile and aerosol size distribution measurements in Iceland (LOAC)

Pavla Dagsson Waldhauserova (1,2), Haraldur Olafsson (1,3,4), Olafur Arnalds (2), Jean-Baptiste Renard (5), Damien Vignelles (5), and Nicolas Verdier (6)

(1) University of Iceland, Department of Physics, Reykjavik, Iceland (pavla@lbhi.is), (2) Agricultural University of Iceland, Faculty of Environment, Hvanneyri, Iceland, (3) Meteorological Office of Iceland, Reykjavik, Iceland , (4) Bergen School of Meteorology, Geophysical Institute, University of Bergen, Norway, (5) LPC2E-CNRS / Université d'Orléans, Orléans, France, (6) CNES, Toulouse, France

Cold climate and high latitudes regions contain important dust sources where dust is frequently emitted, foremost from glacially-derived sediments of riverbeds or ice-proximal areas (Arnalds, 2010; Bullard, 2013). Iceland is probably the most active dust source in the arctic/sub-arctic region (Dagsson-Waldhauserova, 2013). The frequency of days with suspended dust exceeds 34 dust days annually. Icelandic dust is of volcanic origin; it is very dark in colour and contains sharp-tipped shards with bubbles. Such properties allow even large particles to be easily transported long distances. Thus, there is a need to better understand the spatial and temporal variability of these dusts.

Two launch campaigns of the Light Optical Aerosols Counter (LOAC) were conducted in Iceland with meteorological balloons. LOAC use a new optical design that allows to retrieve the size concentrations in 19 size classes between 0.2 and 100 microm, and to provide an estimate of the main nature of aerosols. Vertical stratification and aerosol composition of the subarctic atmosphere was studied in detail. The July 2011 launch represented clean non-dusty season with low winds while the November 2013 launch was conducted during the high winds after dusty period. For the winter flight (performed from Reykjavik), the nature of aerosols strongly changed with altitude. In particular, a thin layer of volcanic dust was observed at an altitude of 1 km.

Further LOAC measurements are needed to understand the implication of Icelandic dust to the Arctic warming and climate change. A new campaign of LAOC launches is planned for May 2014.

Reference:

Arnalds, O., 2010. Dust sources and deposition of aeolian materials in Iceland. Icelandic Agricultural Sciences 23, 3-21.

Bullard, J.E., 2013. Contemporary glacigenic inputs to the dust cycle. Earth Surface Processes and Landforms 38, 71-89.

Dagsson-Waldhauserova, P., Arnalds O., Olafsson H. 2013. Long-term frequency and characteristics of dust storm events in Northeast Iceland (1949-2011). Atmospheric Environment 77:117-127.

Appendix A2

Abstract EGU II. Optical properties and climate forcing of Icelandic dust

Geophysical Research Abstracts
Vol. 16, EGU2014-8640, 2014
EGU General Assembly 2014

Optical properties and climate forcing of Icelandic dust

Pavla Dagsson Waldhauserova (1,2), Haraldur Olafsson (1,3,4), Olafur Arnalds (2), Jindrich Hladil (5), Roman Skala (5), Tomas Navratil (5), Leona Chadimova (5), Maria Gritsevich (6,7), Jouni Peltoniemi (6,7), and Teemu Hakala (6)

(1) University of Iceland, Department of Physics, Reykjavik, Iceland (pavla@lbhi.is), (2) Agricultural University of Iceland, Faculty of Environment, Hvanneyri, Iceland, (3) Meteorological Office of Iceland, Reykjavik, Iceland , (4) Bergen School of Meteorology, Geophysical Institute, University of Bergen, Norway, (5) Institute of Geology AS CR, Prague, Czech Republic, (6) Finnish Geodetic Institute,Masala, Finland , (7) University of Helsinki, Department of Physics,Helsinki Finland

Iceland is an active source of dust originating from glaciogenic and volcanic sediments. The frequency of days with dust suspension exceeded 34 dust days annually in 1949-2011. This figure represents a minimum value as many dust storms occur without the dust passing the weather stations recording the events. Comparison of meteorological synoptic codes for dust observation and direct particulate matter mass concentration measurements in 2005-2013 showed that the mean number of dust days in Iceland can increase up to135 dust days annually. Dust events in NE Iceland occur mostly in May-September, while almost half of all dust events in SW Iceland were at sub-zero temperatures or in winter.
Icelandic dust is different from the crustal dust; it is of volcanic origin and dark in colour. It contains sharp-tipped shards and is often with bubbles. Such physical properties allow large particle suspension and transport to long distances, e.g. towards the Arctic. To estimate the further impacts of dust transport, both laboratory and snow spectropolarimetric measurements were done using the Finnish Geodetic Institute Field Goniospectrometer FIGI-FIGO (http://www.polarisation.eu/index.php/list-of-instruments/view-submission/172), an automated portable instrument for multiangular reflectance measurements. The albedo, hemispherical directional reflectance factor (HDRF), polarization, and other snow properties were monitored on the snow and areas affected by the dust deposition through the following melting period in spring 2013 in Lapland during the Soot on Snow (SoS) 2013 campaign.
Glaciogenic silt deposited on snow made the snow optically darker. The melting, metamorphose and diffusion processes were fast during the measurement time while the sun heated the particles, snow melted around, and the particles diffused inside the snow. Smaller particles diffused faster than the larger. Fine silt particles tended to form larger grains.
Larger volcanic sand particles had lower reflectance than fine silt particles both in laboratory and deposited on snow. Icelandic volcanic sand was of similar optical properties as black carbon both deposited on snow or in laboratory.
This experiment showed that the Icelandic volcanic dust may both directly and indirectly act as a positive climate forcing agent. We suggest that Icelandic dust may be a contributor to the Arctic warming.

We would like to acknowledge all the SOS 2013 participants: A. VIRKKULA., O. MEINANDER, G. DE LEEUW and others.

Paper I

Long-term variability of dust events in Iceland (1949-2011)

P. Dagsson-Waldhauserova[1, 2], O. Arnalds[1], and H. Olafsson[2, 3, 4]

[1]{Agricultural University of Iceland, Hvanneyri, Borgarnes, Iceland}

[2]{University of Iceland, Department of Physics, Reykjavík, Iceland}

[3]{Icelandic Meteorological Office, Reykjavík, Iceland}

[4]{Bergen School of Meteorology, Geophysical Institute, University of Bergen, Norway}

Correspondence to: P. Dagsson-Waldhauserova (pavla@lbhi.is)

Abstract

Long-term frequency of atmospheric dust observations was investigated for the southern part of Iceland and merged with results obtained from the Northeast Iceland (Dagsson-Waldhauserova et al., 2013). In total, over 34 dust days per year on average occurred in Iceland based on conventionally used synoptic codes for dust. Including codes 04-06 into the criteria for dust observations, the frequency was 135 dust days annually. The Sea Level Pressure (SLP) oscillation controlled whether dust events occurred in NE (16.4 dust days annually) or in southern part of Iceland (about 18 dust days annually). The most dust-frequent decade in S Iceland was the 1960s while the most frequent decade in NE Iceland was the 2000s. A total of 32 severe dust storms (visibility < 500 m) was observed in Iceland with the highest frequency during the 2000s in S Iceland. The Arctic dust events (NE Iceland) were typically warm and during summer/autumn (May-September) while the Sub-Arctic dust events (S Iceland) were mainly cold and during winter/spring (March-May). About half of dust events in S Iceland occurred in winter or at sub-zero temperatures. A good correlation was found between PM_{10} concentrations and visibility during dust observations at the stations Vik and Storhofdi. This study shows that Iceland is among the dustiest areas of the world and dust is emitted the year-round.

1 Introduction

Frequency of dust episodes is monitored around many of the major desert areas of the world. Detailed and long-term studies on wind erosion variability can potentially explain the climatological and environmental changes in past. Periodical dust occurrences can affect ecosystem fertility and spatial and temporal distribution of animal and vegetation species similarly to climate variations (Fields et al., 2010). Oceanic ecosystems receive high amounts of nutrient rich dust spread over large areas where deserts occur near the sea (Arnalds et al., 2014). The long-term dust variability studies based on the meteorological observations present up to 90 years old records from North America, Africa, Asia and Australia (N´TchayiMbourou et al., 1997; Qian et al., 2002; Natsagdorj et al., 2003; Ekström et al., 2004; Jamalizadeh et al., 2008; Steenburgh et al., 2012). Engelstaedter et al. (2003) reported high dust activity at many weather stations located in high-latitude regions. Cold climate regions are represented by long-term dust frequency in Northeast Iceland (Dagsson-Waldhauserova et al., 2013). Dust emission intensity and deposition rates in active glacial environment have been found very high, in some cases far exceeding those in lower latitudes (Bullard, 2013). Ganopolski et al. (2009) calculated glaciogenic dust deposition > 50 $gm^{-2}yr^{-1}$ at the last glacial maximum with highest rates over the north-western Europe. Recently, the highest deposition rates of glaciogenic dust > 500 $gm^{-2}yr^{-1}$ are reported from Iceland (Arnalds, 2010, see also Bullard, 2013).

Dust events in Arctic/Sub-Arctic region have been observed in Alaska (Nickling, 1978; Crusius et al., 2011), Greenland (Bullard, 2013), Svalbard (Dornbrack et al., 2010) and Iceland (Arnalds, 2010; Prospero et al., 2012; Thorarinsdottir and Arnalds, 2012). Arctic coastal zones are considered as the windiest regions on Earth (Eldridge, 1980). Strong winds in Iceland are causing some of the most extreme wind erosion events recorded on Earth (Arnalds et al., 2013).

The highest dust emissions in Arctic regions are associated with summer and early autumn (Nickling, 1978; Bullard, 2013; Dagsson-Waldhauserova et al., 2013). Dust concentrations in Sub-Arctic regions peak in spring (April-June, Prospero et al., 2012). Cold and winter periods are, however, of higher glaciogenic dust deposition than warm periods (Ganopolski et al., 2009). Dust events are frequent during dry years (Steenburgh et al., 2012; Dagsson-Waldhauserova et al., 2013), but suspended dust has also been observed during high precipitation and low wind conditions (Dagsson-Waldhauserova et al., 2014).

Iceland is an important source of volcanic sediments that are subjected to intense aeolian activity (Arnalds, 2010; Prospero et al., 2012; Thorarinsdottir and Arnalds, 2012; Arnalds et al., 2013) and is likely the largest glaciogenic dust source area in the Arctic/Sub-Arctic region. Total emissions of dust from Icelandic dust sources are of the range 30 to 40 million tons annually with 5-14 million tons deposited annually over the Atlantic and Arctic Oceans (Arnalds et al., 2014). Seven major dust plume sources have been identified (Arnalds, 2010). These sources are all in vicinity of glaciers. The most active glacial flood plain, Dyngjusandur, covers an area of about 270 km^2 with up to 10 m thick sediments and is the main source for dust events in NE Iceland and towards Arctic (Dagsson-Waldhauserova et al., 2013). The major dust sources in South Iceland are Skeidararsandur, Myrdalssandur, Mælifellssandur, Landeyjasandur resulting in dust events south towards Europe during northerly winds, but alternatively towards Reykjavik and North America during easterly winds. The Hagavatn plume area is the source for frequent dust events towards Reykjavik and North America (the ocean southwest of Iceland). Glaciogenic dust from the Mælifellssandur area contains fine sharp-tipped shards with bubbles and 80 % of the particulate matter is volcanic glass rich in heavy metals (Dagsson-Waldhauserova et al., 2014). Such physical properties of the particles allow rapid suspension of moist particles within only a few hours after rains. *In situ* measurements from other dust plume areas are not available.

Dust suspension is related to reduced visibility. Wang et al. (2008) found a good correlation between PM_{10} concentrations and visibility during dust observation. The visibility-dust formula can be used for dust concentration estimations where no aerosol mass concentration measurements are conducted (Dagsson-Waldhauserova et al., 2013). The relationship between dust concentration and visibility has not been investigated in Iceland.

The main objectives of this study were to explore the long-term (63 years) frequency of dust events in Iceland. Emphasis was given on determining the climatology and character of Arctic and Sub-Arctic dust events. In addition, the relationship between available dust concentrations and visibility during dust observation was investigated and the frequency of dust events placed in an international perspective.

2 Methods

2.1 Meteorological data and PM measurements

A network of 30 weather stations (15 in S Iceland, 8 in NE Iceland, and 7 in NW Iceland) operated by the Icelandic Meteorological Office was chosen for the study (Figure 1). Table 1 shows the duration of station operation with majority of stations in operation since 1949. The data consist of conventional meteorological parameters such as wind velocity, wind direction, temperature and visibility, accompanied by synoptic codes of present weather. Present weather refers to atmospheric phenomena occurring at the time of observation, or which has occurred preceding the time of observation (IMO, 1981). The synoptic codes (ww) for present weather which refer to dust observation are 7-9, and 30-35. In addition, codes 4-6 are considered, but only if the codes for primary or secondary past weather (ww1, ww2) are 3 for blowing soil, dust, sand and dust storm (IMO, 1981; Dagsson-Waldhauserova et al., 2013). Weather observations were made 3-8 times a day.

Meteorological observations (synoptic codes for dust including 04-06 and visibility) were evaluated with available particulate matter (PM) mass concentrations data provided by the Environmental Agency of Iceland (EAI). The PM10 data were obtained from the permanent station in Reykjavik (Grensasvegur, since 1996) and temporary stations in Vík and Kirkjubæjarklaustur (2010-2011). The Reykjavik station is equipped with Thermo EMS Andersen FH 62 I-R instrument, the Kirkjubæjarklaustur station with the Grimm EDM 365 and Thermo 5014 measured concentrations in Vik. Distance between the meteorological and EAI stations in Reykjavik and Kirkjubæjarklaustur is about one kilometer and several kilometers in Vík. Data set of dust concentrations (1997-2002, 2010) from the High-volume Filter Aerosol Sampler in Vestmannaeyjar (Westmann Islands) was used for evaluation of the dust codes and visibility at the Storhofdi station (Prospero et al., 2012). Daily dust concentrations were correlated with the minimum visibility during dust observations during the preceding 24 hours.

Most of the conventional dust studies do not include synoptic codes 04-06 for “Visibility reduced by volcanic ashes”, “Dust haze” and “Widespread dust in suspension in the air” into the criteria for dust observation (Dagsson-Waldhauserova et al., 2013). Comparing these codes with available dust concentration measurements showed that PM10 concentration > 41 μgm^{-3} (about a double mean concentration) was exceeded in about 80 % of the 04-06 code cases. We have not included these codes in this long-term study except that ww1 or ww2 was 3.

2.2 Analysis

The initial dataset was built from the occurrence of "dust observation" made at one or more weather stations. Long-term dust activity was expressed in dust days. A "dust day" was defined as a day when at least one station recorded at least one dust observation. About 29% of the observations did not include information on the present weather and they were excluded from the dataset.

Dust concentration measurements can be compared to the weather observations at few stations in Iceland and for a short time period. For the stations where PM_{10} measurements were available, we applied a power regression to determine the relationship between dust concentrations and visibility during dust codes including 04-06 (methods detailed in Wang et al., 2008). Visibility during dust observation was used to classify the severity of dust events in past (Dagsson-Waldhauserova et al., 2013).

3 Results

3.1 Frequency, spatial and temporal variability in dust production

A mean of 34.4 dust days per year was observed in Iceland during the period 1949-2011. An annual mean of 16.4 dust days (total of 1033 days) was recorded in NE Iceland (Dagsson-Waldhauserova et al. 2013) and about 17.9 dust days (total of 1153 days) occurred annually in southern parts of Iceland in 1949-2011. Figure 2 shows that the most dust active decade in Iceland was the 1960s while the 1980s were the lowest in number of dust days. For the southern part of Iceland, the highest frequency of dust events was in the 1950s-1960s, whereas the 2000s was the most frequent decade in the NE Iceland. The Grimsstadir station (NE) is the dustiest weather observation location in Iceland with > 12 dust days annually. The following dusty stations with > 3 dust days annually are represented in Table 2: Hofn (S), Vatnsskardsholar (S), Egilsstadir (NE), and Hella (S). The stations with highest dust frequency in southern part of Iceland are described in Figure 2 (NE stations published in Dagsson-Waldhauserova et al. 2013a). The stations Hofn and Vatnsskardsholar reported highest number of dust days in the 1950s-1960s, the station Hella observed highest dust period in the 1960s-1970s and a new station in Hjardarland (established in 1990) was the most active in the 2000s. Dust events were less severe in the 2000s than in the 1950s-1990s reflected by increased visibility during dust observations. Mean visibility during dust observations in S Iceland was 23.3 km indicating more severe dust events in S than in the NE

Iceland or that weather stations are closer to major dust sources. Including codes 04-06 into the criteria for dust observation, the annual mean dust-day frequency was 135 dust days with 101 dust days observed in S Iceland and 34 dust days in NE Iceland.

3.1.1. Annual and seasonal dust day variability

An annual number of dust days in 1949-2011 is depicted in Figure 3. The dustiest years were 1955, 1966 and 2010, when over 55 dust days occurred annually. The least dusty period was 1987-1990 with 11-15 dust days annually. Dust events occurred more frequently in southern part of Iceland than in NE Iceland in 1949-1954, 1962-1975, 1978-1981, and 2009-2011. The NE dust events were observed more often in 1955-1961, 1976-1977, 1982-1986, and 1992-2008 (except 1994, 2003). There is clear trend of having either the south or the north more active at a time. The years with relatively severe dust events (and annual visibility during dust observations < 15 km) were 1949, 1966, 1975, 1996, and 1998.

The seasonal distribution of dust days in southern part of Iceland showed that about 47 % of dust events occurred in winter (Nov-March) or during sub-zero temperatures. Dust days, as shown in Figure 4, were most often in May (18 % of dust days), April (13 %) and March (11%). The lowest occurrence of dust days (< 6 %) was in January, December, August and September. Contrarily, dust events in NE Iceland occurred mainly in summer and early autumn (May-September, Dagsson-Waldhauserova et al. 2013).

3.2 Climatology of dust events

3.2.1. Long-term trends in meteorological parameters of dust events (DE)

The mean DE temperature in southern part of Iceland was 3°C with minimum 1.4°C in the 1960s and maximum 5°C in the 2000s (Figure 5A). There was a great variability in DE temperatures, especially during the most active dust decade, the 1960s. The DE were the coldest in NE Iceland during the 1960s as well, but the warmest DE period was the 1950s (Dagsson-Waldhauserova et al., 2013). The mean DE temperature in the NE was significantly higher than in S Iceland, about 10.5°C.

Dust observations in S Iceland reported high mean DE wind velocity of 13.6 ms^{-1}, where the maximum mean of 15.6 ms^{-1} was during the 1980s and the minimum of 11.9 ms^{-1} during the 2000s (Figure 5B). Extreme DE winds exceeding 30 ms^{-1} occurred mainly in the 1960s and

the 1970s. The mean DE wind velocity in NE Iceland was 10.3 ms^{-1} with the maximum of 11.9 ms^{-1} during the 2000s and the minimum of 8.6 ms^{-1} in the 1980s (Dagsson-Waldhauserova et al., 2013).

The most common wind direction during dust events in S Iceland was N-NE, mainly reported from the stations Höfn, Hella, Vatnsskardsholar, Kirkjubaejarklaustur, Storhofdi, Eyrarbakki, Vik, Thingvellir, Hjardarland, Keflavik, and Reykjavik (Figure 6). Dust events were often observed from the wind direction ENE (Haell, Vatnsskardsholar), E-ESE (Storhofdi, Vatnsskardsholar, Thingvellir, Reykjavik, Keflavik), NW-NNW (Höfn), and W-WNW (Vatnsskardsholar). The DE wind directions in NE Iceland were predominantly SW-S and SSE-SE (Dagsson-Waldhauserova et al., 2013).

3.2.2. Seasonal patterns in meteorological parameters of dust events

Seasonal variability in temperature and wind velocity during dust events in S Iceland is depicted in Figure 7. The DE mean temperatures in October-May period are several degrees lower than the long-term monthly temperatures (higher in June-August period). Generally, the DE temperature in S Iceland was about 1.7°C lower than the long-term mean. Contrarily, the DE temperatures in NE Iceland were about 3°C higher than monthly long-term temperatures (Dagsson-Waldhauserova et al., 2013).

The DE wind velocities were significantly higher (5-11 ms^{-1}) than long-term monthly wind velocities (Figure 7B). The highest DE winds in S Iceland were from December to April while the lowest DE winds occurred in summer (June-September). This corresponds to the long-term monthly wind velocity trends. The mean DE wind velocity was 7.7 ms^{-1} higher than long-term mean wind velocity. The difference is most pronounced during the winter months. In NE Iceland, the DE winds were about 4-7 ms^{-1} higher than long-term means with maxima in May and September-October (Dagsson-Waldhauserova et al., 2013). Generally, the DE winds were about 3 ms^{-1} lower in NE than S Iceland.

3.2.3 Dust event classification and meteorology

Reported dust events were of different severity. Where no atmospheric dust measurements are available, visibility during dust observation is used to estimate the dust event severity. Table 2 describes the dust event classes based on the visibility ranges. The most frequent were dust observations of “Suspended” and “Moderate suspended dust” (NE 73%; S 59%) with

visibility 10-70 km, “Severe” and “Moderate haze” (NE 24%; S 32%) with visibility 1-10 km, and “Severe” and “Moderate dust storm” (NE 3%; S 5%) with visibility < 1 km. There were 32 “Severe Dust Storms“ (visibility < 500 m) observed in Iceland (14 in NE mostly in the 1950s, 18 in S mostly in the 2000s).

The DE wind velocity increased with the DE severity, but the DE temperature decreased with the DE severity, except for “Moderate dust storm“ recorded mostly at the Vik station in S Iceland. The parameters show that dust events in southern part of Iceland were observed as more severe than in NE Iceland.

Most of the dust classes in S Iceland occurred in April and May. Severe dust storms were most frequent in March and January at Vik, Hella, Kirkjubæjarklaustur, Hæll, Eyrarbakki and Vatnsskardsholar stations. The station Vik located only about 10 km from the Myrdalssandur dust source reported the mean DE visibility of 2 km indicating very severe dust events. Following stations with the lowest mean DE visibility were Raufarhofn (NE, 15 km), Höfn (18.3 km), Kirkjubæjarklaustur (20.1 km), Storhofdi (20.4 km), and Hella (21.1 km). The highest mean DE velocity was measured at the most windy station Storhofdi (22.6 ms^{-1}) while the lowest mean DE winds were at the station Thingvellir. Thingvellir recorded also the highest mean DE temperature (8.5°C) in S Iceland. The lowest DE temperatures were in Höfn (-2.3°C) located downwind Vatnajökull glacier.

About 18 % of dust events in S Iceland were observed at more stations in the same time (two stations: 12.5 %, three stations: 3.4%, four or more stations: 1.5%). Dust co-observations were mostly in Kirkjubæjarklaustur and Höfn, Kirkjubæjarklaustur and Vatnsskardsholar, and Kirkjubæjarklaustur with Hella. The Reykjavik station observed dust together with Hella or Thingvellir.

3.3 Relationship between PM_{10} concentrations and visibility

Hourly PM_{10} concentrations were compared with corresponding visibility data during dust observations at available stations. Good correlation (R^2=0.73) and considerable correlation (R^2=0.48) were found between dust concentration and visibility by power function fitting at the stations in Vik and Vatnsskardsholar (Figure 8A, 8B). Weak relationship between PM_{10} concentrations and visibility during dust codes (R^2<0.3) was found at the stations Reykjavik and Kirkjubaejarklaustur. Figure 8C shows visibility of all available dust codes plotted against corresponding PM_{10} concentrations together at all stations. Power function analysis

resulted in moderate correlation (R^2=0.37, p<0.01). Daily dust concentrations from the High-volume Filter Aerosol Sampler at Storhofdi during 1997-2002 and 2010 were well correlated with the 24-hour minimum visibility (R^2=0.71, Figure 8D).

4 Discussion

An annual mean of 34 dust days recorded in Iceland is comparable to dust studies from the active parts of China (35 dust days yr^{-1}, Qian et al., 2002), Mongolia (40 dust days yr^{-1}, Natsagdorj et al., 2003), and Iran (Jamalizadeh et al., 2008). The synoptic coding protocols can, however, contribute up to 15 % underestimation of annual dust day number (O´Loingsigh et al., 2010). Moreover, synoptic codes 04-06 showed a good agreement with increased PM_{10} concentrations. Including these codes into the criteria for dust observation, the annual mean dust-day frequency would be fourfold higher than applying conventionally used dust codes. This results in a total of 135 dust days per year on average for Iceland with 101 dust days observed in S Iceland and 34 dust days in NE Iceland. Such frequency can be found in parts of Australia and Africa (Ekström et al., 2004; N´TchayiMbourou et al., 1997). High numbers of dust observations presented here reflect previous studies showing high dust deposition rates in Iceland (Arnalds, 2010; Prospero et al., 2012; Thorarinsdottir and Arnalds, 2012; Bullard, 2013; Arnalds et al., 2013; Arnalds et al., 2014) and places the country among the important dust production areas of the world. Iceland is likely the most largest and active high-latitude cold dust source.

Trends in global dust emissions show high dust frequency during the 1950-1960s and low frequency during 1980s in the USA, Australia and China as well as in Iceland (Steenburgh et al., 2012; Ekström et al., 2004; Qian et al., 2002). The 2000s were reported as the most active decade in Iran and in NE Iceland (Jamalizadeh et al., 2008). Dust periods retrieved from the ice-cores data during GISP2 project in Greenland correlate with the NE Iceland dust frequency 1950-1990 (Donarummo et al., 2002).

Generally, the period 1950-1965 was warm and dry in Iceland resulting in frequent dust suspension (Hanna et al., 2004). For the NE Iceland, the dustiest year 1955 with 37 dust days, coincides with one of the warmest and driest years in NE Iceland (Hanna et al., 2004). For the southern part of Iceland, the most frequent and severe dust event period was during 1965-1968. It was a period of below-average precipitation reported at stations Reykjavik, Stykkisholmur and Vestmannaeyjar (Hanna et al., 2004) while the 1965 was the driest year in

SW Iceland for the past 100 years. The 20th century warm period in Iceland (1920s-1965) ended very abruptly in 1965 with about 1°C drop in mean annual temperature (Hanna et al., 2004). The most exceptional year was, however, the year 1966 with 40 dust days reported in S Iceland. Not only was October 1966 reported as the driest October in Icelandic history, but also February 1966 in Reykjavik. Together with extremely strong maximum winds of more than 40 ms^{-1}, the meteorological conditions in February 1966 caused at least 11 days of extremely severe dust storms. Local newspaper reported several large roofs removed from the houses, ships tore away from the harbors and planes turned around (Morgunblaðið, 1966).

The seventies were cold with high precipitation, but strong winds were often observed in S Iceland bringing the dust into suspension. The 1980s and 1990s were cold and with high precipitation in S Iceland while the 1990s were warm in the NE (Hanna et al., 2004). High frequency of dust events in NE Iceland during the 2000s was associated with dry and warm Junes. High number of dust days in S Iceland in 2010 was often because of resuspension of volcanic ash from the Eyjafjallajökull eruption during very frequent northerly winds (Petersen et al., 2012). The annual differences in dust event frequency do not correspond to trends of the global climate drivers such as the North Atlantic Oscillation (NAO), the Arctic Oscillation or prevailing ocean currents (Dagsson-Waldhauserova et al., 2013). The main driver is likely an orthogonal pattern to NAO, the dipole of Sea Level Pressure (SLP) oscillation oriented east-west (Dagsson-Waldhauserova et al., 2013).

The position of the Icelandic low determines whether dust plumes travel in a northeast or southerly direction. Higher frequency and severity of DE (low visibility and high wind speeds) in S Iceland than in NE Iceland is likely due to the close proximity of the S stations to the dust sources as well as higher number of the stations in the South (Figure 1). The Grimsstadir station is > 100 km from the Dyngjusandur source while the southerly stations are in range of tens of km from the sources. Dust deposition rates and DE severity decrease exponentially with distance from the source (Arnalds et al., 2014). The local dust sources in S Iceland are also affected by milder oceanic climate during the winter while the NE highland dust sources are covered by snow for much of the winter. The dustiest weather station, Grimsstadir, is located downwind from the most active glacial plain in Iceland, Dyngjusandur, N of the Vatnajokull glacier. The most active stations are equally distributed around the areas with very high dust deposition (Arnalds, 2010) from the central NE, SE, S to

SW Iceland. The land reclamation activities from the 1950s and 1970s (Crofts, 2011) result in decreased dust activity at the stations Hella and Höfn (Figure 2).

The seasonal distribution of dust events in Iceland shows that the high dust period is from March to October. The NE dust events are typically warm, occurring during summer/autumn (May-September) while the S dust events are mainly cold, occurring during winter/spring (March-May). This is related to the SLP pattern which controls the warm southerly winds in NE Iceland as well as the cold northerly winds in S Iceland (Bjornsson and Jonsson, 2003). The S dust events are, however, more equally distributed during the year. The winter season is related to mild temperatures and high winds in S Iceland. Relatively high mean dust concentrations were measured during winter (Jan-March) at station Storhofdi (Prospero et al., 2012). The winter cold dust storms were frequently observed also in Mongolia (Natsagdorj et al., 2003). The highest number of dust storms occurred in March-May while the mean March-April temperatures were sub-zero. May is the driest and dustiest month in Iceland while June and September are the driest months only in NE Iceland (Hanna et al., 2004; Dagsson-Waldhauserova et al., 2013). Nevertheless, dust events can be observed also during high precipitation seasons < 4 hours after the rain (Dagsson-Waldhauserova et al., 2014). This agrees that even the highest precipitation year such 1972 can be of relatively high dust frequency.

Visibility during dust observations is an important indicator of dust event severity. To estimate the empirical relationship between visibility and dust concentration in Iceland, we compared available PM_{10} concentrations with visibility based on methods in Wang et al. (2008). We found moderate correlation (R^2=0.37, $p<0.01$) between dust concentrations and visibility which was likely caused due to several factors: i) visibility was observed manually and only the prevailing visibility ($\varphi>180°$) recorded; ii) generally low number of measurements, iii) the stations were located in different distance of each other, iv) time resolution between the dust and weather measurements, and v) station Reykjavik with majority of the measurements was influenced by anthropogenic aerosols. More observations are therefore needed.

Some of the most severe dust events in Iceland during 2007-2011 were captured by the Moderate Resolution Imaging Spectroradiometer (MODIS) flying on NASA's Terra satellite. Several dust plumes, shown on a visible wavelength, exceeded 1000 km travelling towards Europe, North America and Arctic. It was calculated that dust events caused deposition over

370,000 km^2 oceanic area around Iceland carrying 6-14 million tons of dust (Arnalds et al., 2014). The majority of dust, containing high amounts of bioavailable iron, is deposited in early spring in southern parts of Iceland. Oceanic biochemical cycles and productivity might therefore be strongly affected by local aeolian processes. We also emphasize here that considerably high dust event frequency and long-range transport of Icelandic dust may affect the environment and climate on macro scale. Icelandic dust aerosol should be included in climate projections as well as in the European and Arctic air pollution studies.

5 Conclusions

This study of long-term dust observations in Iceland showed that dust-day frequency in cold high-latitude areas can be comparable to the major desert areas in the world. It was found that dust events often occurred during winter and at sub-zero temperatures. Observed dust events were more severe in southern part of Iceland than in NE Iceland, most likely because of close proximity of the southerly weather stations to major dust sources. The highest frequency of dust events was during the 1960s in S Iceland while most of dust events in NE Iceland occurred during the 2000s. The highest number of severe dust storms (visibility < 500 m) was observed in southern part of Iceland during the 2000s. Synoptic codes for dust were in good agreement with available dust concentration measurements; codes 04-06 should be considered in dust studies. There was a moderate correlation found between available PM_{10} concentrations and visibility during the dust observations in Iceland. More synchronised dust and weather measurements are therefore needed. Iceland can be considered as the largest and most active desert and dust source at the boundary of the Arctic and Sub-Arctic region.

Acknowledgements

The work was supported by the Eimskip Fund of The University of Iceland and by the Nordic Centre of Excellence for Cryosphere-Atmosphere Interactions in a Changing Arctic Climate (CRAICC). We would like to thank Joseph Prospero from the University of Miami, USA, and Thorsteinn Johannsson from the Environment Agency of Iceland for providing the PM data for the dust measurements.

References

Arnalds, O.: Dust sources and deposition of aeolian materials in Iceland, Icel. Agr. Sci., 23, 3–21, 2010.

Arnalds, O., Thorarinsdottir, E. F., Thorsson, J., Dagsson-Waldhauserova, P., and Agustsdottir, A. M.: An extreme wind erosion event of the fresh Eyjafjallajökull volcanic ash, Nature Sci. Rep., 3, 1257, 2013.

Arnalds, O., Olafsson, H., and Dagsson-Waldhauserova, P.: Quantification of iron-rich volcanogenic dust emissions and deposition over ocean from Icelandic dust sources, Biogeosciences Dis., 11, 5941–5967, 2014.

Bjornsson, H. and Jonsson, T.: Climate and climatic variability at Lake Mývatn, Aquat. Ecol., 38, 129-144, 2003.

Bullard, J. E.: Contemporary glacigenic inputs to the dust cycle, Earth Sur. Proc. Land., 38, 71–89, 2013.

Crofts, R. (Eds.): Healing the Land, Soil Conservation Service of Iceland, Reykjavik, Iceland, 2011.

Crusius, J., Schroth, A. W., Gasso, S., Moy, C. M., Levy, R. C., and Gatica, M.: Glacial flour dust storms in the Gulf of Alaska: Hydrologic and meteorological controls and their importance as a source of bioavailable iron, Geophys. Res. Lett., 38, L06602, doi:10.1029/2010GL046573, 2011.

Dagsson-Waldhauserova, P., Arnalds, O., and Olafsson, H.: Long-term frequency and characteristics of dust storm events in Northeast Iceland (1949-2011), Atmos. Environ., 77, 117-127, 2013.

Dagsson-Waldhauserova, P., Arnalds, O., Olafsson, H., Skrabalova, L., Sigurdardottir, G. M., Branis, M., Hladil, J., Skala, R., Navratil, T., Chadimova, L., von Lowis of Menar, S., Thorsteinsson, T., Carlsen, H.K., and Jonsdottir, I.: Physical properties of suspended dust during moist and low-wind conditions in Iceland, Icel. Agr. Sci., 27, 2014.

Donarummo, J. J., Ram, M., and Stolz, M. R.: Sun/dust correlations and volcanic interference, Geophys. Res. Lett., 29, 1361, doi:10.1029/2002gl014858, 2002.

Dörnbrack, A., Stachlewska, I. S., Ritter, C., and Neuber, R.: Aerosol distribution around Svalbard during intense easterly winds, Atmos. Chem. Phys., 10, 1473-1490, 2010.

Ekström, M., McTainsh, G. H., and Chappell, A.: Australian dust storms: temporal trends and relationships with synoptic pressure distributions (1960–99), Int. J. Climatol., 24, 1581–1599, 2004.

Eldridge F.R. (Eds.): Wind Machines, Van Nostrand Reinhold, New York, USA, 1980.

Engelstaedter, S., Kohfeld, K. E., Tegen, I. and Harrison, S. P.: Controls of dust emissions by vegetation and topographic depressions: An evaluation using dust storm frequency data, Geophys. Res. Lett., 30, 1294, doi:10.1029/2002GL016471, 2003.

Fields, J. P., Belnap, J., Breshears, D. D., Neff, J. C., Okin, G. S., Whicker, J. J., Painter, T. H., Ravi, S., Reheis, M. C., and Reynolds, R. L.: The ecology of dust, Front. Ecol. Environ., 8, 423–430, 2010.

Ganopolski, A., Calov, R., and Claussen, M.: Simulation of the last glacial cycle with a coupled climate ice-sheet model of intermediate complexity, Clim. Past, 6, 229-244, 2010.

Hanna, E., Jonsson, T., and Box, J. E.: An analysis of Icelandic climate since the nineteenth century, Int. J. Climatol., 24, 1193–1210, 2004.

IMO: Reglur um veðurskeyti og veðurathuganir [Weather Observer Handbook], The Icelandic Meteorological Office, Reykjavik, Iceland, 85 pp., 1981.

Jamalizadeh, M. R., Moghaddamnia, A., Piri, J., Arbabi, V., Homayounifar, M., and Shahryari, A.: Dust Storm Prediction Using ANNs Technique (A Case Study: Zabol City), Proc. World Aca. Sci. Eng. Tech., 33, 529-537, 2008.

Morgunblaðið: Þök fjúka af húsum, skip slitna upp [Roofs blow off houses, boats tore away], 1, available at: http://timarit.is/view_page_init.jsp?issId=113054&pageId=1372641&lang=is&q=1966, last access: 4 Apr 2014, 1966.

N'TchayiMbourou, G., Berrand, J. J., and Nicholson, S.E.: The diurnal and seasonal cycles of wind-borne dust over Africa north of the Equator, J. Appl. Meteorol., 36, 868–82, 1997.

Nickling, W. G.: Eolian sediment transport during dust storms: Slims River Valley, Yukon Territory, Can. J. Earth Sci., 15, 1069-1084.

Natsagdorj, L., Jugder, D., and Chung, Y. S.: Analysis of dust storms observed in Mongolia during 1937–1999, Atmos. Environ., 37, 1401–1411, 1978, 2003.

O'Loingsigh, T., Mc Tainsh, G., Tapper, N., and Shinkfield, P.: "Lost in code: A critical analysis of using meteorological data for wind erosion monitoring", Aeol. Res., 2, 49-57, 2010.

Petersen, G. N., Björnsson, H., and Arason, T.: The impact of the atmosphere on the Eyjafjallajökull 2010 eruption plume, Geophys. Res. Lett., 117, D00U07, doi:10.1029/2011JD016762, 2012.

Prospero, J. M., Bullard, J. E., and Hodgkins, R.: High-latitude dust over the North Atlantic: Inputs from Icelandic proglacial dust storms, Science, 335, 1078, 2012.

Qian, W. H., Quan, L., and Shi, S.: Variations of the dust storm in China and its climatic control, J. Climate, 15, 1216–1229, 2002.

Steenburgh, W. J., Massey, J. D., and Painter, T. H.: Episodic dust events of Utah's Wasatch front and adjoining region, J. Clim. Appl. Meteorol., 51, 1654–1669, 2012.

Thorarinsdottir, E. F. and Arnalds, O.: Wind erosion of volcanic materials in the Hekla area, South Iceland, Aeol. Res., 4, 39-50, 2012.

Wang, Y. Q., Zhang, X. Y., Gong, S. L., Zhou, C. H., Hu, X. Q., Liu, H. L., Niu, T., and Yang, Y. Q.: Surface observation of sand and dust storm in East Asia and its application in CUACE/Dust, Atmos. Chem. Phys., 8, 545–553, 2008.

Table 1. Weather stations in Iceland reporting synoptic observations. Observation period, number of dust observations, dust days and dust days per year are included. Stations are listed in descending order from the highest number of dust days.

Station	Observation period	Dust days	Dust observations	Dust day yr^{-1}
Grimsstadir	1949-2011	791	1685	12.6
Hofn	1949-2011	243	575	3.9
Vatnsskardsholar	1949-2011	234	408	3.7
Egilsstadir	1949-1998	192	386	3.8
Hella	1958-2005	179	368	3.7
Kirkjubaejarklaustur	1931-2011	158	274	2
Storhofdi	1949-2011	118	204	1.9
Haell	1949-2011	94	132	1.5
Hveravellir	1965-2004	91	124	2.3
Eyrarbakki	1957-2011	80	120	1.5
Vik	1961-2011	76	96	1.5
Keflavik	1952-2011	68	96	1.1
Vopnafjordur	1961-2011	64	83	1.3
Thingvellir	1949-1984	56	81	1.6
Reykjavik	1949-2011	41	70	0.7
Raufarhofn	1949-2011	41	61	0.7
Hjardarland	1990-2011	38	56	1.7
Sidumuli	1949-2011	30	37	0.5
Akureyri	1949-2011	26	26	0.4
Galtarviti	1953-1994	15	16	0.4
Stadarholl	1961-2011	12	15	0.2
Stykkisholmur	1949-2011	9	13	0.1
Reykholar	1961-2004	8	9	0.2
Kollaleira	1976-2007	5	7	0.2
Blonduos	1949-2003	5	6	0.1
Natabu	1949-2004	3	4	0.1
Blafeldur	1998-2011	2	2	0.1
Bergstadir	1978-2011	2	2	0.1
Hornbjargsviti	1949-2004	1	1	0.02
Reykir i Hrutafj.	1997-2011	1	1	0.1

Table 2. Dust event classification based on visibility criteria. Frequency of dust events, mean wind velocity, mean temperature, and annual number of dust days of each dust class are included. S represents southern part and NE northeastern part of Iceland.

Dust event class	Visibility (km)	Frequency (%)		Wind velocity (ms^{-1})		Temperature (°C)		Number of dust days yr^{-1}	
		S	NE	S	NE	S	NE	S	NE
Severe dust storm	≤0.5	1.2	< 1	15.7	16.2	-1.7	8.4	0.3	0.2
Moderate dust storm	0.5-1.0	3.5	2	13.6	14.9	4.1	9.4	1.1	0.5
Severe haze	1.0-5.0	14	10	15.0	13.0	1.1	10.6	3.0	2
Moderate haze	5.0-10.0	17	13	14.7	11.3	1.7	10.9	4.1	3
Suspended dust	10.0-30.0	42	46	13.5	9.9	3.0	10.6	10	10
Moderate susp. dust	30.0-70.0	16	27	11.7	10.2	3.7	10.0	6	7

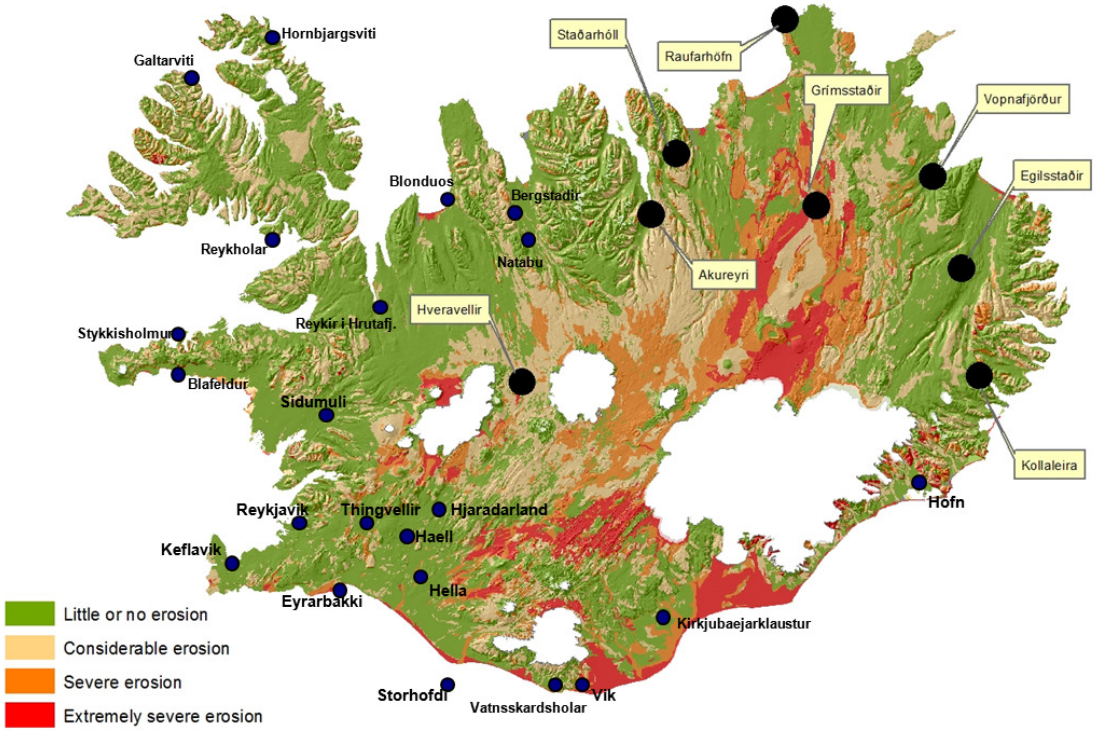

Figure 1. A map showing the locations of weather stations in Northeast and central Iceland (large black circles) and stations in northwestern and southern part of Iceland (small circles). Base map from the Agricultural University of Iceland Erosion Database (Soil Erosion in Iceland).

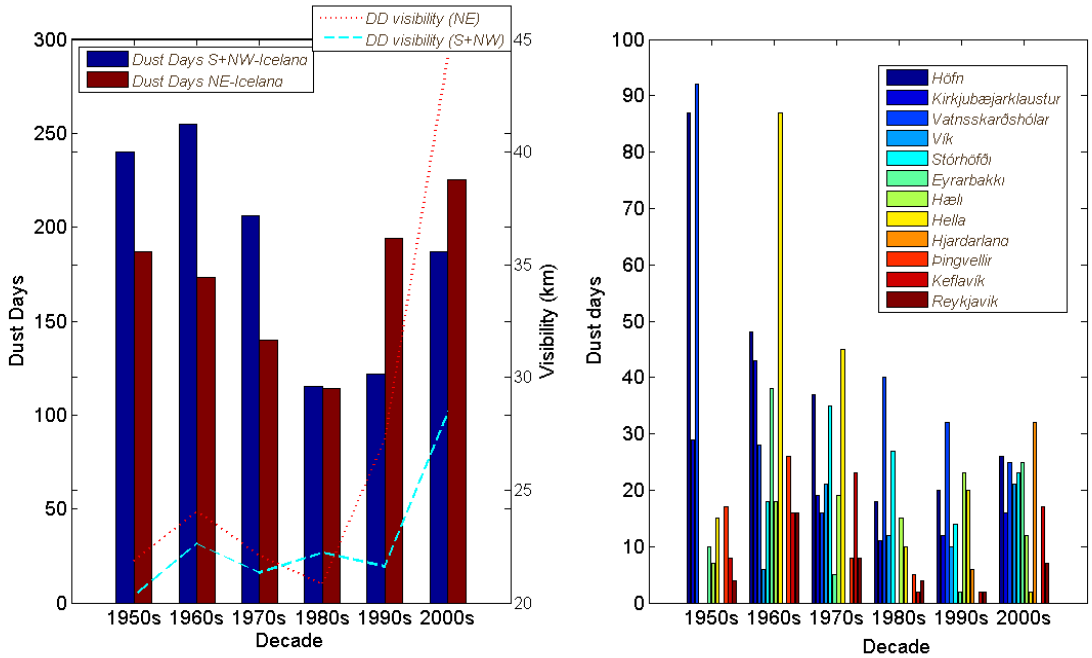

Figure 2. Total number of dust days, all stations combined to the left (blue bars for southern and northwestern part of Iceland, brown bars for Northeast Iceland). Individual stations in South Iceland sorted by decades to the right. Lines represent mean visibility (blue for S, brown for NE Iceland).

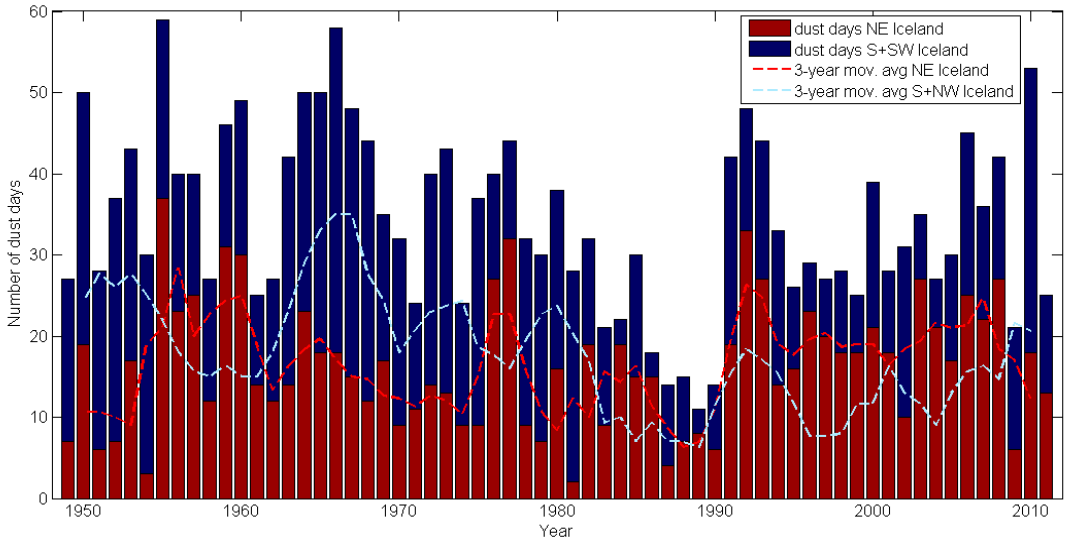

Figure 3. Number of dust days (blue bars for southern and northwestern part of Iceland, brown bars for Northeast Iceland) and 3-year moving averages of dust day frequency (red for NE, light blue for S Iceland).

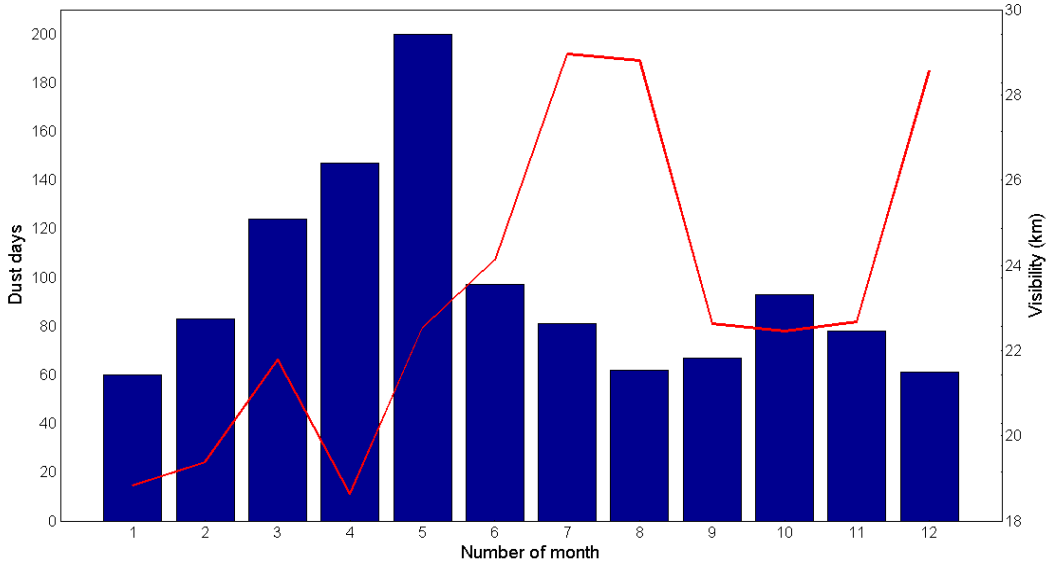

Figure 4. Number of dust days per month (bars) and monthly means of dust visibility (line) in southern part of Iceland in 1949-2011.

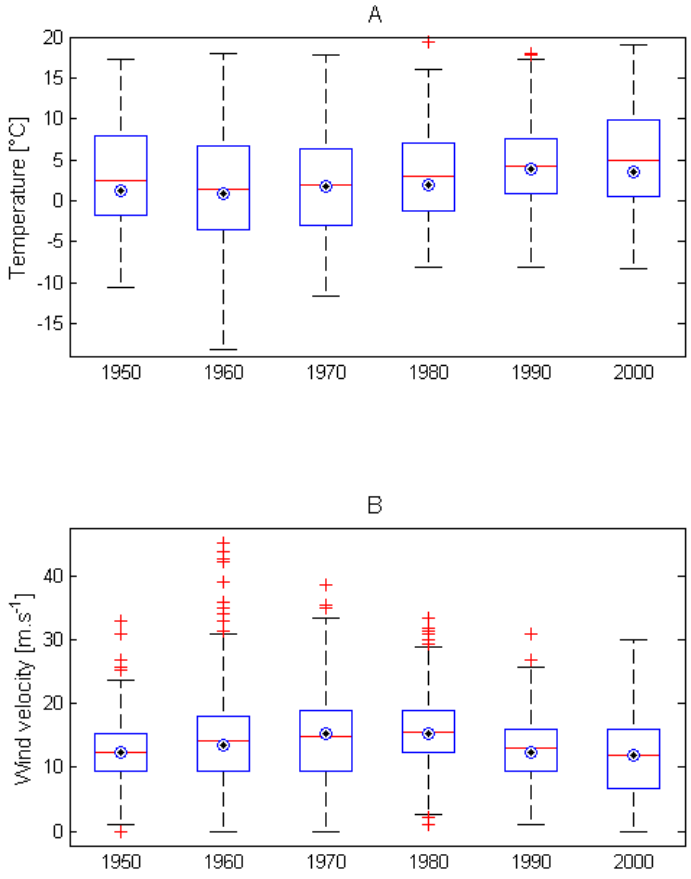

Figure 5. Temperature (A) and wind velocity (B) for dust events in southern part of Iceland in 1949-2011. The boxes demarcate the range in which half the data can be found. The red lines represent the mean and the circles the median.

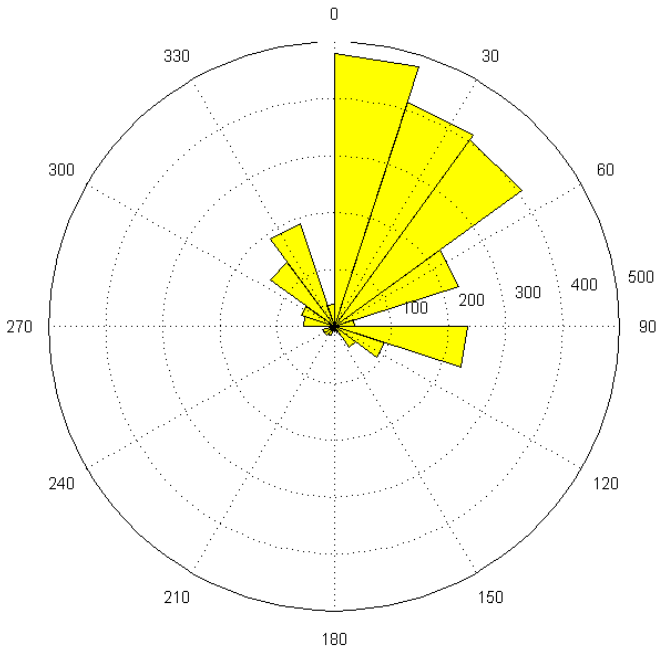

Figure 6. Wind directions (WD) during dust events in southern part of Iceland in 1949-2011. Weather stations that observed mainly WD 0-18° - Höfn, Eyrarbakki, Kirkjubaejarklaustur, Storhofdi, Thingvellir; WD 18-36°- Höfn, Vatnsskardsholar, Hjardarland, Reykjavik, Keflavik; WD 36-54°- Hella, Vatnsskardsholar, Vik; WD 54-72°- Haell, Vatnsskardsholar; WD 90-108°- Storhofdi, Vatnsskardsholar; WD 270-306° - Vatnsskardsholar; and WD 306-342°- Höfn.

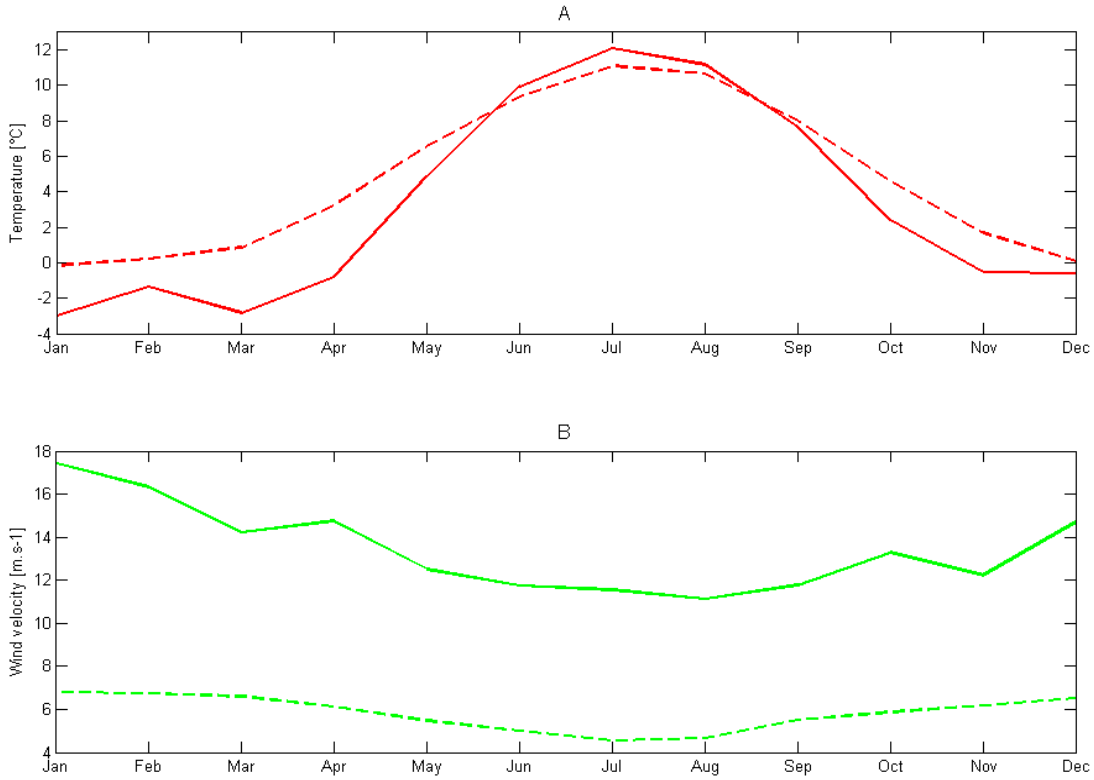

Figure 7. Monthly mean values (solid lines) of temperature (A) and wind velocity (B) during dust events in S Iceland in 1949-2011. Dashed lines represent the total mean values in 1949-2011.

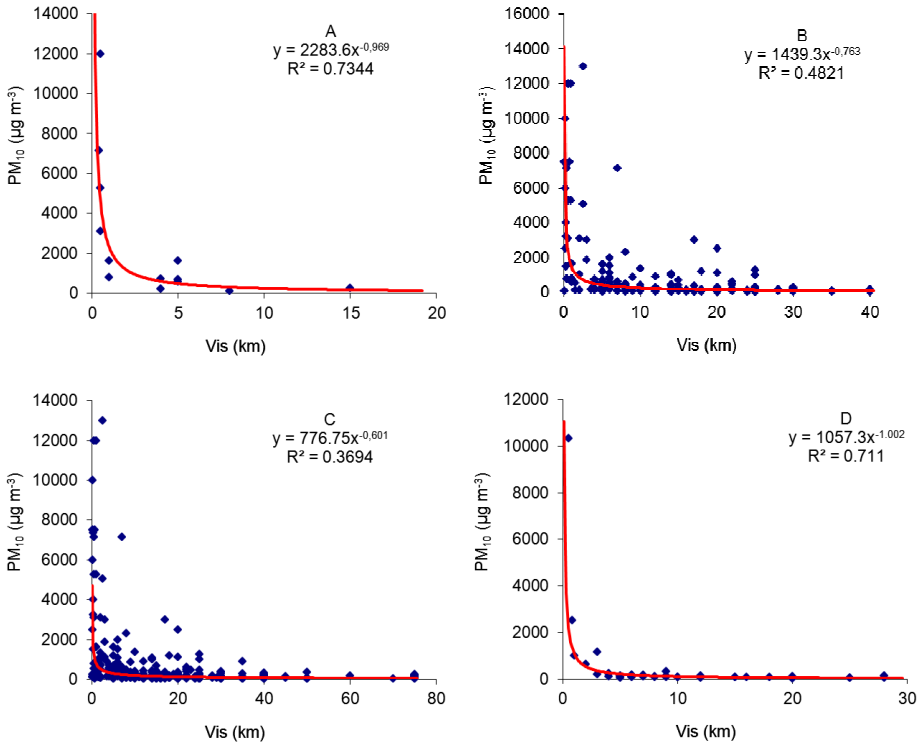

Figure 8. Hourly PM_{10} concentrations with corresponding visibility at stations: A- Vík, B- Vatnsskardsholar, and C – all stations (Reykjavik, Vik, Vatnskardssholar, and Kirkjubæjarklaustur). D represents daily PM_{10} concentrations concentrations from the High-volume Filter Aerosol Sampler with corresponding minimum 24-hour visibility.

Paper II

Physical properties of suspended dust during moist and low wind conditions in Iceland

Pavla Dagsson-Waldhauserova,[1,2] Olafur Arnalds,[1] Haraldur Olafsson,[1,3,4] Lenka Skrabalova,[5] Gudmunda Maria Sigurdardottir,[1,3] Martin Branis,[5] Jindrich Hladil,[6] Roman Skala,[6] Tomas Navratil,[6] Leona Chadimova,[6] Sibylle von Lowis of Menar,[3] Throstur Thorsteinsson,[7] Hanne Krage Carlsen,[8] and Ingibjorg Jonsdottir[7]

[1] University of Iceland, Department of Physics, Reykjavik, Iceland
[2] Agricultural University of Iceland, Faculty of the Environment, Hvanneyri, Iceland.
e-mail: pavla@lbhi.is (corresponding author)
[3] Meteorological Office of Iceland, Reykjavik, Iceland
[4] Bergen School of Meteorology, Geophysical Institute, University of Bergen, Norway
[5] Faculty of Science, Charles University in Prague, Prague, Czech Republic
[6] Institute of Geology AS CR, v.v.i., Prague, Czech Republic
[7] University of Iceland, Institute of Earth Sciences and Environment and Natural Resources, Reykjavik, Iceland
[8] Department of Public Health and Community Medicine, University of Gothenburg, Sweden

ABSTRACT

We measured a dust event which occurred during wet and low wind/windless conditions as the result of surface heating in August 2013. Maximum particle number concentration (PM~0.3-10 μm) reached 149,954 particles cm^{-3} min^{-1} while mass concentration (PM<10 μm) was 1757 μg m^{-3} min^{-1}. The suspended dust was very fine with the highest number of particles in the size range 0.3-0.337 μm, followed by particles 1.5-5 μm in diameter. Close-to-ultrafine particle size distributions showed a significant increase in number with the severity of the measured dust event (during dust peaks). Number concentrations were well correlated with mass concentrations. The mineralogy and geochemical compositions showed that glaciogenic dust contains sharp-tipped shards with bubbles and 80 % of the particulate matter is volcanic glass rich in heavy metals. Wet dust particles were mobilized within < 4 hours. This is the first scientific study of particle size distributions in an Icelandic dust event including findings on initiation of dust suspension.

Keywords: atmospheric measurements, dust storm event, surface heating, dust aerosol, climate aspects

YFIRLIT

Eðliseiginleikar ryks við vindrof í litlum vindi rök veðurskilyrði á Íslandi

Tækjum var komið fyrir á Mælifellsandi norðan Mýrdalsjökuls til mælinga á ryki á upptakasvæði rykmengunar ágúst 2013. Við mældum einn „rykatburð" sem átti sér stað við mjög lágan vindstyrk þegar sandurinn hitnaði í sólskyni. Hámarksstyrkur korna (PM~0,3-10 μm) náði um 150 000 kornum cm^{-3} $mínútu^{-1}$ á meðan þéttleiki (PM<10 μm) var 1757 μg m^{-3} $mínútu^{-1}$. Rykið var mjög fínkorna með flest kornin 0,3-0,337 μm en næst felst af kornastærðinni 1,5-5 μm. Hlutdeild mjög fínna korna jókst með rykmagninu. Fjöldi korna og kornastyrkur fylgdust vel að. Bergfræði og jarðefnafræði kornanna sýndi að þessi jökulættuðu rykkorn voru sum oddhvöss og blöðrótt og að 80% efnanna er gosgler með háu innihaldi af ýmsum þungmálmum. Rykkornin tókust á loft eftir að hafa þornað < 4 tíma. Þessar rannsóknir eru þær fyrstu sem sýna kornastærðir ryks á fokstað þegar rykframleiðsla á sér stað og þær fyrstu til að sýna aðstæður þegar rykmengun verður nánast í logni.

INTRODUCTION

Atmospheric dust has been measured in major desert areas of the world since the 1950s (Chepil & Woodruff 1957, Aston et al. 1973, D´Almeida 1986, Wang et al. 2008). High latitude and periglacial areas are also important sources of dust, but the number of dust studies in cold climate areas is significantly lower than reported for the major dry deserts. Dust measurements within cold region dust sources are mainly seasonal and employ measurement techniques focused mostly on the coarser silt-sized or sand-sized particles (Nickling 1978, Bullard 2013). Air particle monitoring using a range of automatic instruments is conducted far from the dust sources in the Arctic (NILU 2013).

Iceland is an active source of dust originating from glaciogenic and volcanic sediments. Volcanic sandy deserts and glacial outwash plains cover > 22% of the country (Arnalds et al. 2001). These areas are subjected to strong winds and severe wind erosion with dust deposition exceeding 500 g m^{-2} yr^{-1} in some areas (Arnalds 2010). Long-term observations of atmospheric dust show a high frequency of dust events in Iceland with > 34 dust days annually over the last 60 years (Dagsson-Waldhauserova et al. 2013a). The position of the Icelandic low determines whether dust plumes travel in a north-east or southerly direction. An annual mean of 16.4 dust days was recorded in NE Iceland and about 17.9 dust days occurred annually in southern parts of Iceland in 1949-2011 (Dagsson-Waldhauserova et al. 2013a, 2013b). These figures represent minimum values as many dust storm events occur without the dust passing the weather stations that can record the events. The frequency and the amount of dust measured in Iceland places the country among the major dust areas of the world (Mongolia, Iran, USA, China). Furthermore, Icelandic dust storms have been found to be among the most severe wind erosion events recorded on Earth (Arnalds et al. 2012, 2013).

Measurements of particle mass concentrations in Iceland have been mostly related to the Eyjafjallajökull eruption in 2010 (Leadbetter et al. 2012) or areas distal from the dust sources (Thorsteinsson et al. 2011, Blechschmidt et al. 2012). No direct measurements of dust concentrations within the major dust sources in Iceland have been made. Size segregated particle mass concentrations and number-size distributions (number of particles in defined particle size ranges) of dust aerosol can provide a better understanding of physical properties, such as textural, morphological and shape characteristics, and the possible health impacts of dust events (Harrison & Yin 2000, Morman & Plumlee 2013). Studies on number concentrations including particles < 10 μm in Iceland have not been published in the literature to date.

Icelandic dust differs from dust originating from continental dust sources, such as the Saharan and Asian dust. The dust is volcanogenic in origin, of basaltic composition, with lower SiO_2 proportions (<50%) and higher Al_2O_3, Fe_2O_3 and CaO content than crustal dust (Dagsson-Waldhauserova et al. 2013c). Volcanic dust made of glass can be very sharp and porous allowing particles as large as 50 μm to travel long distances (Navratil et al. 2013).

The main objective of this study was to provide an overview of physical properties of Icelandic dust, as exemplified by dust from Mælifellssandur, which is one of Iceland's main dust sources. Results of the first synchronized measurements of particle number and mass concentrations during a dust event directly within a dust source in Iceland are here reported. This information is combined with mineralogical and geochemical analyses of the source material to discuss the possible risk of Icelandic dust to human health.

METHODS

Location

Atmospheric Dust Measurements in Iceland (ADMI 2013) is a pioneering project launched to investigate the physical characteristics of dust aerosol *in situ* at the dust source. The

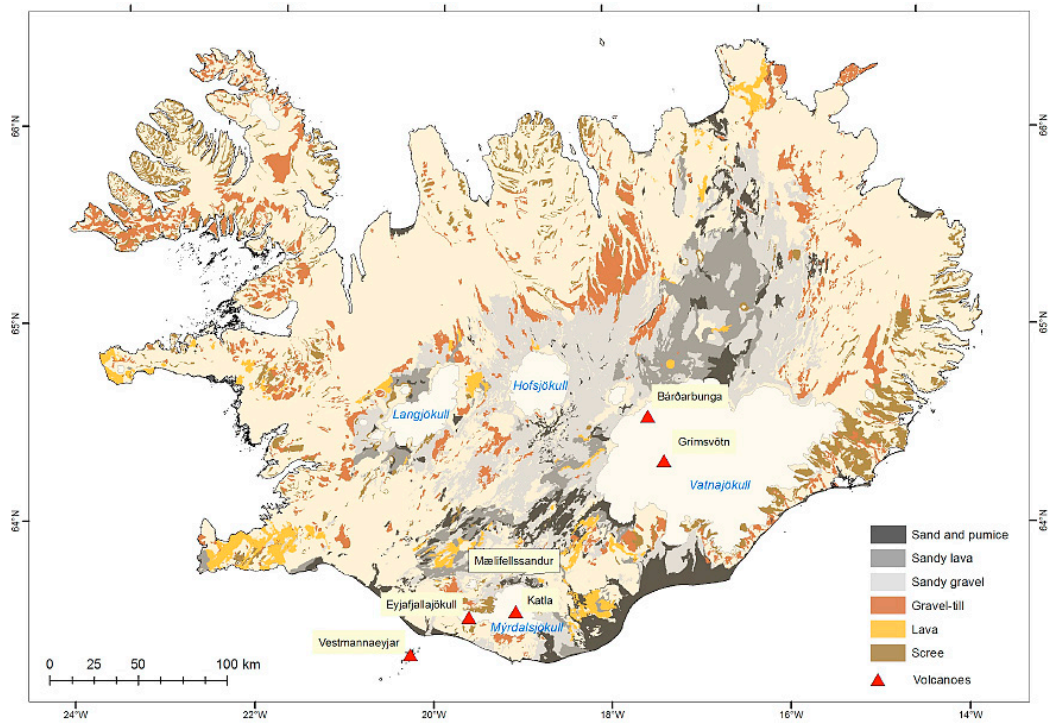

Figure 1. A map of Iceland with location of sampling site (Mælifellssandur) and active volcanoes (marked with red triangles). Based on the Agricultural University of Iceland Nytjaland and Erosion Databases, prepared by Sigmundur Helgi Brink.

ADMI 2013 took place in southern and southwestern Iceland on 8-18 August 2013. It was generally a period of high precipitation and low winds when no major dust storm event was observed. Nevertheless, one short dust event was measured directly at a dust source on 12 August 2013. Instruments were placed on the dust source, the Mælifellssandur sand plain, which is located north of Mýrdalsjökull Glacier in South Iceland (Figure 1, N 63.81569 W 19.12403, 601 m above sea level, 2 km N of glacier). Mælifellssandur is a 50-60 km^2 unstable glaciofluvial plain at 550-650 m elevation. It undergoes widespread flooding during the summer melting of the glacier, leaving unstable, silty materials behind, and is considered one of the major dust sources of Iceland (Arnalds 2010). One of Iceland's most active volcanic systems, Katla, is located under the Mýrdalsjökull Glacier (Thordarson & Höskuldsson 2008), and the materials deposited on the sand plains are derived from this volcanic system. The last eruption of Katla that reached through the glacier was in 1918.

Instrumentation

Two TSI 8520 DustTrak Aerosol Monitors (DustTrak) and one TSI Optical Particle Sizer 3330 (OPS) were placed one meter above the surface on the dust source. The DustTrak is a light-scattering laser photometer that measures aerosol mass concentrations from 0.001 to 100 mg m^{-3} for particles ranging in size from 0.1 to 10 μm. Particle concentrations recorded by DustTrak instruments have been previously found as a reasonably accurate measure of dust storms in Arizona (USA) and Australia (Jayrante et al. 2011). The OPS provides particle concentration and particle size distribution measurements using single particle counting

technology, for particles with optical diameters from 0.3 to 10 µm. It employs optical scattering from single particles where particle pulses are sized and binned in up to 16 different channels.

The DustTraks were calibrated to measure Particle Mass Concentrations (PMC) of two particle diameters (PMC_{10} for particles <10 µm and $PMC_{2.5}$ for particles <2.5 µm). As result, we measured simultaneously two PMCs (PMC_{10}, $PMC_{2.5}$) and Particle Number Concentrations (PNC) from the OPS. The OPS channels that best matched the $PMC_{2.5}$ were of particle diameters 0.3-2.685 micrometers.

Mineralogical and geochemical analysis

We used two instrumental approaches to obtain physical and chemical characteristics of the dust particles collected from the active surface layer of the Mælifellssandur dust source right after the dust event. Firstly, semi-quantitative estimates of mineral content (Bruker D8 Discover) were determined from X-ray powder diffraction (XRD) data using the reference intensity ratio (RIR) method and, secondly, energy dispersive spectrometry EDS/(EDX), with a BRUKER silicon drift detector (SDD) on a VEGA3 XM TESCAN electron microscope (polished sections) was used for elemental characterisation of glass and minerals in the individual particles.

Using the Bruker D8 Discover, the semi-quantitative estimates of the mineral content were determined from X-ray powder diffraction data using the reference intensity ratio (RIR) method as implemented in the Bruker DIFFRAC.EVA software. To make the estimates as accurate as possible the ICDD PDF2 database entries containing experimentally determined RIR values were preferred. Such determined mineral concentrations should be correct within 10-20 rel. % range depending mainly on absolute content of the particular phase in the mixture under investigation, crystallinity of the material, diffraction geometry used to collect the database standard data, and preferred orientation of the studied specimen.

The second approach involved back-scattered-electron (BSE) detection of the size, outline and aggregation parameters of the mineral and glassy components and, subsequently, their EDS chemical element analysis. Such detailed inspection of particle populations allowed us to improve the previously obtained XRD-based estimates of mineral proportions, so that we assumed (although not exactly calculated for each of the minerals) that the possible uncertainty for the mean values was reduced to the order of a few percent.

For volcanic glass, the EDS measurements of clustered points and inspection fields were used. The composition of the volcanic glass was determined with a chemical pattern for eight main oxides which were recalculated to a total of 100 % (Na_2O, MgO, Al_2O_3, SiO_2, K_2O, CaO, TiO_2, and FeO, where the latter denote

Figure 2. Photographs showing the dust suspension event measurements. The surface was exposed to solar radiation for four hours before the event occurred (left). Surface heating resulted in cloud formation and upward air motion causing uplift of dried silt particles from the upper surface layer (middle and right).

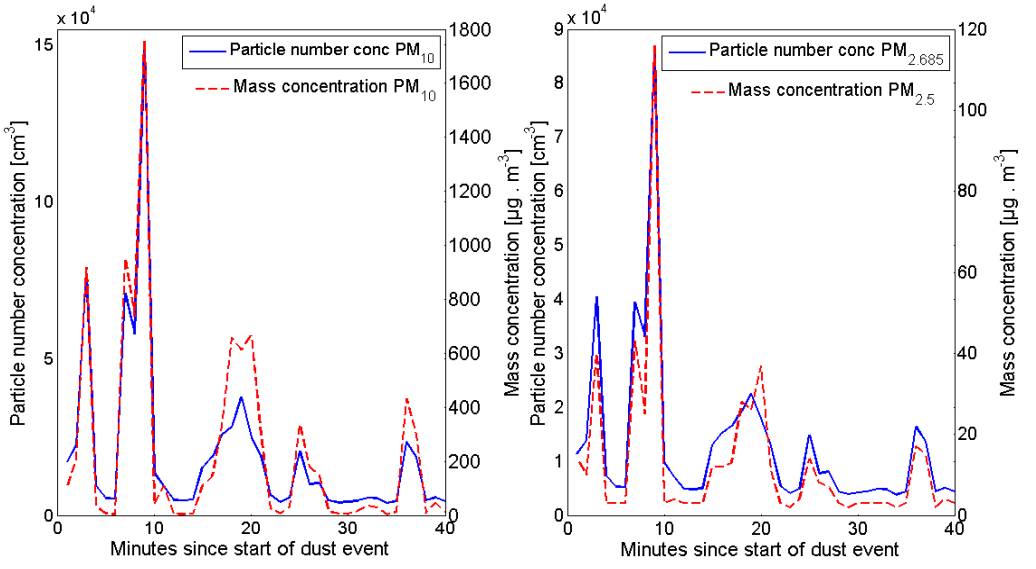

Figure 3. Particle number concentrations (blue) and mass concentrations (red) during the dust event.

FeO = FeO_{total}, ignoring the possibility of the presence of Fe^{3+} in the glass). This provides basic and practical information about these volcanic glass types.

RESULTS

The general physical properties of the dust are described in two sections: i) atmospheric dust measurements and ii) mineralogical and geochemical analyses.

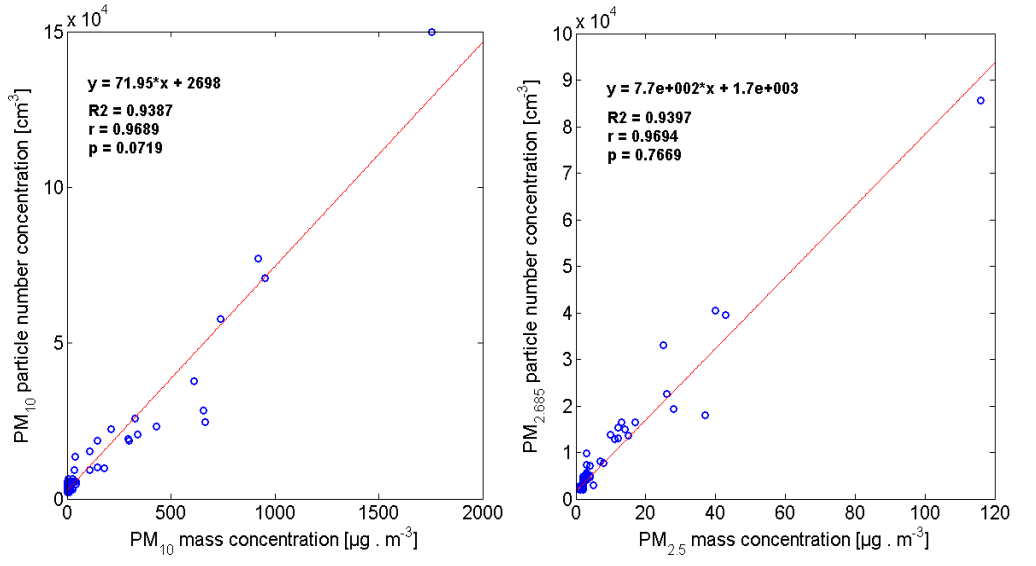

Figure 4. Correlation of particle number concentrations and mass concentrations of PM_{10} (left) and $PM_{2.5(2.685)}$ (right) during all atmospheric measurements.

Atmospheric dust measurements

The dust event was measured under unique conditions, during low wind/windless conditions when the surface was still moist after previous high precipitation. The main driver of dust suspension was direct solar radiation and consequent surface heating. The South Iceland region experienced a period of high precipitation for over a week before and during the measurements. The closest weather station equipped with a rain gauge, Laufbali, had an accumulated precipitation of > 55 mm during a period of five days, ending 14 hours before the event. High relative humidity (77-90 %) and low wind speeds (0-4 m s^{-1}) were measured at the closest weather station, the high altitude station Tindfjöll, 870 m a.s.l., during the dust event. Daily mean temperature was 6.3 °C, similar to the previous five-day mean (6.2 °C). The first dust whirls were visible after the surface was exposed to direct solar radiation for about four hours. Surface heating resulted in cloud formation and upward air motion during which dust started to be mobilized (Figure 2). Substantial dust repeatedly passed the instruments from all wind directions for about 40 minutes and the corresponding dust peaks are visible in Figure 3.

The maximum PNC_{10} (one-min average) was 149,954 particles cm^{-3} and PMC_{10} (one-min average) was 1757 µg m^{-3}. Maximum concentrations of the $PM_{2.5}$ fraction were meas-

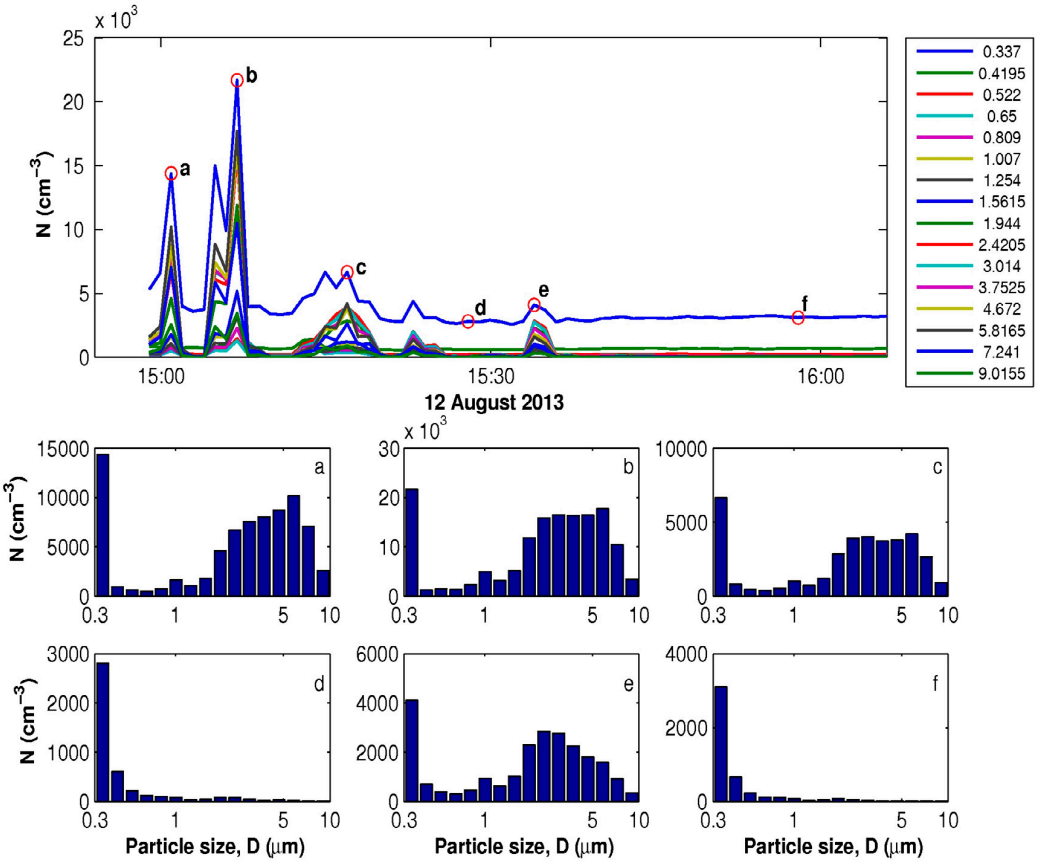

Figure 5. Size distributions of dust particles in size range 0.3 µm to 10 µm determined from the dust peaks (a, b, c, e), between the dust peaks (d) and after the dust event occurred (f). N - particle number concentration.

ured as 85,528 particles cm^{-3} in number concentration, with the mass reaching 116 μg m^{-3}. PNC were well correlated with PMC readings (R^2=0.939; Figures 3, 4). The more prominent the dust plume was, the higher the number of fine particles mobilized and, thus, the mass concentration increased accordingly. The amount of suspended particles, > 7.5 μm, was very small.

Figure 5 shows the particle size distribution in 17 size classes ranging 0.3 to 10 μm for the dust peaks (a, b, c, e), between the dust peaks (d) and after the dust event occurred (f). Very fine particles, 0.3-0.337 μm in diameter, were most abundant during all the measurements. When dust plumes passed through the instruments, the highest number of particles was found in the size range of 0.3-0.337 μm and 1.5-5 μm in diameter. The mean (median) particle diameter during the dust event was 1.69 μm (1.58 μm) with a range of 0.5–3.4 μm. Overall, the mean PMC_{10} and PNC_{10} measured directly on the dust source during the dust event were 234 μg m^{-3} and 19,024 particles cm^{-3}, respectively.

Table 1. Estimated amounts of components in the Mælifellssandur particulate matter. The semi-quantitative estimates are based on XRD analyses, but the smallest mineral contents (around XRD detection limits) also required verification of their presence by means of the chemical composition (EDX) and morphology of crystals (SEM-BSE). Note the predominance of glass (~ 80 wt. %).

MINERAL AND MATERIAL PHASES	wt %
Volcanic glass, amorphous component	78.2
Plagioclases (Na-rich anorthite + bytownite?)	12.2
Pyroxenes (augite)	4.6
Olivine + serpentine minerals (antigorite-lizardite?)	1.8
Zeolites (wairakite?)	1.1
Quartz	0.8
Magnetite + ulvospinel	0.7
Amphiboles (actinolite-tremolite?)	0.3
Undetermined phases and other components	0.3
Total	100.00

Mineralogical and geochemical analyses

The population of volcanogenic particles in the sample was homogenous, consisting mostly of extremely angular, sharp-tipped shards of largely homogeneous volcanic glass containing a small number of bubbles. These were highly polydisperse, nanometric/micrometric to coarse silt-sized (0.1–63 μm) particles. The shard faces were often curved and concave. They corresponded to spontaneous fracture patterns but, in part, also fragmentary outlines of the bubbles which originally exceeded the size of the particles. Most of these small shards resembled the volcanic glass particles which were found after the 2011 Grímsvötn eruption in Scotland (SEPA 2011) and subsequently also in the Czech Republic (unpublished data of the authors). However, this morphological similarity is incidental because of the different elemental compositions of the Mælifellssandur tephra glass (see Table 2 and Oladottir et al. 2005, 2011). According to the XRD analysis and the BSE inspection, the total amount of glass in the particulate matter reached almost 80 wt. % (Table 1).

The grains exceeding silt sizes were rare but their mass contribution was considerable. The large, sand sized clasts (0.063–0.95 mm) also consisted of glass, but mineral crystallites and phenocrysts made up a few to tens of %. In these clasts, the occurrence of Na-rich anorthite and augite was the most typical feature (Table 1, Figure 6). Olivine and antigorite occurred in significant amounts, together with ulvospinel, which typically formed tiny skeleton crystals in the glass. Other clinopyroxenes, biotite, alkali feldspars or quartz, particularly in their common sizes around 10 μm of particle equal diameter, were not found by the techniques applied and amphiboles were rare. Small amounts of zeolites (possibly wairakite based on the XRD signal) were present, mainly in the fine crystalline matrix of well packed, fine-silt lumps, and occasionally could be present with altered augitic aggregates.

The geochemical composition pattern of the

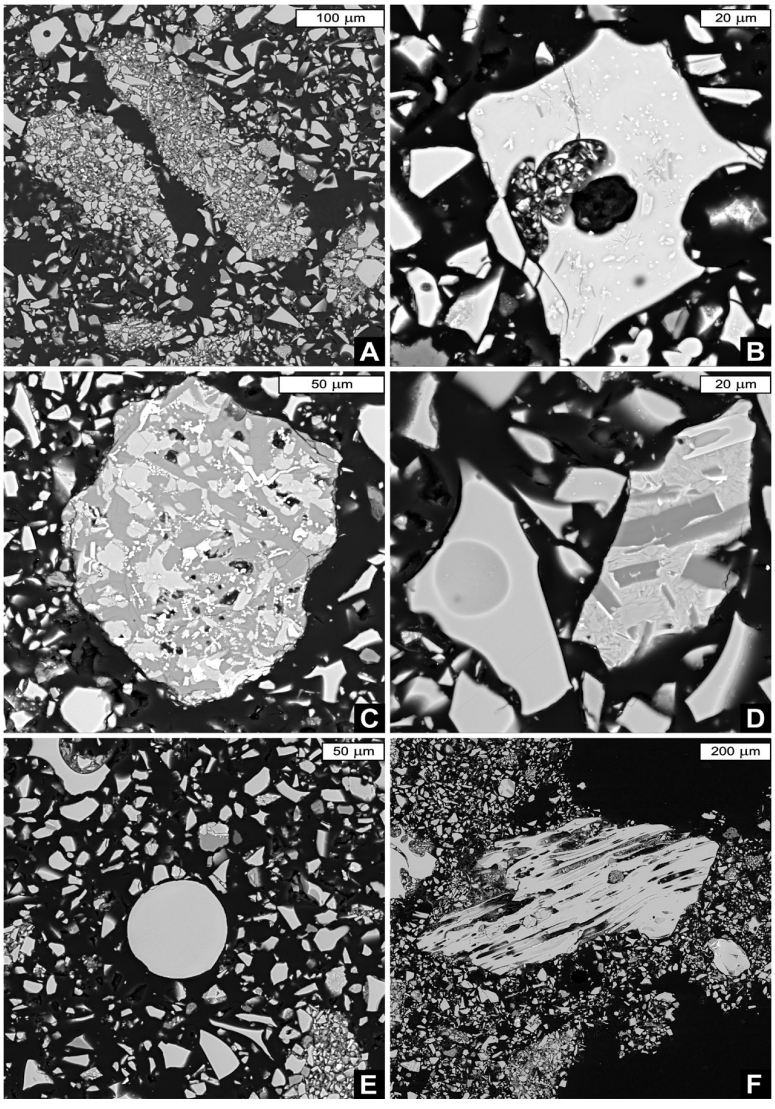

Figure 6. The BSE images of the Mælifellssandur particulate matter polished sections: Several examples of contrasting clusters of larger clasts in otherwise monotonous masses of polydisperse silt-sized (< 63 µm) shards of volcanic glass.

A – Mæli-1, occurrence of friable lumps of sub-millimetre sizes where the smallest glass particles prevailed. These were kept together due to dense packing, adhesion, and the presence of slightly developed (amorphous, crystallite dotted) meniscus and pendant cements (precipitated solutes). B – Mæli-3, a large shard of blocky glass containing small An-rich plagioclase laths (grey) and pyroxene and spinel crystals (relatively bright). The shard contains irregular voids/bubbles, selectively filled by the finest glass-silt fraction. Fractures in glass are fresh and still can expand. C – Mæli-4, a large clast with imperfectly crystallized plagioclases (grey) and pyroxenes (bright). The brightest dots are Fe- and Ti-rich minerals, particularly the skeleton crystals of ulvospinel. D – Mæli-5, pure homogeneous glass shard with a bubble (left) and a rare clast which consists of Na-rich anorthite (dark), altered augitic mass with amphiboles and zeolites (intermediate tones, structured), and an unusual hopper-shaped olivine (brighter, in upper right corner). E – Mæli-6, an uncommon spherical glass grain, with very slight initial crystallite dotting in its central part and exfoliation at the surface. F – Mæli-8, a millimeter-sized clast of fibre-like volcanic glass with long tubular bubbles.

Table 2. The chemical composition of the Mælifellssandur (M) samples based on EDX analyses of polished surfaces of individual glass particles, shown in descending order of FeO values. The eight most important oxides are used to characterize the main chemical pattern of these volcanic glasses from particulate matter recalculated to 100%-total for each set. The Eyjafjallajökull (E) and Katla (K) tephra glass (recalculated from Navratil et al. 2013 and Sigmarsson et al. 2011) are used for comparison, M/E and M/K ratios are shown. Note that M and K values are alike (the individual M/K ratios are close to 1).

GLASS. CODE	Na_2O	MgO	Al_2O_3	SiO_2	K_2O	CaO	TiO_2	FeO	glass - optical appearance in BSE
Mæli-7/3	3.28	4.11	13.60	42.81	0.85	10.44	5.68	19.24	homogeneous glass between nm- to µm-sized crystallites
Mæli-9/1	1.73	5.27	13.23	42.84	0.99	11.58	6.50	17.87	pure volcanic glass with few bubbles of 15-45µm diameters
Mæli-3/4	4.08	4.09	15.29	42.00	0.85	10.51	5.56	17.62	glass closely encircled by mineral crystallites
Mæli-1/2	3.41	5.36	14.11	40.45	0.99	12.39	5.80	17.50	pure blocky glass with few spherical bubbles of 10µm d.
Mæli-5/1	3.23	5.40	13.88	42.13	0.87	11.53	6.07	16.89	pure blocky glass. few spherical bubbles of 20µm diameter
Mæli-6/1	3.21	5.40	13.89	42.10	1.02	12.18	5.47	16.72	a glass spherule of 85µm diameter
Mæli-1/1	3.41	5.59	13.62	41.55	0.89	12.22	6.16	16.55	pure blocky glass with very rare bubbles of 5µm d.
Mæli-3/1	3.42	4.93	14.49	44.58	1.03	10.89	4.20	16.45	pure blocky glass between mm-sized crystals
Mæli-8/1	3.09	5.61	13.95	42.91	0.85	11.66	5.78	16.15	pure fibrous glass. very long parallel bubbles of 5-25µm d.
Mæli-7/5	3.34	3.66	15.93	44.31	0.81	12.12	4.84	14.98	glass closely encircled by mineral crystallites
AVG.VALUES									
M, 2013 (N 10)	***3.22***	***4.94***	***14.20***	***42.57***	***0.92***	***11.55***	***5.61***	***17.00***	Mælifellssandur, this study
E, 2010 (N 15)	*3.91*	*1.43*	*17.60*	*62.58*	*1.86*	*6.02*	*0.84*	*5.74*	Eyjafjallajökull, tephra glass (Navratil et al. 2013)
K, hist. (N n/a)	*3.11*	*4.89*	*13.16*	*48.28*	*0.80*	*9.76*	*4.84*	*15.17*	Katla, historical tephras (Sigmarsson et al. 2011)
M/E ratio	*0.82*	*3.46*	*0.81*	*0.68*	*0.49*	*1.92*	*6.64*	*2.96*	
M/K ratio	*1.04*	*1.01*	*1.08*	*0.88*	*1.15*	*1.18*	*1.16*	*1.12*	

'blackish' particulate matter (PM) glass was relatively stable. Based on the pattern of eight main oxides, this volcanic glass showed a very specific composition which could be easily identified in any mixture of dust deposited at some distance from the source (Table 2) and was notably different to the glass from recent eruptions. In particular, the Mælifellssandur glass had substantially higher amounts of FeO, MgO, CaO and TiO_2 than glass from the recent eruption of Eyjafjallajökull, as shown in Table 2. The glass was more similar to historical tephra from the Katla volcano (Table 2, Boygle 1994, Sigmarsson et al. 2011) with high levels of iron and titanium (FeO~17 %, TiO_2~6 % on average for our sample and FeO~15 %, TiO_2~ 5% for the Katla tephra). The TiO_2 content was particularly high, being 6–7 times higher than the content in the Eyjafjallajökull glass and considerably higher than that reported for tephra from the active Bárðabunga and Grímsvötn volcanic systems under the Vatnajökull glacier to the east (Oladottir et al. 2011). The high concentrations of TiO_2 and FeO were accompanied by depletion of SiO_2 in the glass to about 43 wt. % (Table 2). Such concentrations were lower than that reported for the MgO- and FeO-rich Laki tephra (ca. 50 % SiO_2, Kekonen et al. 2005), for Katla basalts (46-50 %), and for the entire East Volcanic Zone, including Elgdjá and Vestmannaeyjar (Oladottir et al. 2005). Strong depletion of SiO_2 in the Mælifellssandur material was a specific feature having a great potential to characterize the suspended particulates from this main dust source.

In comparing the particle sizes of suspended dust and the surface sample of deposit taken after the dust event, the surface sample was deprived of particles < 10 μm and significantly lower in particles < 2.5 μm than the measured suspended dust. Figure 6 shows that the aggregates consisted of fine and sub-micrometer particles, but 'single' particles were often of larger sizes (> 10 μm).

DISCUSSION

The ADMI measurements showed that dust generation can be activated under specific conditions such as from wet surfaces during the high precipitation season, from low wind speeds and low temperatures. The concentrations and size distributions measured during the short dust event give a unique insight into the initiation of dust storm events. Aerosol concentrations measured during wet background conditions on the dust source were very low; PMC_{10}~1-5 μg m^{-3} and PNC_{10}~222-2550 particles cm^{-3}. A gradual, steady surface heating caused the concentrations to rise with suspension of the dust and, in about four hours of direct sun, the PNCs increased over 100 times while PMCs increased over 600 times. This event was observed during low wind/windless condition and we assume that the time needed to initiate dust production or suspension of the drying silt on the dust source decreases with higher wind velocities.

Comparing PNCs recorded during dust events elsewhere has shown the importance of close-to-ultrafine particles (0.2-0.35 μm) in respect to the total number concentration (Jayrante et al. 2011). The particle diameter mode of 0.2-0.3 μm can contain up to hundreds of thousands particles per cm^{-3} during severe dust storms or volcanic eruptions (Jayrante et al. 2011, Vogel et al. 2012). Background condition concentrations or concentrations measured by counters designed for particle diameter >0.5 μm count up to hundreds of particles per cm^{-3} (Tittarelli et al. 2008, Jayrante et al. 2011, Zhou et al. 2012). Such high PNCs of particles 0.3-10 μm as were measured here have only been reported during a volcanic eruption (Vogel et al. 2012). This shows that glacially derived airborne sediments are very fine with the highest number of suspended particles in sizes 0.3-0.337 μm in diameter, at least during the low wind speed events described here. Therefore, such source material is easily suspended within a short time.

Despite this, the mass concentrations meas-

ured during this small event were significantly lower than those measured during severe dust storms elsewhere and further from major dust sources (Wang et al. 2008, Jayrante et al. 2011, Dagsson-Waldhauserova et al. 2013b). The wind was not strong enough to lift many of the wet particles > 5 μm. The mean PMC_{10} of 234 μg m^{-3} confirmed the long-term estimation of PMC_{10} in NE Iceland calculated from visibility observations (Dagsson-Waldhauserova et al. 2013a).

The special conditions at the dust source during this dust event made the PNC and the PMC strongly correlated (Figures 3, 4); a higher number of dust particles resulted in higher mass concentrations. Such strong relationships most likely resulted from the moist soil conditions and high humidity. The glacial floodplain was still wet and therefore only fine, dried particles were uplifted. The surface sample of deposit taken after the dust event was deprived of 'single' particles < 10 μm while the fine and sub-micrometer particles were only found in the aggregates. We suggest that the fine particles were blown away and transported further from the source. Fine mode particles are usually scavenged by larger particles during dust storms, and thus the mass concentration is estimated to increase with decreasing number of particles (Jayrante et al. 2011, Zhou et al. 2012), which is contrary to our findings. However, the highest number concentrations for submicron particles are generally attributed to wind speeds < 2 m s^{-1} (Weber et al. 2006). The most extreme wind erosion events in Iceland are characterized by limited amounts of particles <125 μm (Arnalds et al. 2013). Further research is therefore needed during the dust events of higher wind velocity to understand the opposite correlation of PNC and PMC.

Mineralogical and geochemical analyses

Considering the chemistry and morphology of the material investigated, we suggest that the Mælifellssandur dust source materials, containing mostly the recycled products of the Katla volcano and adjacent volcanic system, were the main component of dust coming from the area. There are several reasons for this assumption: i) the compositions of the glass shards had narrow ranges in composition; ii) the glass and glassy shards were marked by the raised Ti–Fe concentrations together with a scarcity of well crystallized mineral phases or aggregate rock structures; iii) the marker crystals embedded in the glass were Na-rich anorthite and very small and/or skeleton crystals of ulvospinel; and iv) the majority of the glass shards showed a very uniform morphology which corresponds to explosively and spontaneously fractured, blocky rather than intensely foamed glass. The morphology of the tiny shards resembled the glassy particle deposits from the very recent plumes of the active volcano Grímsvötn, south-west of the Vatnajökull massif. However, the tephra compositions, with markedly low SiO_2 and high TiO_2–FeO concentrations, were different. They can most likely be attributed to the Sléttujökull 'old tephra' source in the Mýrdalsjökull area, or considered as characteristic of the chemistry of the Katla volcanic system (see Larsen 2000, Oladottir et al. 2005, Sigmarsson et al. 2011). This indicates that the fresh volcanic material from recent eruptions has been removed relatively rapidly.

A strongly polydisperse mixture of glass fragments, encompassing the sub-micrometer, silt and even the lower coarse sand classes, was indicative of multiple material sources. This material must have been reworked by fluvial and glaciogenic processes that led to extremely poorly sorted parts of the outwash fans. The rarely observed, millimeter-sized clasts of specific compositions (e.g., resedimented frothy or extremely elongated tephra grains, as exemplified in Figure 6D) belonged to clasts 'floating' in the common matrix of the resedimented tephra. The light frothy clasts could have drifted drift in the top layer of streaming water, whereas the compact, heavy rock fragments were either pushed up in the granular flow (inverse grading) due to the rheological Brazil-nut effect or, more likely, rep-

resented a relict material in deflation zones (clast pavement on the surface of outwash fans, Kjær et al. 2004). Similarly, they could have been separately redeposited with snow and ice cover before their fluvial reincorporation into the sediment.

The studied PM contained few crystals or mineral phases, and zeolites with other secondary minerals were either rare or absent. The well packed to slightly cemented, friable lumps indicative of slightly hardened surfaces (or laminae formed originally close under the surface) contain a small amount of secondary minerals, but even the smallest glass shards in these lumps still have very fresh appearances (Oskarsson et al. 2012). The studied suspended particulates are considerably more uniform than the more diversified, reworked sediment units which characterize other parts of the Mælifellssandur plain and which have been reported as typical for most of the jökulhlaup outwash fans or plains in general (Maizels 1997, Krüger et al. 2010).

Climate implications and health effects

Suspended glaciogenic dust contains substantial numbers of close-to-ultrafine particles which are sharp-tipped, curved, concave, and which contain bubbles. These physical properties allow the dust to be quickly suspended. Iceland is a region with high wind velocities, large desert and ice-proximal areas, favouring dust production. The country is therefore prone to dust generation and frequent, severe dust events. As a result, Iceland is a substantial source of dust on a global level, with particles being transported distances >1000 km from the dust sources during the largest dust events (Arnalds 2010, Navratil et al. 2013). Icelandic cyclones are associated with the uplift of the surface air to the upper troposphere while the tropopause location is lower in altitude than at more southern latitudes, at about 8 km in height. This suggests that Icelandic aerosol can be transported into the stratosphere as well (Rose et al. 2006, Roesli 2008), where the residence time is prolonged up to several weeks. Due to its dark colour, the dust can act as an absorbing aerosol and become an important radiative forcing agent (Meinander et al. 2014). Rose et al. (2006) described the non-volatile portion of the 2000 Hekla eruption particulates, transported to a 10 km altitude to the 75°N latitude in the Greenland Sea, as 'heated aerosols'. Further observations are needed to estimate any direct and indirect effects of Icelandic dust aerosol on Arctic warming. A warming climate with retreating glaciers will result in larger sandy deserts in Iceland, and a warmer climate will also enhance the radiative forcing effect over these dark surfaces.

The fine mineral dust from Mælifellssandur could affect human health because it is often transported towards the capital of Iceland, Reykjavik. A high amount of bioavailable metals in respirable dust increases the inflammatory capacity of PM, which may lead to negative health effects (Morman & Plumlee 2013). Perez et al. (2008) found that the effect of $PM_{2.5-10}$ on mortality rose from 5.0% to 8.4% when an additional 10 μg m^{-3} of metal-rich Saharan dust was present in the atmosphere. Mælifellssandur dust has a 2.4 times higher content of metals than Saharan dust and the mean PMC_{10} was > 180 μg m^{-3} above the health limit of 50 μg m^{-3} (Althingi, 2002). The maximum PMC_{10} was about 30 times above the health limit at the dust source, but we need to emphasize here that this event was very short. However, the PMCs we measured at the dust source are commonly reached at the few stations that measure particulate matter in Iceland, such as in Reykjavik, where PMC_{10} often reaches >100 μg m^{-3} (Thorsteinsson et al. 2011). In vitro studies of Icelandic ash exposure on immune system biomarkers in lung cells found that biomarkers were increased (Horwell et al. 2013) and responses to bacteria were suppressed (Monick et al. 2013).

CONCLUSIONS

Here we introduced the first comprehensive study of the physical and chemical properties

of the Icelandic dust aerosol measured directly within a dust source. This suspended glaciogenic dust contained high concentrations of close-to-ultrafine particles which were sharp-tipped and contained bubbles. The material consisted mostly of volcanic glass rich in iron and titanium. Particles of such morpho-textural characteristics are prone to suspension despite meteorological conditions such as moist surface or low wind. The surface heating of a relatively dark basaltic dust source allows mobilization of moist particles within several hours. The close-to-ultrafine particles have a significant impact on the total particle number concentrations and are likely to contribute to the commonality of Icelandic dust events. PNCs during dust events are comparable to that measured during volcanic eruptions indicating that large Icelandic dust events might have similar-scale impacts on climate. High PNCs were, however, measured at the source and the proportion of smaller particles will increase travel distance from the source while particle surface characteristics may change with time and distance due to leaching. This study brings new scientific findings in the field of dust physics and cryosphere-atmosphere interactions, which should serve as a platform for climate modelling and projections of future changes in climate. We emphasize that further work on the nature of Icelandic dust sources is needed.

ACKNOWLEDGEMENTS

This study is dedicated to Professor Martin Branis († 27 September 2013) from the Charles University in Prague, Czech Republic. The work was supported by the Nordic Centre of Excellence for Cryosphere-Atmosphere Interactions in a Changing Arctic Climate (CRAICC), the Eimskip Fund of The University of Iceland and the FUTUREVOLC funded by the FP7 Environment Programme of the European Commission. The Czech geological team gratefully acknowledges the support of the institute research plan RVO 67985831 and are grateful to Sarka Jonasova, Anna Kallistova and Jaroslava Jaburkova, who were of technical assistance.

REFERENCES

Althingi 2002. *Reglugerð um brennisteinsdíoxíð, köfnunarefnisdíoxíð og köfnunarefnisoxíð, bensen, kolsýring, svifryk og blý í andrúmsloftinu og upplýsingar til almennings [Regulatons on the surface concentration of SO_2, NO_2, CO_2, PM and Pb and information to the public]*. Accessed 11.02.2014 at: http://www.reglugerd.is/interpro/dkm/WebGuard.nsf/key2/251-2002. [In Icelandic]

Arnalds O 2010. Dust sources and deposition of aeolian materials in Iceland. *Icelandic Agricultural Sciences* 23, 3–21.

Arnalds O, Gisladottir FO & Sigurjonsson H 2001. Sandy Deserts of Iceland: An overview. *Journal of Arid Environments* 47, 359-371.

Arnalds O, Gisladottir FO & Orradottir B 2012. Determination of aeolian transport rates of volcanic soils in Iceland. *Geomorphology* 167-168, 4-12.

Arnalds O, Thorarinsdottir EF, Thorsson J, Dagsson-Waldhauserova P & Agustsdottir AM 2013. An extreme wind erosion event of the fresh Eyjafjallajökull volcanic ash. *Nature Scientific Reports* 3, 1257.

Aston SR, Chester R, Johnson LR & Padgham RC 1973. Eolian dust from the lower atmosphere of the eastern Atlantic and Indian Oceans, China Sea and Sea of Japan. *Marine Geology* 14, 15-28.

Blechschmidt AM, Kristjansson JE, Olafsson H, Burkhart JF & Hodnebrog Ø 2012. Aircraft-based observations and high-resolution simulations of an Icelandic dust storm. *Atmospheric Chemistry and Physics Discussion* 12, 7949-7984.

Boygle JE 1994. *Tephra in lake sediments: An unambiguous geochronological marker?* Unpublished PhD. thesis. University of Edinburgh, 227 p.

Bullard JE 2013. Contemporary glacigenic inputs to the dust cycle. *Earth Surface Processes and Landforms* 38, 71-89.

Chepil WS & Woodruff NP 1957. Sedimentary characteristics of dust storms: II. Visibility and dust concentration. *American Journal of Science* 255, 104-114.

D'Almeida GA 1986. A model for Saharan dust transport. *Journal of Climate and Applied Meteorology* 25, 903-916.

Dagsson-Waldhauserova P, Arnalds O & Olafsson H 2013a. Long-term frequency and characteristics of dust storm events in Northeast Iceland (1949-2011). *Atmospheric Environment* 77, 117-27.

Dagsson-Waldhauserova P, Arnalds O & Olafsson H 2013b. Long-term variability of duststorms in Iceland. *Geophysical Research Abstracts* 15, EGU2013-11578-1.

Dagsson-Waldhauserova P, Arnalds O & Olafsson H 2013c. Long term dust aerosol production from natural sources in Iceland. *Journal of the Air & Waste Management Association.* DOI:10.1080/10962247.2013.805703.

Harrison RM & Yin J 2000. Particulate matter in the atmosphere: Which particle properties are important for its effects on health? *Science of the Total Environment* 249, 85–101.

Horwell CJ, Baxter PJ, Hillman SE, Calkins JA, Damby DE & Delmelle P 2013. Physicochemical and toxicological profiling of ash from the 2010 and 2011 eruptions of Eyjafjallajökull and Grímsvötn volcanoes, Iceland using a rapid respiratory hazard assessment protocol. *Environmental Research* 127, 63–73.

Jayaratne R, Johnson G, McGarry P, Cheung H-C & Morawska L 2011. Characteristics of airborne ultrafine and coarse particles during the Australian dust storm of 23 September 2009. *Atmospheric Environment* 45, 3996-4001.

Kekonen T, Moore J, Perämäki P & Martma T 2005. The Icelandic Laki volcanic tephra layer in the Lomonosovfonna ice core, Svalbard. *Polar Research* 24, 33–40.

Kjær KH, Sultan L, Krüger J & Schomacker A 2004. Architecture and sedimentation of outwash fans in front of the Mýrdalsjökull ice cap, Iceland. *Sedimentary Geology* 172, 139–163.

Krüger J, Schomacker A & Benediktsson IO 2010. Ice-marginal environments: Geomorphic and structural genesis of marginal moraines at Mýrdalsjökull. In Kjær KH, Krüger J & Schomacker A (eds.) *The Mýrdalsjökull Ice Cap, Iceland: Glacial processes, sediments and landforms on an active volcano*. Elsevier Science Publishers BV, Amsterdam, pp. 79–104.

Larsen G 2000. Holocene eruptions within the Katla volcanic system, south Iceland: Characteristics and environmental impact. *Jökull* 49, 1–28.

Leadbetter SJ, Hort MC, von Löwis S, Weber K & Witham CS 2012. Modeling the resuspension of ash deposited during the eruption of Eyjafjallajökull in spring 2010. *Journal of Geophysical Research* 117, D00U10. DOI: 10.1029/2011JD016802.

Maizels J 1997. Jökulhlaup deposits in proglacial areas. *Quaternary Science Reviews* 16, 793–819.

Meinander O, Kontu A, Virkkula A, Arola A, Backman L, Dagsson-Waldhauserova P, Jarvinen O, Manninen T, Svensson J, de Leeuw G & Lepparanta M 2014. Brief Communication: Light-absorbing impurities can reduce the density of melting snow. *The Cryosphere Discussion* 8, 259-271.

Monick MM, Baltrusaitis J, Powers LS, Borcherding JA, Caraballo JC & Mudunkotuwa I 2013. Effects of Eyjafjallajökull volcanic ash on innate immune system responses and bacterial growth in vitro. *Environmental Health Perspectives*. *Environmental Health Perspectives* 121, 691-698.

Morman SA & Plumlee GS 2013. The role of airborne mineral dusts in human disease. *Aeolian Research* 9, 203–12.

Navratil T, Hladil J, Strnad L, Koptikova L & Skala R 2013. Volcanic ash particulate matter from the 2010 Eyjafjallajokull eruption in dust deposition at Prague, central Europe. *Aeolian Research* 9, 191-202.

Nickling WG 1978. Eolian sediment transport during dust storms: Slims River Valley, Yukon Territory. *Canadian Journal of Earth Sciences* 15, 1069-1084.

NILU Norwegian Institute for Air Research 2013. *The Zeppelin observatory at Svalbard*. Accessed 21.11.2013 at http://www.nilu.no/Milj%C3%B8overv%C3%A5kning/Zeppelinobservatoriet/tabid/214/language/en-GB/Default.aspx.

Oladottir B, Larsen G, Thordarson T & Sigmarsson O, 2005. The Katla volcano S-Iceland: Holocene tephra stratigraphy and eruption frequency. *Jökull* 55, 53–74.

Oladottir B, Larsen G & Sigmarsson O, 2011. Holocene volcanic activity at Grímsvötn, Bárðarbugna and Kverkfjöll subglacial centres beneath Vatnajökull, Iceland. *Bulletin of Volcanology* 73,1187-1208.

Oskarsson BV, Riishuus MS & Arnalds O 2012. Climate-dependent chemical weathering of volcanic soils in Iceland. *Geoderma* 189, 635–651.

Perez L, Tobias A, Querol X, Künzli N, Pey J & Alastuey A 2008. Coarse particles from Saharan dust and daily mortality. *Epidemiology* 19, 800–807.

Roesli HP 2008. *Winds from ex-hurricane Ike give rise to a remarkable dust cloud over Iceland.* Accessed 19.02.2014 at http://www.eumetsat.int/website/home/Images/ImageLibrary/DAT_IL_08_09_17.html;jsessionid=D1PPTGZC3q8cQfhsYVpTLCkQYzRjktLnw948PRw83Hmp-9cGTQJRl!-521040142.

Rose W, Millard GA, Mather TA, Hunton DE, Anderson B, Oppenheimer C, Thornton BF, Gerlach TM, Viggiano AA, Kondo Y, Miller TM & Ballenthin JO 2006. Atmospheric chemistry of a 33–34 hour old volcanic cloud from Hekla Volcano (Iceland): Insights from direct sampling and the application of chemical box modeling. *Journal of Geophysical Research* 111, D20206. DOI:10.1029/2005JD006872.

SEPA Scottish Environment Protection Agency 2011. *Grímsvötn volcano (Iceland) eruption May 2011: assessing the potential consequences of ash deposition in Scotland*. Accessed 10.11.2013 at http://www.sepa.org.uk/about_us/news/other/grimsvotn_volcanic_eruption.aspx.

Sigmarsson O, Vlastelic I, Andreasen R, Bindeman I, Devidal JL, Moune S, Keiding JK, Larsen G, Höskuldsson A & Thordarson T 2011. Remobilization of silicic intrusion by mafic magmas during the 2010 Eyjafjallajökull eruption. *Solid Earth* 2, 271–281.

Thordarson Th & Hoskuldsson A 2008. Postglacial volcanism in Iceland. *Jökull* 58,197-228.

Thorsteinsson Th, Gisladottir G, Bullard J & McTainsh G 2011. Dust storm contributions to airborne particulate matter in Reykjavík, Iceland. *Atmospheric Environment* 45, 5924-5933.

Tittarelli T, Borgini A, Bertoldi M, de Saeger E, Ruprecht A, Stefanoni R, Tagliabue G, Contiero P & Crosignani P 2008. Estimation of particle mass concentration in ambient air using a particle counter. *Atmospheric Environment* 42, 8543-8548.

Vogel A, Weber K, Fischer Ch, Pohl T, von Löwis S & Moser HM 2012. Ground based stationary and mobile in situ measurements of volcanic ash particles during and after the 2011 Grímsvötn volcano eruption on Iceland. Abstract VA-3 presented at 2012 *Volcanism and the Atmosphere conference*, AGU, Selfoss, Iceland, 10-15 Jun., 71-72.

Wang YQ, Zhang XY, Gong SL, Zhou CH, Hu XQ, Liu HL, Niu T & Yang YQ 2008. Surface observation of sand and dust storm in East Asia and its application in CUACE/Dust. *Atmospheric Chemistry and Physics* 8, 545-553.

Weber S, Kuttler W Weber & K 2006. Flow characteristics and particle mass and number concentration variability within a busy urban street canyon. *Atmospheric Environment* 40, 7565-7578.

Zhou B, Zhang L, Cao X, Li X, Huang J, Shi J & Bi J 2012. Analysis of the vertical structure and size distribution of dust aerosols over the semi-arid region of the Loess Plateau in China. *Atmospheric Chemistry and Physics Discussion* 12, 6113-6143.

Manuscript received 6 December 2013
Accepted 17 March 2014

Paper III

The Cryosphere, 8, 991–995, 2014
www.the-cryosphere.net/8/991/2014/
doi:10.5194/tc-8-991-2014

The Cryosphere
Open Access

Brief communication: Light-absorbing impurities can reduce the density of melting snow

O. Meinander[1], A. Kontu[2], A. Virkkula[1], A. Arola[3], L. Backman[1], P. Dagsson-Waldhauserová[4,5], O. Järvinen[6], T. Manninen[1], J. Svensson[1], G. de Leeuw[1,6], and M. Leppäranta[6]

[1]Finnish Meteorological Institute, Helsinki, Finland
[2]Arctic Research Center, Finnish Meteorological Institute, Sodankylä, Finland
[3]Kuopio Unit, Finnish Meteorological Institute, Kuopio, Finland
[4]University of Iceland, Department of Physics, Reykjavik, Iceland
[5]Agricultural University of Iceland, Faculty of Environment, Hvanneyri, Iceland
[6]Department of Physics, University of Helsinki, Helsinki, Finland

Correspondence to: O. Meinander (outi.meinander@fmi.fi)

Received: 20 November 2013 – Published in The Cryosphere Discuss.: 10 January 2014
Revised: 10 April 2014 – Accepted: 14 April 2014 – Published: 26 May 2014

Abstract. Climatic effects of black carbon (BC) deposition on snow have been proposed to result from reduced snow albedo and increased melt due to light-absorbing particles. In this study, we hypothesize that BC may decrease the liquid-water retention capacity of melting snow, and present our first data, where both the snow density and elemental carbon content were measured. In our experiments, artificially added light-absorbing impurities decreased the density of seasonally melting natural snow. No relationship was found in case of natural non-melting snow. We also suggest three possible processes that might lead to lower snow density.

1 Introduction

For seasonal snow, snow melting is an important part of the natural annual hydrological cycle. It is forced by atmospheric sensible heat flux and solar radiation, where the albedo is a critical factor due to its large variability. Snow albedo depends primarily on the grain size, wetness, impurities in the near-surface snow layer, and directional distribution of the down-welling irradiance. Deposition of anthropogenic emissions to snow cover potentially causes albedo changes. In terms of its climate forcing, black carbon (also known as light-absorbing aerosol) has been hypothesized to be the second most important human emission, and only carbon dioxide is estimated to have a greater forcing (Bond et al., 2013). The climatic effects of black carbon (BC) in snow are due to reduced snow albedo caused by absorption of solar radiation, and induced melt of darker snow, which again lowers the albedo via the albedo feedback mechanism (e.g. Warren and Wiscombe, 1980; Doherty et al., 2010).

Snow melt starts when snow temperature reaches the melting point. Then, if the heating continues, the volume of liquid water increases until the holding capacity or the saturation point of liquid water is reached. This capacity is 3–5 % on a mass basis and depends on snow grain structure and packing (DeWalle and Rango, 2008). When the flow of melt water begins, the impurities may either be washed down through the snow with the flow, or remain in the snow. It has been shown that BC is less likely to be washed down through the snow with melt water (Conway et al., 1996; Doherty et al., 2013).

Hence, if we consider natural snow with anthropogenic BC, we can assume this impurity to remain in the melting snowpack, not to be washed down, and to potentially cause changes in the snow properties and structure, as compared to clean snow. Therefore, we hypothesize that BC in snow might affect the liquid-water retention capacity of melting snow. To test this hypothesis, we use our data of cold and melting snow, where both the snow density and BC content were measured.

2 Materials

All our snow density and BC data have been obtained for natural seasonally melting snow in Sodankylä (67°25′ N, 26°35′ E), Finland, north of the Arctic Circle. By natural snow we refer to a snow pack that has formed from snowfall (i.e. has not been produced by a snow cannon, and has not been affected by human activity, e.g. snow clearing). The data contain cases of cold and melting snow, both with and without experimentally added impurities (Table 1).

The cold snow samples were snow on a lake (17 March 2009), various sites around the Sodankylä area (13 and 19 March 2009 and 23–24 March 2010), and a fenced experimental field (6 and 10 April 2013). The melting snow data were from the experimental field only (17–18 April 2013 before and after rain).

The data originate from three campaigns: the Soot on Snow experiment in 2013 (SoS-2013); the Snow Reflectance Transition Experiment (SNORTEX 2008–2010, see Meinander et al., 2013 for more details); and the SnowRadiance-campaign (SR-2009). The SoS-2013 campaign was carried out at the Sodankylä airport to study the effects of deposition of impurities on surface reflectance, albedo and melt of seasonal snow. The experimental area was a large, flat, fenced open space, and the gravel ground was not covered with concrete or asphalt (Fig. 1). Different amounts of impurities were deposited to snow on different spots, each with diameter of 4 m, and thereafter the spots were monitored until the snow had melted. The sites were left to develop naturally, introducing as little disturbance as possible. Here we used data from three experimental spots with chimney soot, one spot with Icelandic volcanic sand from Ólafur Arnalds (Agricultural University of Iceland) and Haraldur Olafsson (University of Iceland), and one reference spot.

The SnowRadiance (SR) was an ESA-funded project aiming at determining snow properties from optical satellite measurements. The BC samples were collected from the snow over ice on Lake Orajärvi. The lake is frequently used in the winter, e.g. for snowmobiling.

During the SoS-2013, the SNORTEX-2009, and the SR-2009 campaigns, surface snow samples were collected for analysis of their elemental carbon (EC) and organic carbon (OC) concentrations using the filter-based thermal-optical method, described and used in, for example, Forsström et al. (2009). The EC is used as a proxy of BC, due to the measurement technique used. In the SNORTEX-2010 campaign, the sampling, filtering, and laboratory spectrometer analysis followed the procedures presented in Doherty et al. (2010). Several samples were collected from each location.

The snow densities (weight per volume) were measured manually, for either the whole snowpack vertical column (snow tube for SR and SNORTEX data), or for separate horizontal snow layers (density cutter for SoS data to measure the density of the visually dirty surface snow). One density measurement for each location was made. To estimate the standard deviation of the density measurement, an earlier data set of FMI was applied. Sampling of wet snow for density measurements may be difficult since liquid water easily escapes from the sampling box. Here the SoS data for melting snow was obtained for two subsequent days (Table 1), before and after rainfall. The snow was then wet, but not dripping wet, and no water escape from sampling was detected.

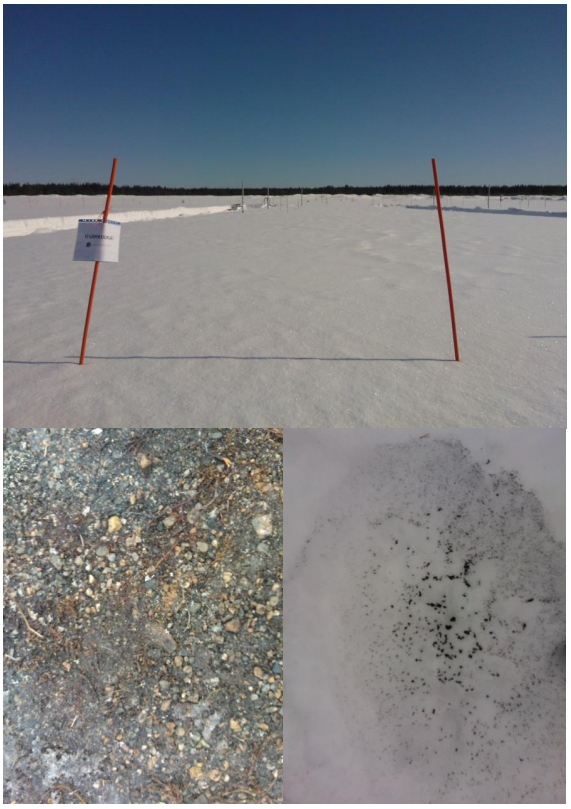

Figure 1. The SoS-2013 experiment. **(a)** Top: the flat and open experimental field with the seasonal snow pack; **(b)** bottom left: the ground under the snow, i.e. a natural gravel surface, not covered by concrete or asphalt, offered an uniform surface for the snow cover; **(c)** bottom right: previously added impurities were visible on the surface of the melting snow, here volcanic sand.

In the SoS-2013 data, snow hardness, grain sizes, and grain shapes were estimated and classified according to the International Classification for Seasonal Snow on the Ground (Fierz et al., 2009).

3 Results

In our data for non-melting natural snow from the SR-2009, SNORTEX-2009, SNORTEX-2010 and SoS-2013 campaigns, the BC concentrations varied between 8 and 126 ppb, and snow densities were 200–264 $\mathrm{kg\,m^{-3}}$. The density did not depend on the BC content (Fig. 2a, the dots inside the circle).

Table 1. The origin of our Sodankylä snow density data coupled with BC analysis results. The campaigns are explained in the text.

Year	Date	Data origin	Location	Snow	Artificial impurities	BC analysis
2009	17 Mar	SR campaign	Snow on lake Orajärvi	Cold snow	No	Thermal-optical
2009	13, 19 Mar	SNORTEX	Sodankylä area	Cold snow	No	Thermal-optical
2010	23, 24 Mar	SNORTEX	Sodankylä area	Cold snow	No	Spectrometer (Doherty et al., 2010)
2013	6, 10 Apr	SoS-2013	Sodankylä airport	Cold snow	Yes	Thermal-optical
2013	17 Apr	SoS-2013	Sodankylä airport	Melting, before rain	Yes	Thermal-optical
2013	18 Apr	SoS-2013	Sodankylä airport	Melting, after rain	Yes	Thermal-optical

However, in our SoS-experiment data of 6 April 2013, the snow with the BC maximum of 1465 ppb (Fig. 2a, one data point for wood burning soot), had the lowest density of all our data, 168 kg m^{-3}. MFcr-grains (melt–freeze crust, as a result of melting and freezing) were 0.25–1.5 mm in diameter, the surface hardness value was 4 (hard snow) and the snow depth was 56 cm. For comparison, with the reference non-sooted natural snow at that time (10 April 2013) on the same experimental field: the Ppir-grains (Precipitation particles) were irregular crystals, of 0.25–0.75 mm in diameter. The BC concentration was 126 ppb, the density was 210 kg m^{-3}, the hardness value was 1 (very soft snow), and the snow depth was 65 cm.

Our experimental data show that for the seasonally melting natural Arctic snow, with and without artificially added soot or volcanic ash, there was a correlation between the density and the BC content of snow (Fig. 2b). This was the case both prior to a rain period, and the next day after the rain. The densities and the corresponding BC contents were measured separately for the top 5 cm of the snow, not for the whole snow pack, and the impurities of volcanic sand, soot from oil burner and wood burning soot were visually observed to remain on the snow surface, too (Fig. 1). All the grains of the surface layer were melt–freeze crust (MFcr).

The BC concentrations in individual snow samples varied from 9 to 730 ppb. From these, the averages for each experimental spot were calculated (92–310 ppb), and plotted in Fig. 2b. The standard deviation (σ) for the clean reference snow samples (no added impurities) was 34 ppb ($n = 7$), and most often σ was larger for spots with added impurities, dependent on the number of samples (from 1 to 5) and the spot properties; e.g. for one spot with added soot, it was $\sigma = 28$ ppb ($n = 5$). The Eq. (1) shows the relation between the snow density ρ_s [kg m^{-3}], and the BC content C_{BC} [ppb] for the melting snow derived from the SoS-2013 data ($R^2 = 0.66$):

$$\rho_s = -0.27 C_{BC} + 440.6, \quad (1)$$

where $C_{BC} = [92,310]$ ppb. The 95 % confidence interval of the slope of the Eq. (1) is from -0.46 to -0.08, that is, we are 95 % confident that the true slope of this equation is in the range defined by -0.27 ± 0.19.

For the snow density, we had one measurement for each location. Therefore, using a previous FMI Sodankylä snow density data set (unpublished data), the average standard deviation was determined, providing a value of 17 kg m^{-3} ($n = 79$ pairwise measurements, $n_{tot} = 158$, $\rho_s = [104,408]$ kg m^{-3}) for the Sodankylä data.

4 Discussion and conclusions

All our data of cold snow and melting snow represent the natural seasonal snow cover in Sodankylä, north of the Arctic Circle. For the cold snow, the density was 200–264 kg m^{-3} with BC 8–126 ppb. Our experimental results for an excessive (1465 ppb) amount of added BC (wood-burning soot) show a reduction of the cold snow density. This result is based on comparison of one sooted vs. one reference spot only; more data are needed to confirm this result. Earlier, Meinander et al. (2013) reported on a larger data set (their Table 3), where the snow BC content, in Sodankylä snow cover in 2009–2011, varied in one sampling location between 9 and 106 ppb in the natural snow cover. Thus, our cold snow data presented here represents well the natural BC variability in Sodankylä.

Artificially added impurities in our experiments on natural snow decreased the snow density of melting snow (Fig. 2, Eq. 1). Moreover, the densities were measured both prior to and after rainfall (4.9 mm water in 3 h), which occurred between two subsequent measurement days. In both cases, the larger the BC content, the smaller the density. Thus the rain did not change this order, which further supported our hypothesis that the impurities may affect the water retention capacity. Furthermore, according to our recent laboratory experiment (unpublished data), we found that snow with artificially added soot released melt water sooner than snow without added soot. For this experiment, we added a known amount of soot to a snow sample, mixed the soot and snow, and let the snow melt indoors, while measuring the melt water on a drip pan as a function of time. The results showed

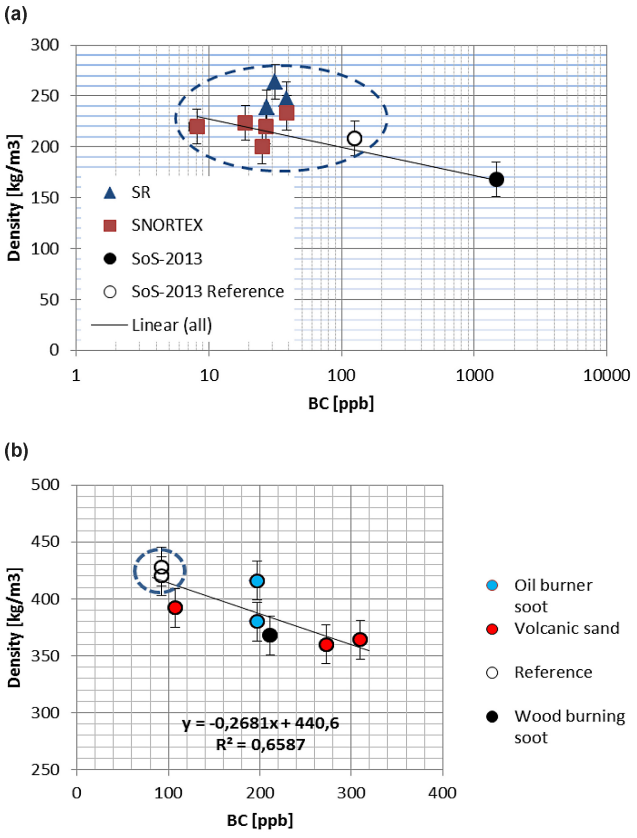

Figure 2. The black carbon (BC) content [ppb] vs. density [kg m^{-3}] for the natural seasonal snow cover in Sodankylä, north of the Arctic Circle with and without artificially added impurities. The line is the least squares linear fit through all the points. **(a)** Cold snowpack: for natural snow without added impurities, BC concentrations were 8–126 ppb, and snow densities were 200–264 kg m^{-3} and for the reference SoS-2013 spot BC was 126 ppb and the snow density was 210 kg m^{-3} (within the circle); when wood-burning soot was artificially deposited to this SoS-spot, BC in snow was measured to be 1465 ppb, and snow density decreased to 168 kg m^{-3} (outside the circle). **(b)** Melting snow: SoS-2013 data for reference spots (within the circle), and spots with artificially added impurities of volcanic sand, soot from oil burner and wood burning soot (outside the circle). The densities and corresponding carbon contents were measured separately for the specified surface layers, not for the entire snow pack.

that while the control snow started to release melt water after 40 min, the snow with added soot released melt water already after 12 min. When cold water was added on snow, the control snow released water after 29 min, while the same amount of water in sooted snow caused water to release already after 7 min. All the snow samples were of the same size (same weight and volume) representing the same natural snow, and mechanically treated the same way whether soot was added or not, for example, the control snow was also mixed although no soot was added. Hence, these new experimental data were found to support our hypothesis that BC may decrease the liquid-water retention capacity of melting snow.

As a summary, according to our experience and observations, we suggest three possible processes that might lead to the lower snow density:

1. *A semi-direct effect of absorbing impurities*. Absorbing impurities would cause melt and/or evaporation from the liquid phase and sublimation from the solid phase of the surrounding snow, resulting in air pockets around the impurities, and thus lower snow density. We have empirical observations, where impurities (both organic and inorganic) in the snow have been surrounded by air pockets.

2. *BC effect on the adhesion between liquid water and snow grains*. If BC reduces adhesion, the liquid-water holding capacity decreases. For linear warming the influence on the density of wet snow is then max 5 % (at this level water flow starts in natural snow). However, with daily cycles, warm days and cold nights, the weaker adhesion may push liquid water down more day-by-day and then the influence to the density would be larger. This way also melt–freeze metamorphosis would produce less dense snow.

3. *BC effect on the snow grain size.* Absorbing impurities would increase the melting and metamorphosis processes, resulting in larger snow grains, which would lower the water retention capacity. Earlier, Yamaguchi et al. (2010) have suggested that the water retention curve of snow could be described as a function of grain size using soil physics models. Here our data showed some slight indication for the possibility of soot in snow to result in larger snow grain sizes via increased melt and metamorphosis, and our data did not show clear evidence against this possibility.

Volcanic sand is assumed not to contain BC (Dadic et al., 2013, Fig. 12a). This assumption is further supported by our own EC analysis of volcanic sand samples with the thermal – optical method showing hardly any EC. Instead, the BC in our volcanic sand spot can be assumed to originate either from long-range transport, or from our other experimental spots with added soot; carbonaceous material in volcanic aerosols has also been proposed to be due to tropospheric air that is entrained into the volcanic jet and plume (Andersson et al., 2013). Our observations and measurements indicate that for a visually darker snow surface, the analyzed BC content is larger and the measured snow density is smaller, regardless of whether soot or volcanic sand had been added to the spot.

The significance of our results on reduction of snow density, and possibly also decreasing water holding capacity due to the black carbon, may be due to the fact that (i) snow density is an important snow parameter that has been found to

correlate with several factors affecting the snow melt, such as snow age and liquid-water holding capacity (Kuusisto, 1984); (ii) snow density multiplied by snow depth equals the important climate model parameter of snow water equivalent (SWE); and (iii) our results may have potential in reducing the uncertainties (IPCC, 2013) related to the effect of black carbon on snow melt and climate change.

In nature, the low density of new dry snow increases due to gravitational settling, wind packing, sintering, and melt–freeze events. These processes depend on the grain size, shape and organization, and snow temperature. The density of snow is also affected by water vapour diffusion in the snow pack, as well as by the temperature and the vegetation under the snow. In our experimental data, we can assume similar environmental conditions with only the impurity contents in snow being the varying factor; our results are for natural snow on natural ground, and we did not have data for drainage of melt water in the snowpack. Here we reported our first results, and more data are needed to further study the effect of light-absorbing impurities on density and water retention capacity of melting snow.

Acknowledgements. The authors thank all the participants of the campaigns of SoS-2013, SNORTEX-2010, SNORTEX-2009 and SR-2009, especially Antti Aarva. Filters from the 2010 snow samples were analyzed for BC by S. Doherty. We gratefully acknowledge support from the Academy of Finland (A4-project), and the Nordic Center of Excellence (NCoE), Nordic Top Research Initiative "Cryosphere-atmosphere interactions in a changing Arctic climate" (CRAICC), and the EU Life+ project Mitigation of Arctic warming by controlling European black carbon emissions, MACEB (project no. LIFE09 ENV/FI/000572).

Edited by: M. Boy

References

Andersson, S. M., Martinsson, B. G., Friberg, J., Brenninkmeijer, C. A. M., Rauthe-Schöch, A., Hermann, M., van Velthoven, P. F. J., and Zahn, A.: Composition and evolution of volcanic aerosol from eruptions of Kasatochi, Sarychev and Eyjafjallajökull in 2008–2010 based on CARIBIC observations, Atmos. Chem. Phys., 13, 1781–1796, doi:10.5194/acp-13-1781-2013, 2013.

Bond, T. C., Doherty, S. J., Fahey, D. W., Forster, P. M., Berntsen, T., DeAngelo, B. J., Flanner, M. G., Ghan, S., Kärcher, B., Koch, D., Kinne, S., Kondo, Y., Quinn, P. K., Sarofim, M. C., Schultz, M. G., Schulz, M., Venkataraman, C., Zhang, H., Zhang, S., Bellouin, N., Guttikunda, S. K., Hopke, P. K., Jacobson, M. Z., Kaiser, J. W., Klimont, Z., Lohmann, U., Schwarz, J. P., Shindell, D., Storelvmo, T., Warren, S. G. and Zender, C. S.: Bounding the role of black carbon in the climate system: A scientific assessment, J. Geophys. Res.-Atmos., 118, 5380–5552, doi:10.1002/jgrd.50171, 2013.

Conway, H., Gades, A., and Raymond, C. F.: Albedo of dirty snow during conditions of melt, Water Resour. Res., 32, 1713–1718, 1996.

Dadic, R., Mullen, P. C., Schneebeli, M., Brandt, R. E., and Warren, S. G.: Effects of bubbles, cracks, and volcanic tephra on the spectral albedo of bare ice near the Transantarctic Mountains: Implications for sea glaciers on Snowball Earth, J. Geophys. Res.-Earth, 118, 1658–1676, doi:10.1002/jgrf.20098, 2013.

DeWalle, D. R. and Rango, A.: Principles of snow hydrology, Cambridge University Press, Cambridge, UK, 2008.

Doherty, S. J., Warren, S. G., Grenfell, T. C., Clarke, A. D., and Brandt, R. E.: Light-absorbing impurities in Arctic snow, Atmos. Chem. Phys., 10, 11647–11680, doi:10.5194/acp-10-11647-2010, 2010.

Doherty, S. J., Grenfell, T. C., Forsström,S., Hegg, D. L., Brandt, R. E., and Warren, S. G.: Observed vertical redistribution of black carbon and other insoluble light-absorbing particles in melting snow, J. Geophys. Res.-Atmos., 118, 5553–5569, 2013.

Fierz, C., Armstrong, R. L., Durand, Y., Etchevers, P., Greene, E., McClung, D. M., Nishimura, K., Satyawali, P. K. and Sokratov, S. A.: The International Classification for Seasonal Snow on the Ground, IHP-VII Technical Documents in Hydrology No. 83, IACS Contribution No. 1, UNESCO-IHP, Paris, 2009.

Forsström, S., Ström, J., Pedersen C. A., Isaksson, E., and Gerland, S.: Elemental carbon distribution in Svalbard snow, J. Geophys. Res., 114, D19112, doi:10.1029/2008JD011480, 2009.

IPCC, "Climate Change 2013: The Physical Science Basis. Working Group I Contribution to the IPCC 5th Assessment Report – Changes to the Underlying Scientific/Technical Assessment" (IPCC-XXVI/Doc.4), http://www.ipcc.ch/report/ar5/wg1/ (last access: 22 May 2014), 2013.

Kuusisto, E.: Snow accumulation and snowmelt in Finland. Publications of the Water Research Institute, National Board of Waters, Finland, No. 55, 149 pp., 1984.

Meinander, O., Kazadzis, S., Arola, A., Riihelä, A., Räisänen, P., Kivi, R., Kontu, A., Kouznetsov, R., Sofiev, M., Svensson, J., Suokanerva, H., Aaltonen, V., Manninen, T., Roujean, J.-L., and Hautecoeur, O.: Spectral albedo of seasonal snow during intensive melt period at Sodankylä, beyond the Arctic Circle, Atmos. Chem. Phys., 13, 3793–3810, doi:10.5194/acp-13-3793-2013, 2013.

Warren, S. G. and Wiscombe, W. J.: A model for the spectral albedo of snow. II: Snow containing atmospheric aerosols, J. Atmos. Sci., 37, 2734–2745, 1980.

Yamaguchi, S. Katsushima, T., Sato, A., and Kumakura, T.: Water retention curve of snow with different grain sizes, Cold Reg. Sci. Technol., 64, 87–93, doi:10.1016/j.coldregions.2010.05.008, 2010.

Paper IV

Biogeosciences Discuss., 11, 5941–5967, 2014
www.biogeosciences-discuss.net/11/5941/2014/
doi:10.5194/bgd-11-5941-2014

Biogeosciences Discussions Open Access

Quantification of iron-rich volcanogenic dust emissions and deposition over ocean from Icelandic dust sources

O. Arnalds[1], H. Olafsson[2,3,4], and P. Dagsson-Waldhauserova[1,2]

[1]Agricultural University of Iceland, Hvanneyri, 311 Borgarnes, Iceland
[2]University of Iceland, Reykjavik, Iceland
[3]The Icelandic Meteorological Office, Reykjavik Iceland
[4]Bergen School of Meteorology, Geophysical Institute, University of Bergen, Norway

Received: 27 February 2014 – Accepted: 7 April 2014 – Published: 28 April 2014

Correspondence to: O. Arnalds (oa@lbhi.is)

Published by Copernicus Publications on behalf of the European Geosciences Union.

Abstract

Iceland has extremely active dust sources that result in large scale emissions and deposition on land and sea. The dust has volcanogenic origin of basaltic composition with about 10 % Fe content. We used two independent methods to quantify dust emission from Iceland and dust deposition on sea. Firstly, aerial extent (map) of deposition on land was extended to ocean areas around Iceland. Secondly, survey of number of dust events over the past decades and calculations of emissions and sea deposition for the dust storms were made. The results show total emissions range from 30.5 (dust event based calculation) to 40.1 million tons (map calculation), which places Iceland among the most active dust sources on Earth. Ocean deposition ranges between 5.5 (dust events calculations) and 13.8 million tons (map calculation). Calculated iron deposition from Icelandic dust ranges between 0.56 to 1.4 million tons, which are distributed over wide areas (> 370 000 km^2) and consist of fine reactive volcanic materials. The paper provides the first quantitative estimate of total dust emissions and oceanic deposition from Iceland. Iron is a limiting nutrient for primary production in the oceans around Iceland and the dust is likely to affect Fe levels in Icelandic ocean waters.

1 Introduction

Dust emissions from barren areas have pronounced influences on Earth's terrestrial and oceanic ecosystems, the atmosphere, climate and human health (Field et al., 2010; Ayris and Delmelle, 2012a). Global estimates of mean annual dust emissions range from 500 to 5000 million tons per year with most estimates between 1000 and 2000 million tons, but the global oceans are commonly estimated to receive 300–500 million tons (reviewed by Engelstaedter et al., 2006). Dust production is mainly attributed to unstable barren areas in dry climates with northern Africa being the largest contributor of dust to the atmosphere (Engelstaedter et al., 2006). Other commonly cited dust sources include Mongolia (e.g., Natsagdorj et al., 2003), Aral Sea Basin (Singer et al.,

2003), Middle East (Jamalizadeh et al., 2008), Australia (Ekström et al., 2004; Leys et al., 2011) and southern USA (e.g., Sweeney et al., 2011). However, dust emissions from the Arctic and Antarctic have received increased attention (Arnalds, 2010; Bullard, 2013; Gillies et al., 2013; Muhs et al., 2013). Research shows frequent dust storms in South Iceland into the North Atlantic Ocean (Arnalds and Metúsalemsson, 2004; Prospero et al., 2012) and into the Arctic from Northeast Iceland (Dagsson-Waldhauserova et al., 2013a), and it has been suggested that Iceland is among the world's most active dust sources (Arnalds, 2010; Prospero et al., 2012; Blechschmidt et al., 2012; Bullard, 2013).

Volcanic eruptions have recently become a focus of attention due to possible global nutrient additions to the oceans, including significant iron inputs that are potentially important for primary production (e.g., Duggen et al., 2010; Olgun et al., 2011; Ayris and Delmelle, 2012a). Achterberg et al. (2013) measured significantly elevated iron levels south of Iceland during the 2010 Eyjafjallajökull eruption. Volcanic ash is commonly subjected to intense aeolian redistribution (see Arnalds, 2010, 2013; Ayris and Delmelle, 2012a; Bullard, 2013), as was witnessed after the 2010 Eyjafjallajökull eruption (Thorsteinsson et al., 2012). Furthermore, some glaciogenic Arctic dust sources are composed of iron rich volcanic deposits, such as in Iceland (Baratoux et al., 2011; Prospero et al., 2012; Dagsson-Waldhauserova et al., 2013b) and some parts of Alaska (Muhs et al., 2013). In Iceland, these aeolian materials are primarily poorly crystallized basaltic materials (glass) containing high quantities of iron, which can have a substantial impact on the ocean chemistry and fertility. The iron from dust has pronounced effects on the global carbon cycle and atmospheric CO_2 (Jickells et al., 2005; Mahowald et al., 2005; Misumi et al., 2014). Schulz et al. (2012) noted that little is known about the mechanics and quantities of dust deposition in the oceans, with large uncertainties of the iron contents available for marine phytoplankton.

In spite of the importance for the oceanic nutrient cycles, little is known how much volcanic material is blown to the oceans around Iceland. Here we present the first quantitative estimate of the total dust emissions from Iceland and the first quantitative

estimate of aeolian redistribution of the volcanic materials and iron to the ocean areas from Iceland. These estimates are based on: (i) number of dust-events generated from weather records over several decades throughout Iceland; (ii) numerical calculations of selected dust storms; (iii) modification and extension of established sedimentation rates on land to oceanic areas.

2 Setting: the Icelandic dust sources

Iceland is a volcanic island on the active Mid-Atlantic Ridge, with about 30 active volcanic systems with volcanic eruptions occurring every 3–5 years on average (Thordarson and Höskuldsson, 2008). About 10 % of the country is covered with glaciers, including the 8100 km^2 Vatnajökull Glacier (Fig. 1). Many active volcanoes are located under the glaciers, including the Katla volcanic system under Mýrdalsjökull Glacier, and the Grímsvötn and Bárdarbunga systems under the Vatnajökull Glacier (Fig. 1).

Glacial rivers bring heavy sediment loads, creating extensive glacio-fluvial outwash plains in many areas. These plains are often flooded during summer melt, leaving sediments on the surfaces that are extremely vulnerable to redistribution by wind (Fig. 2). Many of these areas have been identified as major dust plume sources or dust hotspots (Arnalds, 2010). Sandy deserts of Iceland are, however, much larger than these main dust plume sources, or about 15 000 km^2 in all, and most of these areas can emit dust during the highest intensity dry winds (see Arnalds, 2010). In addition to plume areas (hot spots) and the sandy areas in general, there can be periods of dust generation after deposition of ash from volcanic eruptions on poorly vegetated and barren land, as witnessed after the 2010 Eyjafjallajökull and 2011 Grímsvötn eruptions (Leadbetter et al., 2012; Arnalds et al., 2013). Furthermore, fluvial outburst events associated with eruptions under glacier can leave unstable sediments that result in frequent dust events (Prospero et al., 2012).

Most dust emission events in NE Iceland are driven by low sea level pressure (SLP) west of Iceland (and/or high SLP east of Iceland) which leads to warm geostrophic

southerly winds. Dust events in S Iceland are generally linked to reserved east-west SLP which turns to cold geostrophic Arctic winds (Björnsson and Jonsson, 2003; Dagsson-Waldhauserova et al., 2013a, b).

3 Methods

3.1 Dust event frequency

Visibility is an important indicator of dust event severity where dust concentration measurements are not available. Long-term frequency of atmospheric dust observations has been investigated in detail for NE Iceland (Dagsson-Waldhauserova et al., 2013a) and for the southern part of Iceland (Dagsson-Waldhauserova et al., 2013c) based on present weather observations at 8 weather stations in NE Iceland, 15 stations in S Iceland and 7 stations in NW Iceland. A dust day was defined as a day when at least one station observed at least one dust observation. For this study, we included synoptic codes 04-06 for "Visibility reduced by volcanic ashes", "Dust haze" and "Widespread dust in suspension in the air" into the criteria for dust observation (see Dagsson-Waldhauserova et al., 2013a for details). The most frequent were dust observations of "Suspended" and "Moderate suspended" dust (NE 73 %; S 52 %) with visibility 10–70 km, "Severe" and "Moderate haze" (NE 23 %; S 42 %) with visibility 1–10 km, and "Severe" and "Moderate" dust storm (NE 4 %; S 6 %) with visibility less than 1 km. The total number of dust days in Iceland, based on averages presented (Dagsson-Waldhauserova et al., 2013a, b), is 135 dust days per year on average in Iceland in 1949–2011. About 34 dust days were observed annually in NE Iceland and about 101 dust days annually in southern part of Iceland.

3.2 Calculated dust storm emissions and transport to oceanic areas

The estimation of dust transport was based on several sources of atmospheric data. Similar methodology has been used to calculate emissions from single storms by Leys

et al. (2011). The concentration of dust is based on: (i) observed visibility at manned weather stations; (ii) the horizontal extension of the dust plumes; and (iii) the representativeness of the visibility observations are estimated from MODIS satellite images. The winds in the atmospheric boundary-layer were estimated from ground-based and upper-air observations as well as numerical simulation, and the thickness of the boundary-layer was estimated from the upper-air observations and numerical simulations. The upper-air observations are made at 00:00 and 12:00 UTC at Keflavik, SW-Iceland and Egilsstaðir, E-Iceland. The numerical model, Harmonie (based on Arome, see Seity et al., 2011) was run with subgrid 1-D turbulence scheme based on Cuxart et al. (2000) with a horizontal resolution of 2.5 km. The simulations are based on initial and boundary-conditions from the operational suite of the ECMWF.

Four dust-storms originating at Dyngjusandur major dust source north of Vatnajökull (Fig. 1) were selected for estimation of the total transport of suspended dust. In all four storms, the visibility in the dust plume was observed and recorded, and the vertical, horizontal and temporal extension of the plume was estimated from the available data. For a 1–2 km thick convective boundary-layer the dust can be expected to be quite well mixed vertically after advection of about 100 km in 1–2 h. The sea front is located at 200 km from the dust source in NE Iceland and 140 km in east Iceland, but the window was calculated at about 90 km for NE direction (three storms) and 155 for the E direction (one storm), which is determined by the location of weather stations. The boundary-layer winds are typically 15–23 $m\,s^{-1}$ and the height of the boundary layer is of the order of 1–2 km. This may sound low, but it should be kept in mind that dust-storms occur typically in stable stratified flow and that there is limited heating from the ground due to little solar radiation in Iceland and short advection time of the air-mass over land. The selected storms all lasted less than 24 h. The calculated total amount emitted materials was from 215 000 to 384 000 tons. Materials transported as dust through the calculated window ranged from 75 000 to 160 000 tons in each storm (Table 1).

3.3 GIS-based dust deposition distribution

An aeolian deposition map for Iceland was presented by Arnalds in 2010. The map is based on soil metadata showing thicknesses between tephra layers (volcanic ash) of known age, main dry winds from each major dust source and landscape parameters downwind from the sources. This deposition illustrated on the map has close relationship with iron content measured in mosses which is primarily wind deposited (data and map published by Magnússon, 2013), fertility of ecosystems as reflected bird abundance (Gunnarsson et al., 2014), but also many basic soil parameters such as pH, organic content and clay formation (Arnalds, 2008, 2010). We have extended the map to oceanic areas and included categories for very low deposition furthest away and extreme deposition closest to the aeolian sources. The map now shows six broad categories of deposition in $g\,m^{-2}\,yr^{-1}$: (i) very low, 1–15 (added to the previous map of Arnalds, 2010); (ii) low, 10–50; (iii) medium, 25–100; (iv) high 75–250; very high (v) 250–500 $g\,m^{-2}\,yr^{-1}$ and (vi) and extreme, 500–800 $g\,m^{-2}\,yr^{-1}$ (added to the previous map). The map is presented in Fig. 3. Note that the deposition range for each class overlaps with the next. The highest class (extreme) is expected to receive > 800 $g\,m^{-2}\,yr^{-1}$ at some landscape positions. Mean deposition on glaciers was estimated at 400 g $m^{-2}yr^{-1}$ based on the deposition map. The aerial distribution of the deposition classes over sea is in part based on a number of satellite images (MODIS; Aqua and Terra) taken over the past decade. These images show plumes extending several hundred km south into the Atlantic Ocean and northeast into the Arctic Ocean. We expect that most of the dust settles relatively close to the source with a logarithmic drop in sedimentation with distance from the source (Fig. 4).

3.4 Iron content of the dust materials

The chemical composition of the major of sand sources can be determined from published materials. The common range for iron in Icelandic volcanic rocks is from 6.5 to 12.5 % with an average about 9.4 % judging from review data presented by Jakobsson

et al. (2008) (andesite and basalts). The Dyngjusandur plume source, the primary dust source in NE Iceland has 9.4 % Fe content, made of volcanic glass (Baratoux et al., 2011). The Hagavatn plume source has similar iron content, but is made of more crystalline basalt grains (Baratoux et al., 2011). Óladóttir et al. (2011) reported slightly lower Fe content in tephra for volcanic systems under Vatnajökull glacier (Bárdarbunga and Grímsvötn) or 9.2 %, based on a large number of determinations. Tephra from the Katla volcanic system under Mýrdalsjökull glacier has similar but slightly higher Fe contents, mostly 10–11 % (Óladóttir et al., 2008). The Katla, Grímsvötn systems are responsible for the majority of dust going south from Iceland, which is the majority of the Icelandic oceanic dust. Thus, in this paper we have selected the average of 10 % Fe in volcanic dust from Iceland.

4 Results

4.1 Dust quantities based on frequency and calculated emissions

We found that there are 135 dust storm events that occur on average in Iceland each year. However, some storms are unnoticed by weather stations, (north winds at the Mýrdalssandur and Skeidarársandur dust sources). The total emissions derived are 30.5 million tons per year over land and sea. Majority is deposited on land (25 million tons), while 5.6 million tons are deposited over sea, mostly from the south shore (Table 2). The emissions per medium storm are about 300 000 tons per storm according to these calculations, but "minor" storms of about 100 000 ton emissions are most frequent (75.6 annually).

The path of dust over land is much longer in NE Iceland, or 130–150 km from the Dyngjusandur major source, but shorter distances from other sandy areas. More is therefore deposited over land from NE Iceland and we estimate that only 10 % of dust emitted from the NE Iceland reaches the oceans, based on the calculations presented in Sect. 3.2, which gave transport through a window at 90–155 km distance of the order

of 75 000 to 160 000 tons in each storm (see Table 1). This drop in deposition rates with distance from the source is supported by the drop indicated by the deposition map (see graph in Fig. 4 above), but it is a conservative estimate of the proportion of dust materials reaching the sea in NE Iceland considering dust storm calculations presented in Table 1. Many of the major dust sources of South Iceland are located close to the shoreline (Fig. 1), and we estimate that 50 % of the dust emissions reach oceanic areas, which we consider a conservative estimate.

4.2 Total deposition on land and sea based on GIS deposition map

The results from the calculations of dust deposition on land and oceans around Iceland are presented in Table 3. There is a logarithmic drop in deposition with distance from the source. We used the lower 25 % percentile for deposition within each range, reflecting the logarithmic drop, as the areas increase in size away from the sources. The results show that about 40.1 million tons are deposited annually on land, glaciers and sea. This number compares to the 30.5 million tons of total emissions calculated from storm frequency and dust intensity. These results for the total emissions (40.1 vs. 30.5 million tons) are relatively comparable and provide the first estimate of total dust emissions from Icelandic dust sources.

About 14 million tons are deposited on about 370 000 km^2 ocean area according to the GIS deposition map, but about 26 million tons on about 103 000 km^2 on land (including glaciers). These map-based deposition values for land and glaciers (26 million tons) is very comparable to the 25 million tons calculated from number and the severity of storms for land. However, the map calculations indicate higher (14 million tons) deposition to oceans than the storm calculation method (5.5 million tons).

4.3 Oceanic iron deposition from Iceland

The values obtained from calculations of emissions on one hand (Sect. 3.1) and deposition based on the GIS map (Sect. 3.2.) give a range for probable rates of deposition to

the oceans, from 5.5 to 13.8 million tons, respectively. Using these numbers, it can be inferred that the total iron deposition to the oceans (about 1/10 of the weight), is about 0.5–1.4 million tons in total per year (Table 3). The Fe sediment rates vary immensely from 0.1–0.5 $g\,m^{-2}\,yr^{-1}$ for areas far from Iceland to > 13 $g\,m^{-2}\,yr^{-1}$ close to the southern shore. The last column in Table 3 shows an estimate of bioavailable Fe based on evidence presented by Achterberg et al. (2013) after the 2010 Eyjafjallajökull eruption (see Discussion). The bioavailable iron ranges from 0.02–0.1 $mg\,m^{-2}\,yr^{-1}$ far from the sources to 2.8–10 $mg\,m^{-2}\,yr^{-1}$ closest to the sources in South Iceland. Maximum numbers of > 50 $mg\,m^{-2}\,yr^{-1}$ can be expected in localized areas.

5 Discussion

5.1 Total dust emissions from Iceland

Our research indicates that total emissions of dust from Icelandic dust sources are of the range 30 to 40 million tons annually, with the majority of the sediments deposited on land. The two different values reflecting this range are obtained by independent methods, but are, however, in relatively good agreement. The deposition rates used for obtaining the total emissions from the GIS map are in good agreement with local and regional deposition values reviewed by Lawrence and Neff (2009), especially close to the sources. More uncertainties are in the values far from the sources with deposition rates as low as 1 $g\,m^{-2}\,yr^{-1}$, with large areal extent. Judging from the difference between the calculated deposition (from number of events and their severity), and extending the aeolian deposition map, it is likely that deposition on distant sources is somewhat overestimated. Data for deposits on land acquired for the construction of the deposition map is also less reliable for those areas (thin deposits and fewer ash-layer markers).

The uncertainties associated with quantifying each of the storms and amount carried to the sea are several. Horizontal extension of the windstorms and their duration is

estimated to be of the order of 10–20 %, while the uncertainty of the concentration estimated from horizontal visibility as well as the vertical extension of the dust plumes is estimated to be 30–50 %. The uncertainty of the concentration is twofold. Primarily, it is related to uncertainty in the manual estimation of the visibility and how well it represents the entire dust plume. Secondly, observations that may deviate from the present cases in terms of particle size distribution and optical properties which are not known and presumably variable to some extent, even from case to case in Iceland. Furthermore, the uncertainty in the estimate of how much of emitted materials reach the sea is unknown. Yet, the relatively similar quantities derived for the total emissions and sea emissions compared to values obtained from the deposition maps show that these estimates are adequate as first approximations.

The dust emissions in Iceland presented here (31–40 million t) are of the order of 0.6–7.2 % of the total estimate for global dust emissions of 500 to 5000 million tons given in a review by Engelstaedter et al. (2006). They noted that North Africa is by far the largest source of dust with 170–1600 million t, but our numbers are 1.9–21 % of these estimates of North African dust.

The total oceanic deposition from Iceland ranges between 5.5 and 14 million t annually, according our results. Engelstaedter et al. (2006) reviewed estimates of mean annual dust depositions to the oceans, which range between 314 and 910 million $t\,yr^{-1}$ to the oceans globally but from 140 to 260 million $t\,yr^{-1}$ to North Atlantic Ocean. The North Atlantic estimates are close to values reported in a review by Mahowald et al. (2005), suggesting that the North Atlantic receives about 200 million tons of dust annually, mostly from Africa. The Icelandic dust to oceans amounts to 2.8–7 % of this quantity. The dust deposition per unit area west of the Sahara is considered to be about $10\,t\,km^{-2}\,yr^{-1}$ (Duce et al., 1991). The corresponding average number from the data presented here is $10.4–25.7\,t\,km^{-2}\,yr^{-1}$ on average over 370 000 km^2 sea area, equal to or substantially greater than the rates reported by Duce et al. It is therefore evident that Icelandic dust sources rate among the globally most active sources, and contributing a sizeable share of atmospheric dust to the North Atlantic Ocean, and most likely

the majority of dust deposits to the northern part of the North Atlantic Ocean and the Atlantic part of the Arctic Ocean (Greenland and Norwegian Seas).

5.2 Oceanic iron deposition with dust

Jickells et al. (2005) indicated that atmospheric sources of iron were of the order of 16 million tons Fe per year. The Icelandic aeolian sediments are exceptionally iron rich, which explain high values of deposited iron to Icelandic water. Iron deposition to oceans from Icelandic sources is of the order 0.56–1.39 million t (Table 4), which is a sizeable proportion of the estimate of the global total (3.5–8.7 %). However, Jickells et al. (2005) report fluvial (625–962 million t) and glacial sediments (34–211 million t) as much larger sources for flux of iron to the oceans, but their spread is naturally considerably more limited, closer to the outlets.

There is evidence that the oceans south of Iceland are Fe limited during and after peak bloom, and the Irminger Basin waters have been identified as an area of low dissolved Fe (Nielsdóttir et al., 2009; Ryan-Keogh et al., 2013). Achterberg et al. (2013) found elevated Fe levels in surface waters south of Iceland during the 2010 Eyjafjallajökull eruption, indicating that volcanic activity can raise the oceanic Fe numbers. They, however, pointed out that the potential positive effect of such nutrient pulses as provided by eruptions are depended on other conditions such as nitrogen availability, and the effects are potentially short-lived. We do, however, concur with Prospero et al. (2012) that the numerous periodic dust plumes over the Icelandic waters can have a prolonged effect on Fe availability south of Iceland, and also in other Icelandic waters. Furthermore, many of the dust-storm events occur in spring in South Iceland (March–May), which further enhances possible positive growth effects during early summer.

Only part of the iron in the ash becomes available. Iron solubility has generally been calculated as 1–5 % (see Mahowald et al., 2005), but Buck et al. (2010) reported 9±5 % sea water solubility for iron in aerosol over oceans. How much of this iron becomes bioavailable is uncertain (Jickells et al., 2005). A range of Fe bioavailability has been reported in the literature (e.g., Ayris and Delmelle, 2012b) with 0.004–0.04 % bioavail-

ability reported by Olgun et al. (2011; see also Ayris and Delmelle, 2012a). Achterberg et al. (2013) studying the 2010 Eyjafjallajökull deposition indicated that only 0.02 % of the Fe would become bioavailable. We made an effort of quantifying bioavailable iron based on 0.02 % bioavailability, which is presented in the last column in Table 4, which shows that bioavailable Fe from dust sources are of the order 0.04 to > 10 mg m^{-2} yr^{-1}. It should, however, be noted that Jones and Gislason (2008) showed that 7 year Hekla ash (from the 2000 eruption) released substantially less iron than the freshly deposited ash.

The continuous river and aeolian distribution to the oceanic waters have more stable effects on the nutrient contents of the surface waters than volcanic pulses. Icelandic rivers bring annually about 60–70 million tons of sediments to the ocean on average (research reviewed by Gíslason, 2008) compared to 5.6–14 million tons deposited by aeolian processes. In addition to this mean annual flow, large scale floods in relation to volcanic activity and draining of sub-glacial lakes create temporary pulses of sediment release to the oceans from Iceland (and also often dust pulses). The high river inputs will result in high concentrations near the river outlets, dwarfing the aeolian inputs. However, the river fed sediments are not as widespread as the aeolian deposition. Furthermore, dust far from the sources is relatively fine-grained material, more reactive than the coarser glacio-fluvial sediments, and is more likely to affect nutrient contents, such as Fe, in much of the oceanic waters around Iceland. Iron solubility has been suggested to be higher in areas remote from desert plumes (Baker et al., 2005). However, the effect of particle size, hence the small grains distributed over the oceans, is poorly understood (Ayris and Dalmelle, 2012b). There are published experiments on the solubility of iron from fresh volcanic ash, less is known about the iron solubility in volcanic materials redistributed by aeolian processes, but it is likely to be less than for the fresh volcanic ash, as the readily soluble salts adsorbed onto the fresh ash particles have been washed away (e.g., Duggen et al., 2010).

6 Implications and conclusions

We present the first available estimates of total dust emissions from Icelandic dust sources, which are obtained using two independent methods, and yielding 30 to 40 million tons of dust annually. These figures are significant in relation to global emissions and are likely to have widespread effects on atmospheric conditions in the North Atlantic Ocean and in the Arctic. This dust needs to be considered in climate models for the area, and is likely to have impact on albedos of snow, sea ice, and glaciers, thus enhancing snow melt in Iceland and possibly Greenland and Svalbard.

Our research also presents the first estimate of oceanic dust deposition of volcanic materials from Iceland. The amount is in the range of 5.5–13.8 million tons annually, which is a substantial proportion of the dust deposited to the North Atlantic Ocean and the Arctic, and large contribution of materials to the ocean surface at northerly latitudes (e.g., > 55° N). The 5.5–13.8 million t of materials deposited as dust is an addition to the 60–70 million tons that are fluvial (Gíslason, 2008), but the aeolian materials are distributed more evenly and over larger areas than the fluvial sediments. This large amount and distribution shown in Fig. 4 can be used for improving ocean nutrition models for the ocean waters around Iceland.

The iron content of volcanic dust materials deposited from the Icelandic dust sources is high (10 %). Therefore, the dust is expected to release relatively high concentrations of bioavailable iron. This iron release can potentially have marked influence on the primary productivity in oceans around Iceland and needs to be considered for nutrient budgets for the area. Even though the numbers are substantially lower than fluvial deposition of suspended materials from Iceland, the extensive spread is potentially just as an important factor. Considering the importance for ocean productivity and fisheries, we suggest that the effect on Icelandic dust plumes on the primary production should be investigated in greater detail.

Icelandic glaciers are currently retreating due to climate change (Björnsson and Pálsson, 2008). Dust emissions are likely to increase over the next decades with retreating

glaciers as some of the major dust source areas (mainly Dyngjusandur, Maelifellssandur and Myrdalssandur, see Fig. 1) leave behind larger floodplains subjected to intense aeolian redistribution of fine sediments. It is important to increase understanding of the aeolian nature of these major dust source areas, including loading, erosion processes, deflation, dust generation and other factors.

The amount of dust emissions calculated from the deposition map presented here includes periodic pulses from volcanic eruptions, which may result in lower emissions during average years (without eruptions), which can in part explain the difference between calculated deposition from frequency and emissions of storms compared to estimates from deposition on land. Our results provide a best estimate in a subject area where data of this nature did not exist previously, but is needed for improved understanding of oceanic biochemical cycles, productivity and atmospheric conditions.

References

Achterberg, E. P., Moore, C. M., Henson, S. A., Steigenberger, S., Stohl, A., Eckhardt, S., Avendano, L. C., Cassidy, M., Hembury, D., Klar, J. K., Lucas, M. I., Macey, A. I., Marsay, C. M., and Ryan-Keogh, T. J.: Natural iron fertilization by the Eyjafjallajökull volcanic eruption, Geophys. Res. Lett., 40, 921–926, 2013.

Arnalds, O.: Soils of Iceland, Jökull, 58, 409–421, 2008.

Arnalds, O.: Dust sources and deposition of aeolian materials in Iceland, Icel. Agric. Sci., 23, 3–21, 2010.

Arnalds, O.: The influence of volcanic tephra (ash) on ecosystems, Adv. Agron., 121, 331–380, 2013.

Arnalds, O. and Metúsalemsson, S.: Dust emissions from South Iceland 5 October 2004, Náttúrufraedingurinn, 72, 90–92, 2004 (in Icelandic).

Arnalds, O., Thorarinsdottir, E. F., Thorsson, J., Dagson-Waldhauserova, P., and Agustsdottir, A. M.: An extreme wind erosion event of the fresh Eyjafjallajökull 2010 volcanic ash, Nature Sci. Rep., 3, 1257, doi:10.1038/srep01257, 2013.

Ayris, P. M. and Delmelle, P.: The immediate environmental effects of tephra emission, B. Volcanol., 74, 1905–1936, 2012a.

Ayris, P. and Delmelle, P.: Volcanic and atmospheric controls on ash iron solubility: a review, Phys. Chem. Earth, 45–46, 103–112, 2012b.

Baker, A. R., Jickells, T. D., Witt, M., and Linge, K. L.: Trends in the solubility of iron, aluminium, manganese and phosphorus in aerosol collected over the Atlantic Ocean, Mar. Chem., 98, 43–58, 2005.

Baratoux, D., Mangold, N., Arnalds, O., Bardintzeff, J.-M., Platevoet, B., Grégorie, M., Pinet, P.: Volcanic sands of Iceland – Diverse origins of aeolian sand deposits revealed at Dyngjusandur and Lambahraun, Earth Surf. Proc. Land., 36, 1789–1808, 2011.

Björnsson, H. and Jonsson, T.: Climate and climatic variability at Lake Mývatn, Aquat. Ecol., 38, 129–144, 2003.

Björnsson, H. and Pálsson, F.: Icelandic glaciers, Jökull, 58, 365–386, 2008.

Blechschmidt, A.-M., Kristjansson, J. E., Olafsson, H., Burkhart, J. F., and Hodnebrog, Ø.: Aircraft-based observations and high-resolution simulations of an Icelandic dust storm, Atmos. Chem. Phys. Disc., 12, 7949–7984, 2012.

Buck, C. F., Landing, W. M., Resing, J. A., and Measures, C. I.: The solubility and deposition of aerosol Fe and other trace elements in the North Atlantic Ocean: observations from the A16N CLIVAR/CO2 repeat hydrography section, Mar. Chem., 120, 57–70, 2010.

Bullard, J. E.: Contemporary glacigenic inputs to the dust cycle, Earth Surf. Proc. Land., 38, 71–89, 2013.

Cuxart, J., Bougeault, P., and Redelsperger, J. L.: A turbulence scheme allowing for mesoscale and large-eddy simulations, Q. J. Roy. Meteor. Soc., 126, 1–30, 2000.

D'Almeida, G. A.: A model for Saharan dust transport, J. Clim. Appl. Meteorol., 25, 903–916, 1986.

Dagsson-Waldhauserova, P., Arnalds, O., and Olafsson, H.: Long-term frequency and characteristics of dust storm events in Northeast Iceland (1949–2011), Atmos. Environ., 77, 117–127, 2013a.

Dagsson-Waldhauserova, P., Arnalds, O., and Olafsson, H.: Long term dust aerosol production from natural sources in Iceland, J. Air Waste Manage. Assoc., doi:10.1080/10962247.2013.805703, 2013b.

Dagsson-Waldhauserova, P., Arnalds, O., and Olafsson, H.: Long-term variability of dust-storms in Iceland, Geophys. Res. Abstr., 15, EGU2013-11578-1, 2013c.

Duce, R. A., Liss, P. S., and Merill, J. T.: The atmospheric input of trace species into the World Ocean, Global Biochem. Cy., 5, 193–259, 1991.

Duggen, S., Olgun, N., Croot, P., Hoffmann, L., Dietze, H., Delmelle, P., and Teschner, C.: The role of airborne volcanic ash for the surface ocean biogeochemical iron-cycle: a review, Biogeosciences, 7, 827–844, doi:10.5194/bg-7-827-2010, 2010.

Ekström, M., McTainsh, G. H., and Chappell, A.: Australian dust storms: temporal trends and relationships with synoptic pressure distributions (1960–99), Int. J. Climatol., 24, 1581–1599, 2004.

Engelstaeter, S., Tegen, I., and Washington, R.: North African dust emissions and transport, Earth-Sci. Rev., 79, 73–100, 2006.

Fields, J. P., Belnap, J., Breshears, D. D., Neff, J. C., Okin, G. S., Whicker, J. J., Painter, T. H., Ravi, S., Reheis, M. C., and Reynolds, R. L.: The ecology of dust, Front. Ecol. Envir., 8, 423–430, 2010.

Gillies, J. A., Nickling, W. G., and Tilson, M.: Frequency, magnitude and characteristics of aeolian sediment transport: McMurdo Dry Valleys, Antarctica, J. Geophys. Res.-Ea. Surf., doi:10.1029/2012JF002473, 2013.

Gislason, S. R.: Weathering rates in Iceland, Jökull, 58, 387–408, 2008.

Gunnarsson, T. G., Arnalds, O., Appleton, G., and Gill, J. A.: Ecosystem recharge by volcanic dust drives large-scale variation in bird abundance, Global Ecol. Biogeogr., submitted, 2014.

Jamalizadeh, M. R., Moghaddamnia, A., Piri, J., Arbabi, V., Homayounifar, M., and Shahryari, A.: Dust storm prediction using ANNs technique (a case study: Zabol City), Proc. Wrld. Acad. Sci. E., 33, 529–537, 2008.

Jakobsson, S. P., Jónasson, K., and Sigurdsson, I. A.: The three igneous rock series of Iceland, Jökull 58, 117–138, 2008.

Jickells, T. D., An, Z. S., Andersen, K. K., Baker, A. R., Berametti, G., Brooks, N., Cao, J. J., Boyd, P. W., Duce, R. A., Hunter, K. A., Kawahata, H., Kubilay, N., LaRoche, J., Liss, P. S., Mahowald, N., Prospero, J. M., Didgwell, A. J., Tegen, I., and Torres, R.: Global iron connections between desert dust, ocean biogeochemistry, and climate, Science, 308, 67–71, 2005.

Jones, M. T. and Gislason, S. R.: Rapid releases of metal salts and nutrients following the deposition of volcanic ash into aqueous environments, Geochim. Cosmochim. Ac., 72, 3661–3680, 2008.

Lawrence, C. R. and Neff, J. C.: The contemporary physical and chemical flux of aeolian dust: a synthesis of direct measurements of dust deposition, Chem. Geol., 267, 46–63, 2009.

Leadbetter, S. J., Hort, M. C., von Löwis, S., Weber, K., Witham, C. S.: Modeling the resuspension of ash deposited during the eruption of Eyjafjallajökull in spring 2010, J. Geophys. Res., 117, D00U10, doi:10.1029/2011JD016802, 2012.

Leys, J. F., Heidenreich, S. K., Strong, C. L., McTainsh, G. H., and Quigley, S.: PM_{10} concentrations and mass transport during "Red Dawn" – Sydney 23 September 2009, Aeol. Res. 3, 227–342, 2011.

Mahowald, N. M., Baker, A. R., Bergametti, G., Brooks, N., Duce, R. A., Jickells, T. D., Kubilay, N., Prospero, J. M., and Tegen, I.: Atmospheric global dust cycle and iron inputs to the ocean, Global Biogeochem. Cy., 19, GB4025, doi:10.1029/2004GB002402, 2005.

Magnússon, S. H.: Heavy metals and sulfur in mosses in Iceland 1990–2010: impact of industry (*Þungmálmar og brennisteinn í mosa á Íslandi 1990–2010: áhrif iðjuvera*), Icelandic Institute of Natural History Report NÍ-13003, Reykjavik, Iceland, 2013 (in Icelandic).

Misumi, K., Lindsay, K., Moore, J. K., Doney, S. C., Bryan, F. O., Tsumune, D., and Yoshida, Y.: The iron budget in ocean surface waters in the 20th and 21st centuries: projections by the Community Earth System Model version 1, Biogeosciences, 11, 33–55, doi:10.5194/bg-11-33-2014, 2014.

Muhs, D. R., Budahn, J. R., McGeehin, J. P., Bettis III, A. E., Skipp, G., Paces, J. B., and Wheeler, E. A.: Loess origin, transport, and deposition over the past 10 000 years, Wrangell-St. Elias National Park, Alaska, Aeol. Res., 11, 85–99, 2013.

Natsagdorj, L., Jugder, D., and Chung, Y. S.: Analysis of dust storms observed in Mongolia during 1937–1999, Atmos. Environ., 37, 1401–1411, 2003.

Nielsdóttir, M. C., Moore, C. M., Sanders, R., Hinz, D. J., and Achterberg, E. P.: Iron limitation of the postbloom phytoplankton communities in the Iceland Basin, Gobal Biogeochem. Cy., 23, GB3001, doi:10.1029/2008GB003410, 2009.

Óladóttir, B. A., Sigmarsson, O., Larsen, G., Thordarson, T.: Katla volcano, Iceland: magma composition, dynamics and eruption frequency as recorded by Holocene tephra layers, B. Volcanol., 70, 475–493, 2008.

Óladóttir, B. A., Sigmarsson, O., Larsen, G., Devidal, J- L.: Provenance of basaltic tephras from Vatnajökull subglacial volcanoes, Iceland as determined by major- and trace-element analyses, Holocene, 21, 1037–1048, 2011.

Olgun, N., Duggen, S., Croot, P. L., Delmelle, P., Dietze, H., Schacht, U., Óskarsson, N., Siebe, C., Auer, A., and Grabe-Schönberg, D.: Surface ocean iron fertilization: the role of airbonre volcanic ash from subduction zone and hot spot volcanoes and related iron fluxes

into the Pacific Ocean, Global Biogeochem. Cy., 25, GB4001, doi:10.1029/2009GB003761, 2011.

Prospero, J. M., Bullard, J. E., and Hodgkins, R.: High-latitude dust over the North Atlantic: inputs from Icelandic proglacial dust storms, Science, 335, 1078–1082, 2012.

Ryan-Keogh, T. J., Macey, A. I., Nielsdottir, M. C., Lucas, M. I., Steigenberger, S. S., Stinchcombe, M. C., Actherberg, E. P., Bibby, T. S., and Moore, C. M.: Spatial and temporal development of phytoplankton iron stress in relation to dynamics in the high-latitude North Atlantic Ocean, Limnol. Oceanogr., 58, 533–545, 2013.

Schulz, M., Prospero, J. M., Baker, A. R., Dentener, F., Ickes, L., Liss, P. S., Mahowald, N. M., Nickovic, S., García-Pando, C. P., Rodríguez, S., Sarin, M., Tegen, I., and Duce, R. A.: Atmospheric transport and deposition of mineral dust to the ocean: implications for research needs, Environ. Sci. Technol., 56, 10390–10404, 2012.

Seity, Y., Brousseau, P., Malardel, S., Hello, G., Bénard, P., Bouttier, F., Lac, C., and Masson, V.: The AROME-France convective-scale operational model, Mon. Wea. Rev., 139, 976–991, 2011.

Singer, A., Zobeck, T., Poberzsky, L., and Argaman, E.: The PM_{20} and $PM_{2.5}$ dust generation of soils/sediments in the Southern Aral Sea Basin, Uzbekistian, J. Arid Environ., 54, 705–728, 2003.

Sweeney, M. R., McDonald, E. V., and Etyemezian, V.: Quantifying dust emissions from desert landforms, eastern Mojave Desert, USA, Geomorphology, 135, 21–34, 2011.

Thordarson, T. and Höskuldsson, Á.: Postglacial volcanism in Iceland, Jökull, 58, 197–228, 2008.

Thorsteinsson, T., Jóhannsson, T., Stohl, A., and Kristiansen, N. I.: High levels of particulate matter in Iceland due to direct ash emissions by the Eyjafjallajökull eruption and resuspension of deposited ash, J. Geophys. Res., 117, B00C05, doi:10.1029/2011JB008756, 2012.

Wang, Y. Q., Zhang, X. Y., Gong, S. L., Zhou, C. H., Hu, X. Q., Liu, H. L., Niu, T., and Yang, Y. Q.: Surface observation of sand and dust storm in East Asia and its application in CUACE/Dust, Atmos. Chem. Phys., 8, 545–553, doi:10.5194/acp-8-545-2008, 2008.

Table 1. Calculation of four storms based on visibility determined at weather stations and wind data for each storm, using equations converting visibility into PM_{10} concentrations by D'Almeida (1986) and Wang et al. (2008) (factor −1.418); see also Dagsson-Waldhauserova et al. (2013). Total emissions calculated by formula given by Leys et al. (2011) and the deposition curve presented in Fig. 4, which reflects drop in concentration. All storms occurred at the Dyngjusandur dust source in NE Iceland. The column "Distance from source" indicates the location of the calculated window through which materials in the last column are transported. "Emissions through window" means how much material is transported through the window (e.g., to sea).

Storm	Size	Distance from source km	Total emissions from source thousand tons	Emissions through window thousand tons
23 Sep 2008	Medium-large	90	384	160
24 Sep 2011	Medium	90	255	110
25 May 2012	Medium-large	90	365	150
9 Aug 2012	Medium	155	215	75

Table 2. Annual number of dust-day events in South, North and all Iceland to the left. The dust events are split in three intensity classes each with calculated average emissions to give total emissions for each North and South Iceland. The results are shown as total emissions (land and sea) and emissions over sea (northeast and south of Iceland and total emissions to the sea, last three columns).

Intensity	Dust events in NE Iceland per year	Dust events in S Iceland per year	Total dust events in Iceland per year	Average emissions per event	Total deposition, land and ocean	Emissions to oceans NE (10 % of total)	Emissions to oceans S (50 % of total)	Total emissions to oceans
					million tons			
Major	1.5	6.3	7.8	1	7.8	0.150	3.150	3.300
Medium	7.8	42.5	50.3	0.3	15.1	0.234	1.275	1.509
Minor	25.3	52.2	75.6	0.1	7.6	0.253	0.522	0.775
Total	**34.6**	**101**	**135.6**		**30.5**	**0.637**	**4.917**	**5.554**

Table 3. Deposition on land and sea based on a map of deposition on land (Arnalds 2010) and extension of the data to oceanic areas around Iceland.

	Average	Areal extent		Deposition		
Category	Deposition	Land	Ocean	Land	Ocean	Total
	$t\,km^{-2}$	km^2		million tons		
1	5	10 085	173 637	0.05	0.89	0.92
2	20	8,370	109 845	0.17	2.20	2.36
3	44	17 367	48 761	0.76	2.15	2.90
4	119	11 699	22 594	1.39	2.69	4.08
5	350	16 680	12 188	5.84	4.27	10.10
6	500	27 297	3244	13.65	1.60	15.27
Glaciers	400	11 185		4.47		4.47
Total		**102 683**	**370 269**	**26.33**	**13.79**	**40.11**

Table 4. Range in annual dust deposition over sea area from Iceland, total and per unit area, iron deposition and a calculation of bioavailable iron from Icelandic dust (0.02 % of total Fe, Achterbert et al., 2013). Range in dust deposition found by (i) frequency determination and dust load calculation (lower values), and (ii) map-based deposition numbers (higher values).

	Deposition per year	Sea area	Total dust	Fe	Total Fe on sea	Bioavailable Fe[$]
Deps. categ.	$t km^{-2}$ or $g m^{-2}$	km^2	million $t yr^{-1}$	$g m^{-2} yr^{-1}$	thousand $t yr^{-1}$	$mg m^{-2} yr^{-1}$
1	2–5	173 637	0.35–0.86	0.2–0.5	35–87	0.04–0.1
2	8–20	109 845	0.89–2.2	0.8–2	89–220	0.16–0.4
3	17–44	48 761	0.88–2.1	1.7–4.4	87–215	0.36–0.88
4	48– 119	22 594	1.1– 2.7	4.8–11.9	109–269	0.97–2.38
5	142–350	12 188	1.7–4.3	14.2–35.0	173–427	2.8–7
6	203–500	3244	0.7–1.6	20.3–50.0	66–162	4.1–10
Total		**370 269**	**5.6–13.8**		**560–1390**	

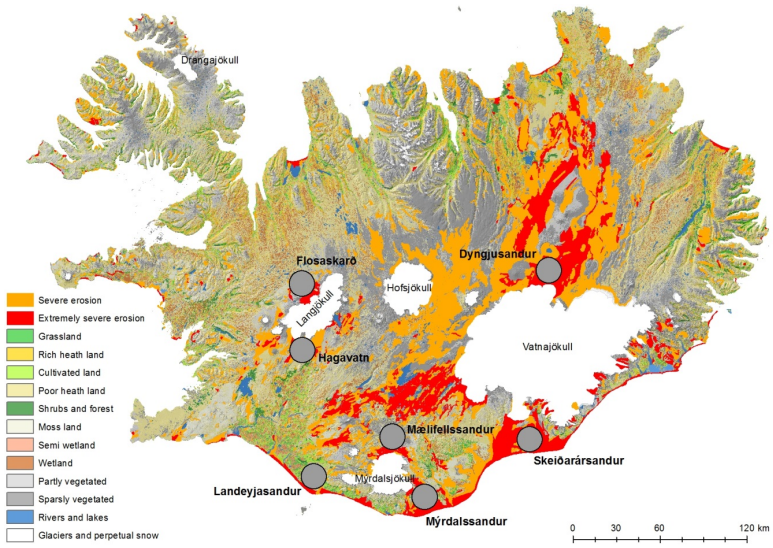

Fig. 1. Location of major plume areas in Iceland shown as circles. Sandy areas with unstable surfaces shown as red (very unstable) and orange (unstable), but glaciers are white. The map is based on the Agricultural University of Iceland land cover database.

Fig. 2. Typical plume area in Iceland: Maelifellssandur, north of Myrdalsjökull. The photo shows approximately 3 km of the glacial front but the plume area is > 25 km^2. The sand-fields are flooded during warm summer days, charging the surface with silty materials (lighter colored areas, deposited from higher water flow the previous day or days). Some of the channels dry out as the water percolates into the surface, with the sediment loads being left on the surface. The more coarse materials are left on the ground after wind erosion events (saltation, the darker materials). The water channels change frequently. Dust storms are extremely common within this area during summer (often daily), but less frequent during winter when this highland area is usually covered with snow. Photo July 2012 (OA).

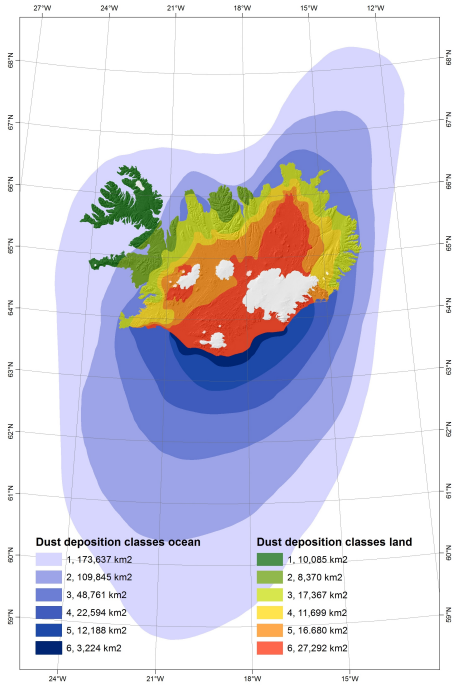

Fig. 3. Average distribution of aeolian sediments and volcanic ash around Iceland. Deposition is split in six categories (see map legend), and is an extension of previously published map for terrestrial Iceland (Arnalds, 2010). Extension to sea is partly based on satellite images showing dust-storm events. Main extension is to the south from the southern Iceland dust plume areas, and to the northeast, mainly from the Dyngjusandur dust plume source.

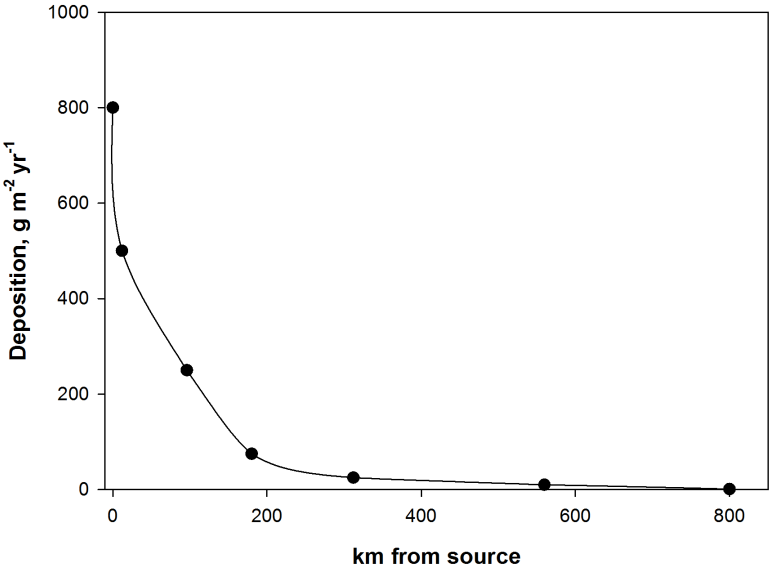

Fig. 4. The logarithmic drop in sedimentation with distance from the sediment source. Transect south from the dust sources at the southern tip of Iceland. The transect from Dyngjusandur in NE Iceland has x-axis scale approximately divided by 2.

Paper V

Atmospheric Environment 77 (2013) 117–127

Contents lists available at SciVerse ScienceDirect

Atmospheric Environment

journal homepage: www.elsevier.com/locate/atmosenv

Long-term frequency and characteristics of dust storm events in Northeast Iceland (1949–2011)

Pavla Dagsson-Waldhauserova [a,b,*], Olafur Arnalds [a], Haraldur Olafsson [b,c,d]

[a] Agricultural University of Iceland, Hvanneyri, Borgarnes IS 311, Iceland
[b] University of Iceland, Department of Physics, Reykjavík, Iceland
[c] Icelandic Meteorological Office, Bústaðavegi 9, Reykjavík IS 150, Iceland
[d] Bergen School of Meteorology, Geophysical Institute, University of Bergen, 5007, Norway

HIGHLIGHTS

- Present weather and visibility observations in Northeast Iceland.
- There were 1033 dust days in 1949–2011 with the annual mean of 16.4 dust days.
- Dust event frequency is comparable to major desert areas in the world.
- Dust production occurred during summer months, mostly June and September.
- Median concentrations were calculated as 106 μg m^{-3}.

GRAPHICAL ABSTRACT

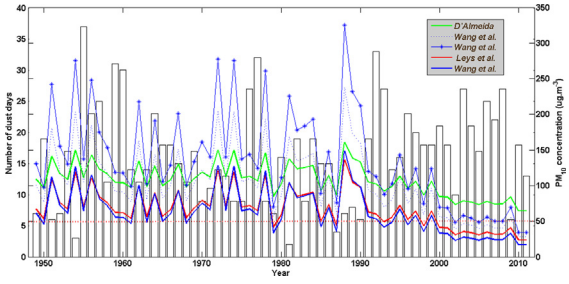

ARTICLE INFO

Article history:
Received 24 October 2012
Received in revised form
26 April 2013
Accepted 30 April 2013

Keywords:
Climatology
Visibility
Aerosol dust concentration
Dust event classification
Wind erosion

ABSTRACT

Long-term records of meteorological dust observations from Northeast Iceland were analysed and frequency of dust events from Icelandic deserts calculated. A total of 1033 dust days were reported during the period 1949–2011 with an annual mean of 16.4 dust days $year^{-1}$, placing the area among the dustiest areas in the world. The most active decades were the 2000s, 1990s and 1950s. Monthly dust event frequency is bimodal with primary and secondary maxima in June and September. A total of 14 severe dust storms (visibility < 500 m) occurred during the period. Median dust event concentration was calculated as 106 μg m^{-3} from the visibility observations. The frequency and severity of dust events depend on Sea Level Pressure (SLP) oscillation which controls the southerly winds in NE Iceland. The availability of fine sediments susceptible to dust production in outwash plains controlled by the flow rate of glacial river is also important. Volcanic ash from eruptions in 2010 and 2011 barely affected the dust event frequency in NE Iceland. Icelandic dust may be substantial source for large scale air pollution in the Arctic.

1. Introduction

Natural dust is emitted from many desert areas on Earth. The global dust belt, where most of the dust sources are located, extends from Africa, through the Middle East, into Central Asia (Formenti et al., 2011). Globally, fine dust particles may be transported at altitudes of up to 10 km and can be carried distances of >10,000 km (Husar, 2004). Grousset et al. (2003) suggested that dust particles can travel over a 20,000 km in two weeks. Dust is considered to contribute to the Arctic haze phenomena (Raatz, 1984; Quinn et al., 2002).

Although dust is most often associated with dry and warm desert areas, dust is also frequently emitted in cold climate regions and at high latitudes, foremost from glacially-derived sediments of riverbeds or ice-proximal areas (Arnalds, 2010; Crusius et al., 2011;

* Corresponding author. Agricultural University of Iceland, Keldnaholt, 112 Reykjavík, Iceland. Tel.: +354 4335267; fax: +354 4335201.
E-mail addresses: pavla@lbhi.is, paw2@hi.is (P. Dagsson-Waldhauserova), oa@lbhi.is (O. Arnalds), haraldur@vedur.is (H. Olafsson).

1352-2310/$ – see front matter © 2013 Elsevier Ltd. All rights reserved.
http://dx.doi.org/10.1016/j.atmosenv.2013.04.075

Prospero et al., 2012; Bullard, 2013). Glaciers produce sediments during the grinding and abrasion by ice over bedrock and meltwater transports fine particles to floodplains from which they are deflated by strong glacier-driven or katabatic winds. Eldridge (1980) considered the Arctic and Antarctic coastal zones as the windiest regions on Earth which may increase the severity of regional dust events. Furthermore, threshold wind velocities for a given particle size are lower in cold conditions than in warmer areas (Bullard, 2013). Dust emission intensity and deposition rates in glacial areas sometimes exceed those at lower latitudes (Bullard, 2013). Canada (Hugenholtz and Wolfe, 2010), Iceland (Arnalds, 2010), USA, China, and New Zealand (McGowan et al., 1996) are among areas with the highest deposition rates (Bullard, 2013). Blechschmidt et al. (2012) suggested that Icelandic deserts should be considered as major dust sources in global and regional climate models.

Iceland is an example of glaciogenic dust source area at high latitudes. In addition, Iceland is an important source of volcanic sediments that are subjected to intense aeolian processes and dust production (Arnalds et al., 2001, 2012, 2013; Arnalds, 2010; Prospero et al., 2012; Thorarinsdottir and Arnalds, 2012). Many of the major source areas for the dust have been identified (Arnalds, 2010) and the sandy deserts have been mapped (Arnalds et al., 2001). The Northeast is one of the most active aeolian areas of Iceland, with frequent dust plumes rising up from the Dyngjusandur source area and other sandy areas in the region, with dust plumes extending several hundred km from the sources (Arnalds, 2010). The Dyngjusandur active aeolian sandsheet covers an area of 270 km^2 with up to 10 m thick sediments (Mountney and Russell, 2004). Desert areas near Dyngjujokull are a result of glaciofluvial flooding, often associated with volcanic eruptions under the Vatnajokull glacier, enhanced by widespread volcanic deposition (Arnalds et al., 2001).

Atmospheric dust can reduce visibility and cause health risks. The World Health Organization considers that annual $PM_{2.5}$ concentration of 10 μg m^{-3} and estimated visibility 67 km indicates health risk, or daily standard of 35 μg m^{-3} and visibility range 31 km (WHO, 2005). In comparison, visual range can be over 300 km in dry climates and 100 km in humid climates on clear days (Hyslop, 2009). Observations of visibility during dust events are a key indicator of the severity of dust events where no aerosol measurements are conducted.

Many factors affect dust activity, such as sediment availability and climate factors. It is important to monitor changes in dust activity in time, especially in relation to climate and environmental changes. Atmospheric dust and visibility observations are available at weather stations in Iceland for more than 60 years (Arason et al., 2010). These data are ideal for studying long term variability in dust production and severity of historical dust events.

The main objectives of the study presented here were: (i) to explore the long term (63 years) variability in dust activity in NE Iceland (ii), to determine climatological characteristics of episodic dust events in a subarctic region, (iii) to place Icelandic dust production into international perspective.

2. Methods

2.1. Meteorological data

A network of eight weather stations in NE Iceland was chosen for the study. Fig. 1 depicts the location of the stations at Akureyri

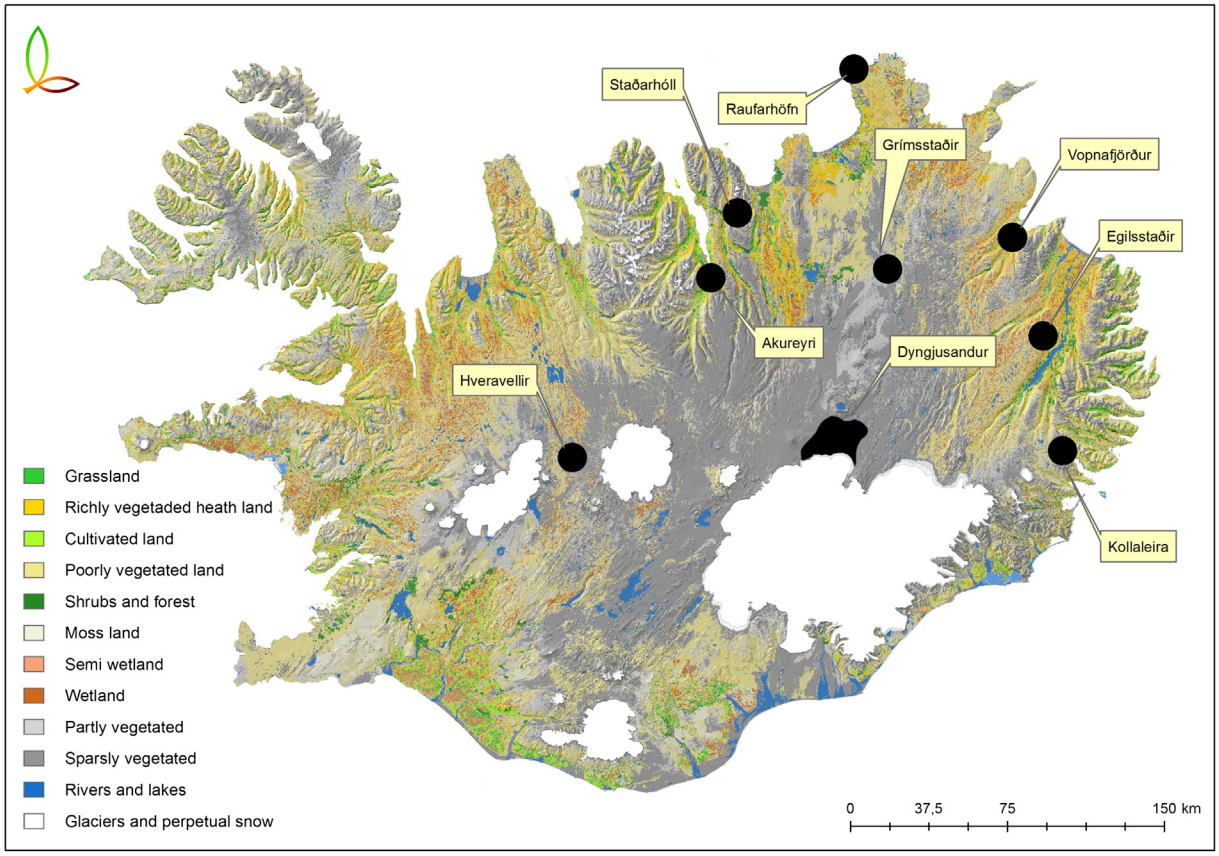

Fig. 1. A map showing the locations of weather stations in Northeast Iceland [Akureyri (AK), Egilsstadir (EG), Grimsstadir (GS), Raufarhofn (RH), Stadarholl (SH), Vopnafjordur (VO), Kollaleira (KL)] and a station in central Iceland [Hveravellir (HV)]. Base map from the Agricultural University of Iceland land use database (Nytjaland).

(AK), Egilsstadir (EG), Grimsstadir (GS), Raufarhofn (RH), Stadarholl (SH), Vopnafjordur (VO), Kollaleira (KL), and additionally Hveravellir (HV). HV is the only manned weather station located in central Iceland (Fig. 1) where dust events have been observed mostly during southerly winds and therefore affecting northern Iceland. The duration of operation varies: AK, ES, GS, and RH have been operated since 1949 (giving 63-year time series), EG 1949–1998 (50 years), SH and VO since 1961 (51 years), HV 1965–2004 (40 years), and KL from 1976 to 2007 (32 years). The weather stations are operated by the Icelandic Meteorological Office where the data are stored after strict quality control.

The data consist of conventional meteorological parameters such as wind velocity, wind direction, temperature and visibility, accompanied by synoptic codes of present weather. Present weather refers to atmospheric phenomena occurring at the time of observation, or which has occurred preceding the time of observation (The Icelandic Meteorological Office, 1981). In this study only atmospheric phenomena such as for 'moldrok' (blowing soil/dust), 'sandfok' (blowing sand/dust), 'sandbylur'(extreme blowing sand/dust), and codes for dust haze, suspended dust, blowing dust and dust whirls, were used and defined as 'dust observation'. The synoptic codes (*ww*) for present weather which refer to dust observation are 7–9, 30–35, and 4–6 only if the codes for primary or secondary past weather (ww_1, ww_2) are 3 for blowing soil, dust, sand and dust storm (The Icelandic Meteorological Office, 1981). At all stations, the weather was observed every day of the year 3–8 times a day.

2.2. Analysis

The initial dataset was built from the occurrence of 'dust observation' made at one or more weather stations. Long-term dust activity is expressed in dust days. A 'dust day' was defined as a day when at least one station recorded at least one dust observation. About 29% of the observations did not include information on the atmospheric phenomena and they were excluded from the dataset.

There are no continuous dust concentration measurements conducted in NE Iceland and therefore there are no *in situ* dust concentrations available for our dust observations. However, visibility observation during a dust event can be applied to estimate dust concentration using empirical relationships (Leys et al., 2011). Dust concentrations were derived from an equation (Table 1) based on conversion between horizontal visibility and suspended particle concentration presented in a paper by D'Almeida (1986). Additional formulas with different coefficients from Wang et al. (2008) and Leys et al. (2011) were used for comparison of mass concentrations which were measured in desert, semi-desert and loess environments (see Section 3.3.2.1).

Dust events were classified from visibility ranges (Table 2) based on criteria provided by Leys et al. (2011) and Wang et al. (2008). Dust events with visibility less than 500 m are often classified as "severe dust storms" (CMA, 1979; Tao, 2011), which is used in the present study. We classify dust event in visibility range 11–30 km as "suspended dust" and visibility range above 30 km as "moderate suspended dust". Visibility >10 km has been used in the literature to represent floating dust or suspended dust (Natsagdorj et al., 2003; Tao et al., 2002).

3. Results

3.1. Frequency, spatial and temporal variability in dust production

There was a considerable variability between weather stations in the total number of dust observations recorded over the 63 year period. The Grimsstadir station (GS) located downwind from the main dust source made 1685 dust observations (Table 3). The GS station also had by far the greatest frequency of dust days, with 65% (640 dust days) of the total 1033 dust days recorded over the 63 years. Egilsstadir (EG) counted for 15% (155 dust days), followed by 7% at HV and 5% at VO. The number of dust days per decade is shown in Fig. 2. The total number of dust days (defined in Section 2.2) is to the left, but numbers of dust days at individual stations are shown to the right. The annual mean is 16.4 dust days per year. Looking at decades separately reveals that there are frequent dust days during first decade of 21st century but also during the 1990s and the 1950s. The occurrence of total dust observations is, however, the highest in the 1990s and during the first decade of the 2000s.

The lowest number of dust days occurred in the 1980s but with a more evenly spread observations between the weather stations. EG observed most dust events in the 1980s, fewest events in the 1990s, but dust monitoring was discontinued there in 1998. The most active decade, the first decade in the 2000s has double mean frequency compared to the least active decade, the 1980s.

The mean visibility observed during all dust observations was 26.7 km (shown as the solid line in Fig. 2). It was the lowest during the 1980s, 20.8 km, and the highest for dust observations during the 2000s, up to 44 km. Occurrence of dust days was generally higher after the year 2000 but visibility during dust events (DE) was almost double compared to the rest of the decades.

Table 1
Aerosol dust concentration formulas estimated from visibility and PM_{10} concentration relation. PM_{10} is particulate matter concentration in $\mu g\ m^{-3}$ and V is horizontal visibility in m (except D'Almeida (1986) where V is in km).

Aerosol dust concentration formulas	Surface type	Reference
$PM_{10} = 914.06Vexp(-0.73) + 19.03$	Saharan desert	D'Almeida (1986)
$PM_{10} = 1E + 08Vexp(-1.3687)$	Chinese sandy land	Wang et al. (2008)
$PM_{10} = 3E + 08Vexp(-1.4519)$	Chinese steppe area	Wang et al. (2008)
$PM_{10} = 1E + 08Vexp(-1.418)$	China – all areas	Wang et al. (2008)
$PM_{10} = 6E + 06Vexp(-1.1303)$	Australian sand plains	Leys et al. (2011)

Table 2
Dust event classification based on visibility categories. Mean visibility of each dust class is recalculated into PM_{10} concentration using the formula for steppe areas in Wang et al. (2008) and the formula from D'Almeida (1986). PM_{10} concentrations are based on an average obtained using the formulas by Wang and D'Almeida.

Dust event class	Visibility (km)	PM_{10} concentration ($\mu g\ m^{-3}$)
Severe dust storm	≤0.5	31,027
Moderate dust storm	0.5–1.0	8209
Severe haze	1.0–5.0	1265
Moderate haze	5.0–10.0	368
Suspended dust	10.0–30.0	126
Moderate suspended dust	30.0–70.0	52

Table 3
Total dust observations, mean annual number of dust days and mean dust day visibility at all stations.

Station	Total dust observations	Dust days per year	Mean dust day visibility
GS	1685	12.5	24.8
EG	368	3.9	24.1
HV	132	2.3	38.1
VO	96	1.2	24.1
RH	61	0.7	15
AK	26	0.4	30.6
SH	13	0.24	42.7
KL	6	0.16	24.2

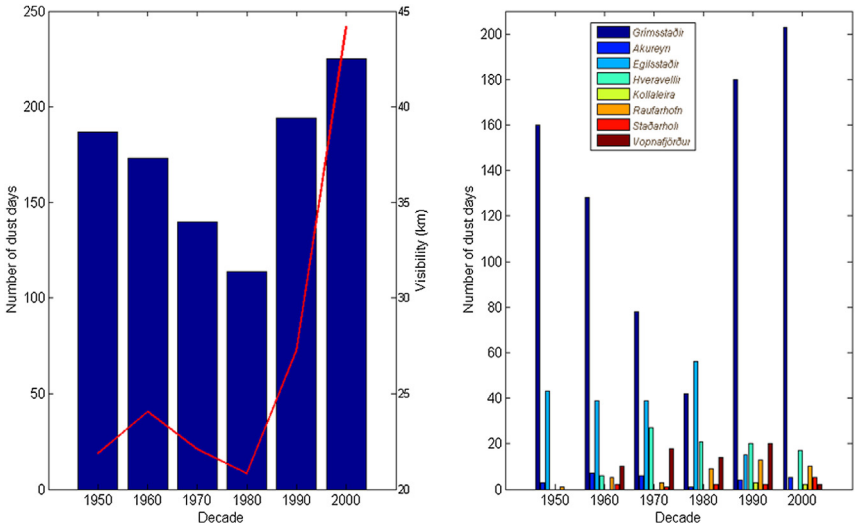

Fig. 2. Total number of days with dust observations, all stations combined to the left. Individual stations sorted by decades to the right. Solid line represents mean visibility.

3.1.1. Annual dust day variability and visibility

The annual number of dust days at all stations in NE Iceland is presented in Fig. 3. Note that 80% of reported dust days relate to the GS and the EG stations. The most active year was 1955 with 37 days of reported dust events with average visibility of 23.2 km, about 3 km less than mean dust day visibility. Other years with high occurrence of dust days in NE Iceland were 1992, 1977, 1960, and 1959. The 3-year moving average of dust day frequency (dashed line) depicts four periods of high dust activity in 1955–1960, 1976–1977, 1992–1993 and 2006–2008. The mean visibility during dust days varies and was notably low in 1954, 1972, 1974, and 1978. The lowest mean annual visibility during dust observations (12.8 km) was recorded in 1988 when dust events of high severity were observed including the severe dust storm on 18 June 1988, so called '*The June 88 storm*', which has been used to illustrate a severe dust storm (Arnalds et al., 2012).

Table 3 summarizes the mean number of dust days per year and visibility at all stations. The GS station is located only about 90 km downwind from the main dust source of Dyngjusandur and was the most active station with over 12 dust days reported annually. The horizon at GS is not blocked by mountains and there are also some local dust sources. Consequently, it is of no surprise that GS provides a large majority of dust days into our database. The second was the EG station with almost 4 dust days annually, while over half of the stations observed <1 dust day annually. The RH station is located at the north-eastern shore and might be influenced by coagulation of dust particles and water (fog) droplets in marine regions, resulting in low DE visibility.

3.1.2. Seasonal patterns in dust activity and visibility

The seasonal distribution of dust events (mostly driven by the GS station) is depicted in Fig. 4. The highest occurrence was in June with almost 22% of all dust events, followed by September (19%). Low dust season started in December and ended in April. The lowest DE visibility was in May, 24.7 km. From April to November the mean visibility during dust events did not exceed 29 km.

The decadal changes in monthly distribution of dust events are shown in Fig. 5 (including only months with at least 5% of the total number of dust days). June had the highest occurrence of dust days early on and showed similar trend after 2000, while September dominated during the 1970s. August had relatively high occurrence of dust events during the 1980s and the 1990s, and May showed a contribution mainly in the 1950s. Absolute numbers of monthly dust days per decade are shown on the graph to the right. Dust events in May in the 1950s were about 2 °C warmer than in other decades. September events in the 1980s were, however, over 2 °C colder than in September during the other decades.

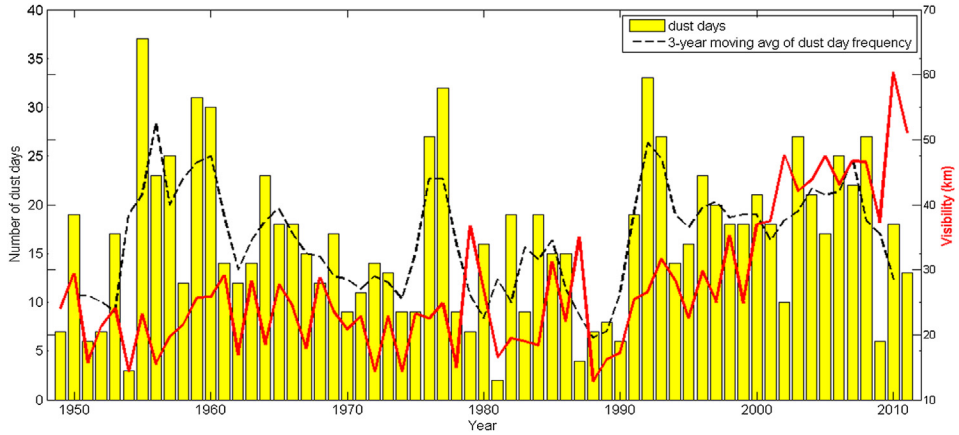

Fig. 3. Number of dust days (bars) and mean annual visibility during dust events (solid line) at all stations. Dashed line represents a 3-year moving average of dust day frequency.

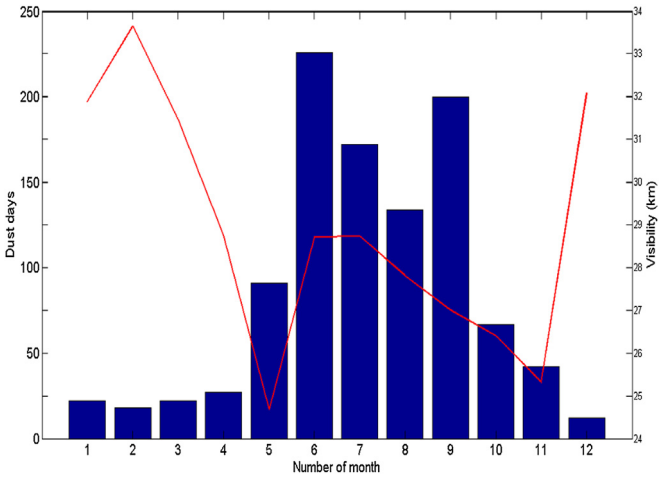

Fig. 4. Number of dust days per month (bars) and monthly means of dust visibility (solid line) for period 1949–2011.

3.2. Climatology of dust events in NE Iceland

3.2.1. Long term trends in meteorological characteristics of dust events

The mean temperature during dust events (DE) ranged from 9.6 to 11.4 °C. The DEs which occurred in the 1950s were the 'warmest' with an average DE temperature of 11.4 °C, but DE temperature dropped to 9.6 °C in the 1960s (Fig. 6A). Wind velocity correlates well with the dust event occurrence as would be expected. The fewest DE per decade were recorded in the 1980s and they occurred at the average wind velocity of 8.6 m s^{-1}. The DE wind velocities increased substantially from the 1990s (11.4 m s^{-1}) to the highest average velocity of 11.9 m s^{-1} during the 2000s (Fig. 6B). Most of the DE meteorological data in the 1950s and the 2000s were obtained at the GS station and the DE wind velocities at other stations are lower (yellow line, Fig. 6B). The RH station changed from manned to automatic station in 2005. Previous meteorological observations at this station were made more frequent than at the other stations and the data have the highest quality. The DE wind velocity at this coastal station remained similar throughout the period with a maximum in the 1990s and the lowest velocity in the 1980s (dotted line, Fig. 6B). During the dust events, the inland stations had higher wind velocities than the coastal stations.

The most common wind directions of the dust events in NE Iceland were SW–S–SE (Figs. 6C and 7). During the 1950s and the 1960s, SE storms were more frequent than in following decades. In the 1980s, dust events were mostly during winds from the SW and the first decade in the 2000s was dominated by southerly winds.

In order to gain better understanding of the frequency of the DEs, the long term variability in southerly winds was investigated in greater detail. The most active station (GS) was chosen to determine prevailing winds during dust events. GS is located in relatively flat highland area at some distance from mountains that can affect wind direction. The proportion of annual southerly air flow (winds from directions 100°–280°) on total air flow (all winds) was identified for this station. Fig. 8 depicts strong correlation between years of positive southerly air flow (>50% of winds were from directions 100°–280°, Fig. 8A) and years with high number of dust days (Fig. 8B). Low number of southerly winds in the 1980s correspond to low dust days frequency in this decade. This coincides with a drop in the frequency of southerly winds exceeding wind speed of 8 m s^{-1} during the active dust season (May–November) on total winds in the 1980s at the station RH (Fig. 8C).

3.2.2. Seasonal patterns in meteorological characteristics of dust events

Monthly mean values for temperature, wind velocity and most frequent wind direction of dust events (solid line) are shown in Fig. 9. Dashed lines depict total mean temperature and wind velocity in 1949–2011. The DE temperatures were about 3 °C higher than monthly long-term temperatures and DE wind velocities were about 4–7 m s^{-1} higher than long-term wind velocities. The major differences in temperature and wind velocity were in May, September and October. The reason is likely the occasional presence of snow within the Dyngjusandur dust source during these months and therefore the threshold wind velocity and temperature of DE are higher. The DE temperatures were warmest in June–August, with a maximum 14.4 °C in July. The highest DE wind

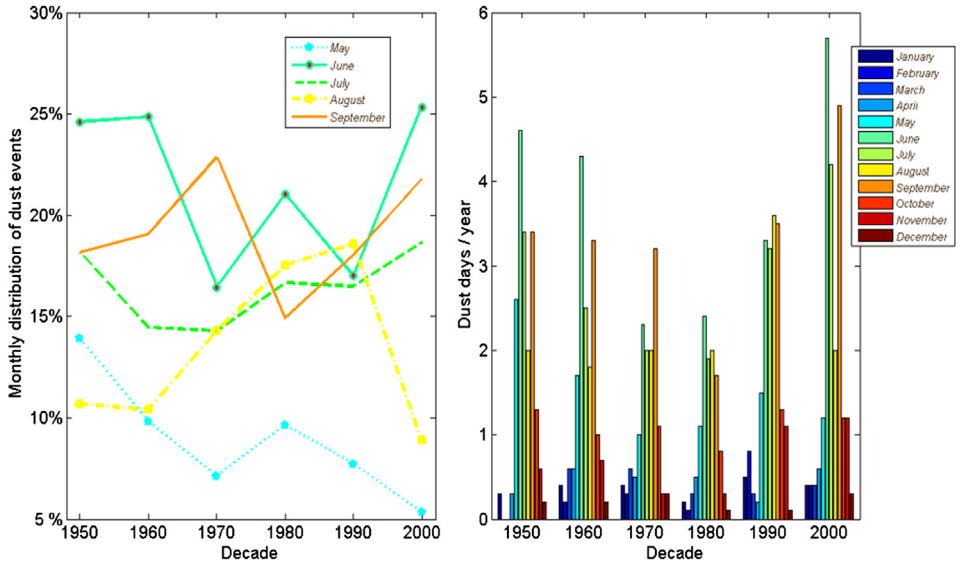

Fig. 5. Frequency of dust events during individual months of the year. The thick lines depict the fraction of June (light green) and September (orange) dust observations by decades. The dashed lines show remaining months with at least 5% of the total number of dust days. The absolute numbers of dust days each month per decade is on the right. (For interpretation of the references to colour in this figure legend, the reader is referred to the web version of this article.)

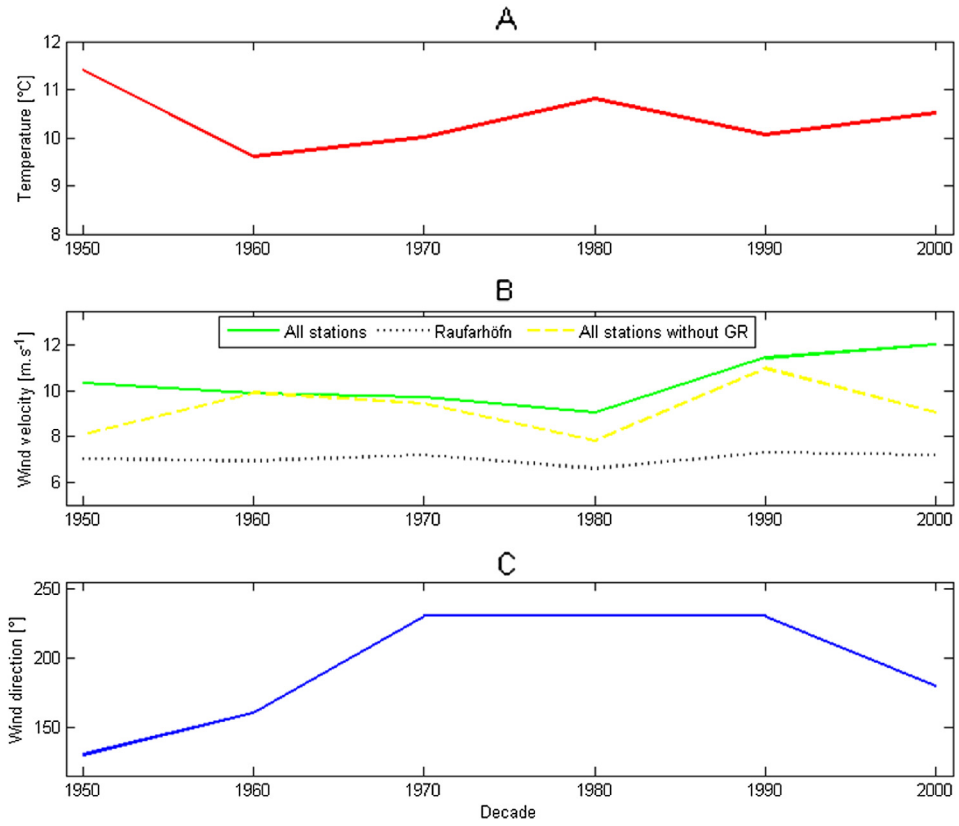

Fig. 6. Meteorological parameters for dust events 1949–2011. A-mean temperature, B-mean wind velocity, C-most frequent wind direction. Mean wind velocity during dust events at all stations is marked with a green line. Dashed yellow line shows mean wind velocities at all stations except Grimsstadir (GS, most active station) and dotted line shows mean wind velocity at the coastal station Raufarhofn (RH). (For interpretation of the references to colour in this figure legend, the reader is referred to the web version of this article.)

velocities occur in September and October, 11.4–11.9 m s^{-1}, and in May (10.9 m s^{-1}). There is a characteristic decrease in wind velocities during the summer season in June–August to about 9.9 m s^{-1}. Dust events are mostly associated with S and SW winds. Such winds are dominant in the late season (July–September), while there is a considerable contribution of dust events with SE winds during the early season (May–June).

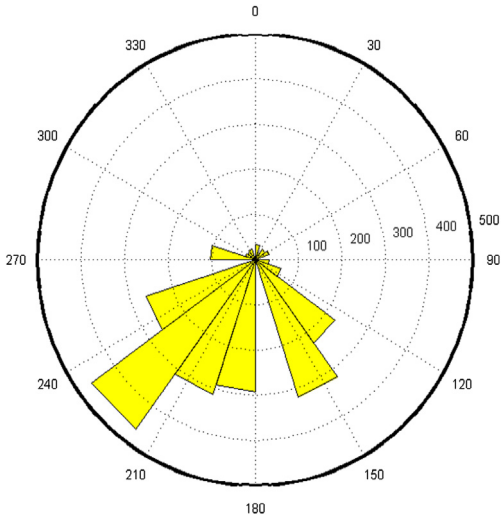

Fig. 7. Wind directions during dust events at all stations 1949–2011.

3.3. Dust event classification and aerosol dust concentrations

3.3.1. Dust event classes and climatology

Most of the dust events during the study period were classified within the 'suspended dust' class (46%) with visibility 10–30 km (Table 4). About 13% of dust events (192 dust days) had visibility <5 km. In total, we observed 14 severe dust storms with visibility less than 500 m.

The DE wind velocity generally increased with the DE severity as stated earlier. However, DE temperature was colder than average for the most severe DE classes (Table 4). The 'moderate haze' and 'suspended dust' had the highest DE temperatures because they occurred more often during the summer period (July–August).

The frequency of meteorological parameters of individual dust event classes from 1949 to 2011 is depicted in Fig. 10. Severe and moderate dust storm classes (visibility 0–1 km) were most often recorded in the 1950s and the 1990s but only once observed in the 2000s. About 50% of dust events had visibility <10 km in the 1950s. There is an increase in DE wind velocities within all classes between the 1990s and the 2000s. The DE temperatures of individual classes vary between stations during decades. The DE temperature when 'haze' classes were recorded, were warmer at the inland GS station in the 2000s compared to the 1990s but colder at the coastal RH station in the 2000s compared to the 1990s.

Duration of dust events in NE Iceland ranges from one day up to seven days of continuous dust observations. About 70% of the dust observations lasted one day or less, about 15% lasted two days and 7% for three days. More two- and three-day DEs were observed

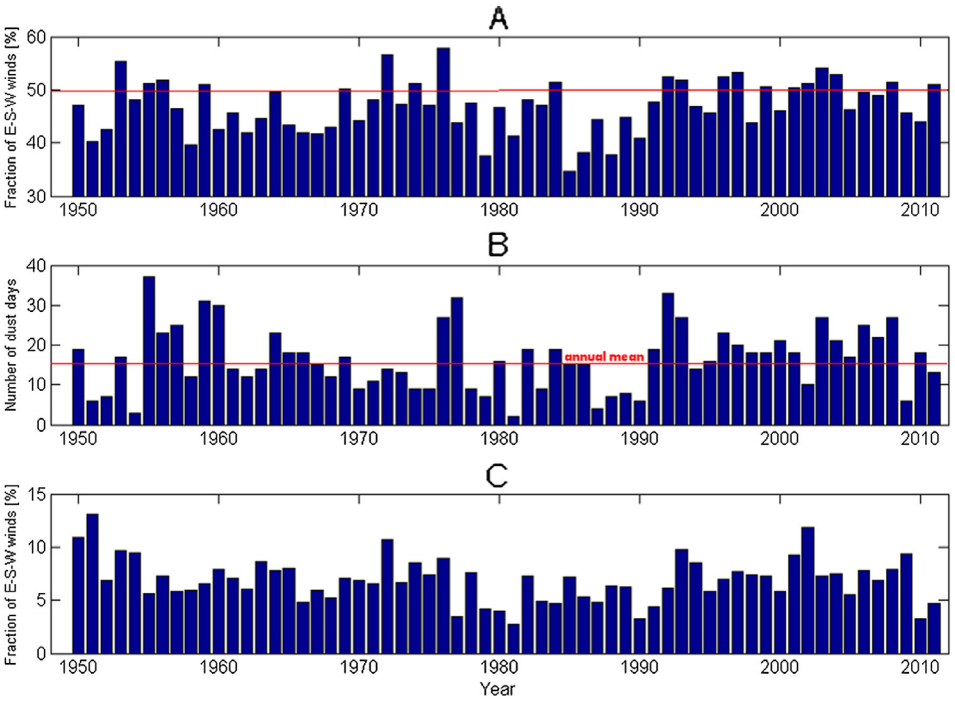

Fig. 8. Annual proportion of E–S–W (wind directions 100°–280°) winds of total winds. A-percentage of E–S–W winds of total wind observations at station GS, B-annual number of dust days, C-proportion of E–S–W winds exceeding wind speed of 8 m s^{-1} in May–November of total wind observations at station RH.

during the 1950's, but seven-day observations of moderately suspended dust were reported during the 2000s.

The Moderate Resolution Imaging Spectroradiometer (MODIS) flying on NASA's Terra satellite has captured many images of dust plumes blowing off the northern and northeastern coast of Iceland over the Arctic Ocean. Unfortunately, there are no clean pictures of severe or moderate dust storms in NE Iceland because of cloud cover over the region. One of the most severe events captured by MODIS was the 'severe haze' on September 17, 2008 (Fig. 11), which caused reduced visibility at GS station for seven days. The lowest visibility was observed as 1.5 km and mean wind velocity was about 19 m s^{-1}. Visible part of the plume extended >350 km (red line (in the web version)).

3.3.2. Relationship between visibility and dust concentration

3.3.2.1. Aerosol dust concentration formulas. Unfortunately, dust aerosol measurements are not made in NE Iceland and it is

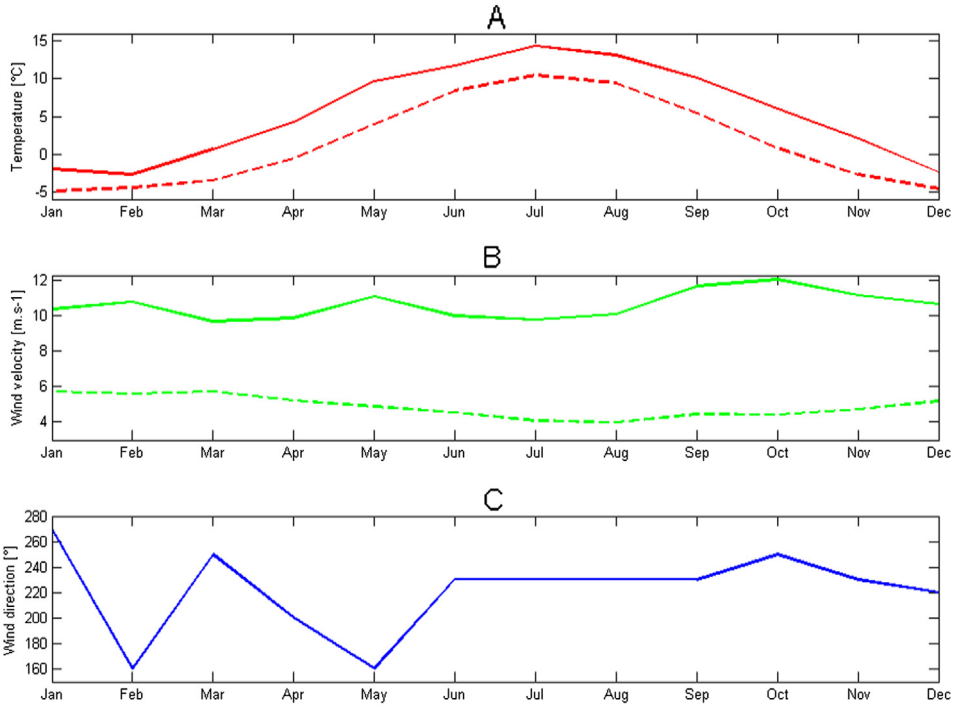

Fig. 9. Monthly mean values of meteorological parameters during dust events in 1949–2011. A-mean temperature, B-mean wind velocity, C-most frequent wind direction.

Table 4
Dust event classification based on visibility ranges, frequency of dust events in different classes and annual number of dust days. Mean wind velocity and mean temperature of each dust class are included.

Dust event class	Visibility (km)	Frequency (%)	Wind velocity ($m\ s^{-1}$)	Temperature (°C)	Number of dust days yr^{-1}
Severe dust storm	≤0.5	< 1	16.2	8.4	0.2
Moderate dust st.	0.5–1.0	2	14.9	9.4	0.5
Severe haze	1.0–5.0	10	13.0	10.6	2
Moderate haze	5.0–10.0	13	11.3	10.9	3
Suspended dust	10.0–30.0	46	9.9	10.6	10
Mod. susp. dust	30.0–70.0	27	10.2	10.0	7

therefore necessary to estimate the concentrations based on visibility observations. Several attempts have been made to relate visibility with total suspended particle concentration in the literature. D'Almeida (1986) found a good correlation ($r^2 = 0.95$) between horizontal visibility and PM_{10} during Saharan sand storms (Table 1). The green line in Fig. 12 shows calculated annual PM_{10} concentrations from DE visibility observations in NE Iceland using his formula. Wang et al. (2008) obtained formulas for visibility and PM_{10} mass concentration based on *in situ* measurements in desert, semi-desert and loess environments in Asia in 2001–2006. They obtained a strong relationship ($r^2 = 0.9$) between visibility and PM_{10} concentration. Leys et al. (2011) similarly calculated relationship for the famed 'Red Dawn' storm in Australia in 2003. Fig. 12 shows the mean annual PM_{10} dust concentrations during DE in NE Iceland using these formulas from different surfaces. The calculations suggest that the maximum mean annual concentration was obtained in 1988 when dust events caused on average concentration between 140 and 330 μg m^{-3}depending on which formula is used for the conversion. Generally the concentrations are lower in the 2000s. Concentrations calculated from DE visibility in Iceland are higher using formulas for steppe surfaces than for deserts. Using the formula derived for steppe conditions (Wang et al., 2008) resulted in the highest aerosol mass concentrations in

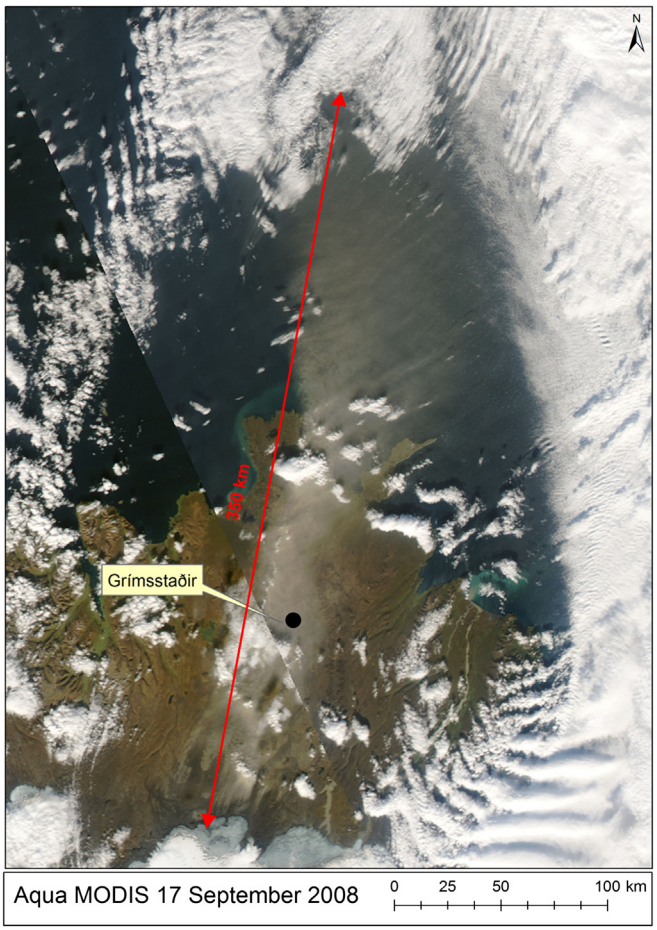

Fig. 11. Severe haze blowing off the northern coast of Iceland over the Arctic Ocean on September 17, 2008 (NASA, 2012).

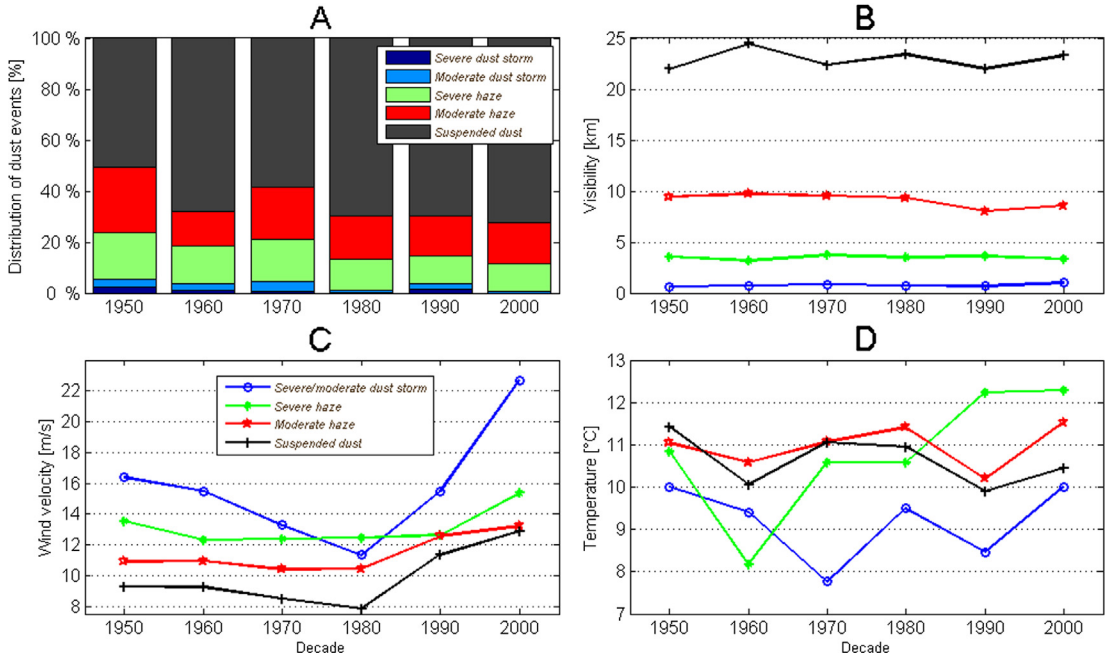

Fig. 10. Meteorological parameters of dust event classes 1949–2011. A-distribution of dust event classes; B-visibility range; C-wind velocities; D-temperature. Severe dust storm (visibility V ≤ 0.5 km), Moderate dust storm (V = 0.5–1 km), Severe haze (V = 1–5 km), Moderate haze (V = 5–10 km), Suspended dust (V = 10–30 km).

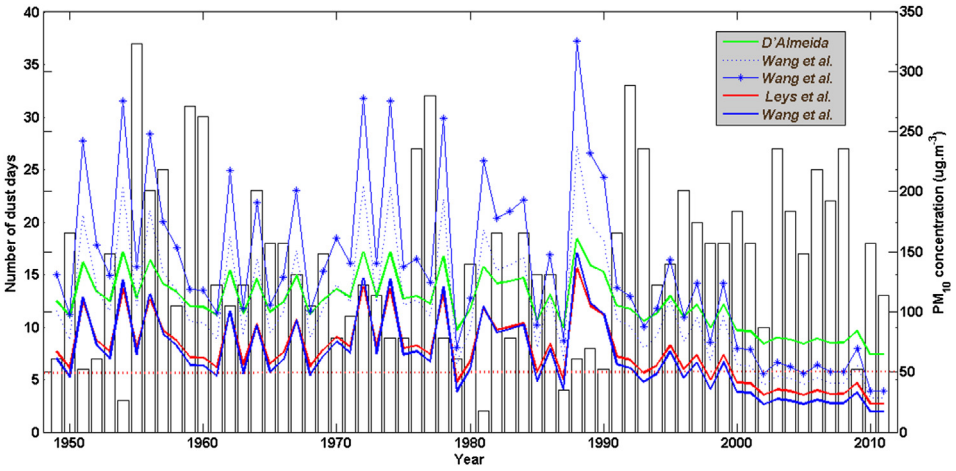

Fig. 12. Calculated mean annual PM_{10} concentration during dust events in NE Iceland based on formulas developed for different surfaces (formulas in Table 1). Bars depict number of dust days and lines indicate mean PM_{10} concentration during dust events. Blue lines are calculated values based on Asian surfaces (Wang et al., 2008), green line for African desert (D'Almeida, 1986), and red line for Australian desert (Leys et al., 2011). The European guideline determines the limit value for health protection 50 μg m^{-3} over 24 h (2008/50/EG available at http://eur-lex.europa.eu/LexUriServ/LexUriServ.do?uri=OJ:L:2008:152:0001:0044:EN:PDF). (For interpretation of the references to colour in this figure legend, the reader is referred to the web version of this article.)

general and most likely represents Icelandic fine glaciogenic sediments.

3.3.2.2. Seasonal variability in aerosol dust concentrations. Fig. 13 shows results for the mean and the median dust concentrations calculated from visibility using the formula from D'Almeida (1986). The mean dust concentration during dust events in NE Iceland is 237 μg m^{-3} during the period 1949–2011. Maximum is in April with 805 μg m^{-3}, a month which represents only 2% of total dust events. Median dust concentration is 106 μg m^{-3}, the highest in May and September (122 μg m^{-3}), followed by June, July and August. The highest frequency of the severe dust storms is also in September (37% of all severe dust storms) and May (21% of severe dust storms). Clearly, the highest median dust concentrations occurred during months with frequent dust events.

4. Discussion

Meteorological observations around major dust source regions worldwide include continuous atmospheric dust and sand observations. Annual mean of 16.4 dust days in NE Iceland is similar to that found in Iran (Jamalizadeh et al., 2008), more active than Utah (4.3 dust days $year^{-1}$; Steenburgh et al., 2012) but less frequent than in the northern part of Africa (up to 150 dust days $year^{-1}$; N'TchayiMbourou et al., 1997), Australia (50 dust storm days $year^{-1}$; Ekström et al., 2004), Mongolia (40 dusty days $year^{-1}$; Natsagdorj et al., 2003), or in active parts of China (35 dust days $year^{-1}$; Qian et al., 2002). As for the Arctic regions, Nickling (1978) observed 15 dust storms within 59 summer days in the Yukon Territory in 1972–1973, and Bullard (2013) recorded 7 days with high dust emissions in West Greenland in summer 2007. Dust activity can also be monitored by measuring deposition rates. Iceland rates

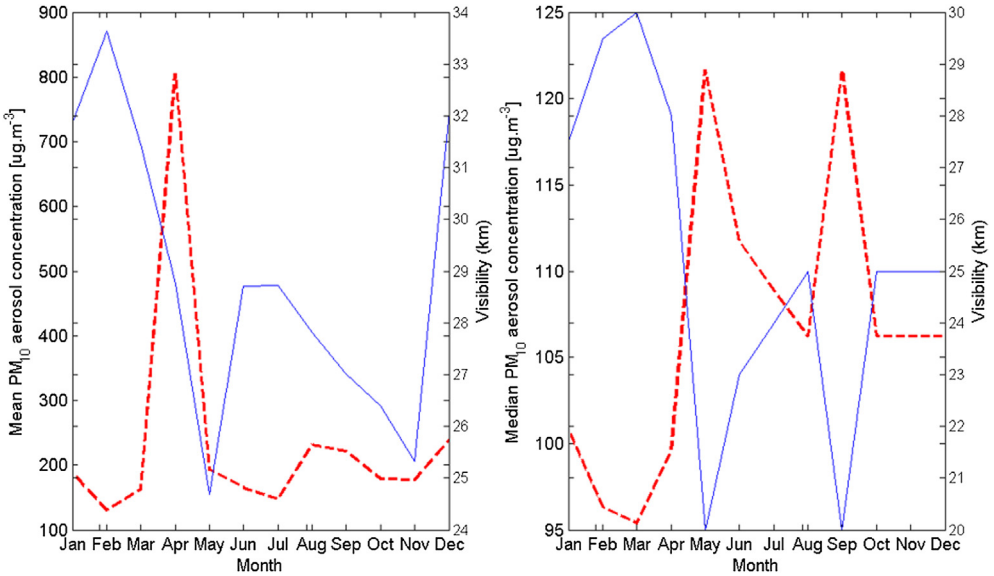

Fig. 13. Mean (left) and median (right) dust concentration of dust events. Red dashed line represents dust concentration and blue line shows visibility. (For interpretation of the references to colour in this figure legend, the reader is referred to the web version of this article.)

among the highest dust deposition areas worldwide (Arnalds, 2010; Bullard, 2013), indicating that large amount of sediments are released during the dust events. The major sources have been identified as glacial floodplains (Dyngjusandur, Fig. 1) and the sandy deserts north of the Vatnajökull glacier (Arnalds, 2010).

Trends in dust emissions vary between regions over the past six decades. Generally, dust activity was relatively high in the 1950s and 1960s, and low in the 1980s in the USA (Steenburgh et al., 2012), Australia (Ekström et al., 2004) and China (Qian et al., 2002). The 2000s were reported as the most active decade in Iran (Jamalizadeh et al., 2008). Long term trend in dust production in NE Iceland correlates well with these regions. Donarummo et al. (2002) found several dust periods in ice-cores during GISP2 project in Greenland. Two periods of high (1955–1960, 1975–1978) and one period of low (the 1980s) dust concentrations correlate with Icelandic dust trend between 1950 and 1990.

The dustiest year in NE Iceland was 1955 with 37 dust days. This year was dry and warm, but the year before had high precipitation in the Northeast Iceland. Hanna et al. (2004) reports the summer of 1955 as the warmest in the 20th century at Grímsey, an island of the coast of North Iceland. The same year had also a dust storm peak in the Tarim Basin, China, where 50 dust storms were recorded (Qian et al., 2004). The year 1955 was calculated with the highest total dust flux in Utah in 1950–2010 by Steenburgh et al. (2012). In China, year 1955 was one of the four most severe drought events in 1951–2009 (Wu et al., 2011) and part of extreme drought period 1952–1956 in the USA (Nace and Pluhowski, 1965). Worldwide peaks in dust production in the 1950s coincide with NE Iceland where higher temperatures and lower than average precipitation were measured at the time (Bjornsson and Jonsson, 2003; Hanna et al., 2004). There was a significant drop in temperature in NE Iceland in the late 1960s continuing through the 1970s. However, the annual temperature at inland stations in the 1990s had reached similar values as were observed in the 1950s (Bjornsson and Jonsson, 2003), which correlates well with increased DE frequency. Increased number of dust events in June in the 2000s is associated with dry and warm months of Junes in 2000, 2004, 2006 and 2007. For the 10 dustiest years in NE Iceland, the annual temperatures were above the average. This would result in peak discharge of water to the glaciofluvial floodplains that make up the main dust source area.

Dust is primarily emitted during southerly (SW–S–SE) winds. Spring DEs are often associated with SE winds. There was a drop in frequency of SE winds in the 1970s and the 1990s, compared to high frequency in the 1950s and the 1960s. SE winds were infrequent in May of the 2000s. Low dust occurrence in the 1980s coincides with low frequency of southerly winds (wind direction 100°–280°). Only about 40% of all winds blew from southerly directions and strong May–Nov southerly winds were also low (Fig. 8C). The springs of the 1980s were cold and with long lasting snow cover.

We found no significant correlation between high dust seasons and global climate drivers such the North Atlantic Oscillation (NAO), the Arctic Oscillation or prevailing ocean currents (Olafsson, 1999). The long term temperature and precipitation trends in Iceland are often in contrast to the North Hemisphere land averages or not consistent with the global averages (Hanna et al., 2004). Although the NAO correlations were not significant, they were highly suggestive of a possible relationship (Hanna et al., 2004; Bjornsson and Jonsson, 2003; Olafsson, 1999). Hanna et al. (2004) suggest the Iceland – southern Greenland – northwestern North Atlantic region is driven by special climatic conditions. Furthermore, Iceland is near one dipole of the NAO and the NAO is driving westerly winds, and therefore weakly correlated with DEs in the NE Iceland driven by southerly winds. However, there is an orthogonal pattern to NAO, described as a dipole of sea level pressure (SLP) field that is oriented east–west (Bjornsson and Jonsson, 2003). Low SLP west of Iceland (and/or high SLP east of Iceland) will lead to warm geostrophic southerly winds and if the east–west dipole is reserved it will turn to cold geostrophic northerly winds. DEs in the NE Iceland are linked with strong southerly winds and therefore with high SLP east of Iceland.

Dust events occur most frequently in June and September which coincides with July and August having more precipitation on average than June and September at the GS station. May is the driest month but occasionally with snow covering dust sources and thus with fewer dust days than later in the season. September and May feature the greatest wind speeds during active dust season which is in harmony with the average wind speed at inland stations (Bjornsson and Jonsson, 2003). Dust storms in Canada are most frequent in May–July when rivers are at low stage exposing freshly deposited sediments (Nickling, 1978). In contrast, DEs in Alaska occur predominantly in September when low precipitation and strong winds take place (Crusius et al., 2011). Such processes cause that highest frequency of severe dust storms (visibility < 500 m) in September also in Iceland.

Dust storms (visibility < 1 km) occur during the highest wind speeds and the lowest temperatures (Fig. 10). Mean DE wind velocity of 10.3 m s^{-1} corresponds to threshold value for aeolian transport 5–10 m s^{-1} reported from glacierised regions (Bullard, 2013), but Icelandic research reports common threshold values of 6–10 m s^{-1}(Arnalds et al., 2012).

The 1990s were most frequent in 'dust observations' with the events being more severe (lower visibility) than during the 2000s. This coincides with exceptionally high frequency of south-westerly winds exceeding wind speed of 8 m s^{-1} during the May–November period (Fig. 10C). The highest number of 'dust days' was recorded in the 2000s but DE visibility doubled (about 45–50 km) indicating less severe DEs in spite of strong southerly winds. This may indicate less availability of fine materials susceptible to dust production determined by changes in flow rate at the Jokulsa a Fjollum river in the 1990s and the 2000s, but the reason remains unclear.

Volcanic ash deposited during the 2010 Eyjafjallajokull and 2011 Grimsvotn eruptions caused serious dust storms in South Iceland (Schumann et al., 2011; Leadbetter et al., 2012; Petersen et al., 2012) but no increase was recorded in dust activity in NE Iceland after these events. This shows that fresh volcanic ash is not required for high occurrence of DE in NE Iceland although ash deposited there would undoubtedly increase the frequency in the region.

The major dust emissions are towards north over NE Iceland and further into the Arctic region. Icelandic dust periods correlate with published dust concentrations from Greenland (Donarummo et al., 2002). Furthermore, Drab et al. (2002) identified Icelandic dust in ice-core samples in central Greenland. Several forward trajectories during dust events in NE Iceland confirmed that air parcels were moved to central Greenland and further north. We therefore suggest that Iceland could be a long-term source of dust into the Arctic.

5. Conclusions

The severity and frequency of dust storms events in Northeast Iceland are comparable to many of the major dust areas of the world. In the long term, the most active aeolian area in NE Iceland is inland of Grimsstadir. There is great within-year and decadal variability in the frequency of the dust storms. The most active periods were during the 1950s and the period from the early 1990s until 2008. The study indicates that Icelandic dust may be a substantial source for not only local, but also larger scale air pollution in the Arctic.

Relating visibility observations obtained from long term weather records can give a comprehensive account of dust

frequency and behaviour on a regional basis. The results have relevance to a range of topics, such as on respiratory health research, aeolian deposition and ecosystem development both on land and sea, and by providing information about aerosol production on a regional scale in general.

Acknowledgement

This work was supported by the Nordic Centre of Excellence for Cryosphere–Atmosphere Interactions in a Changing Arctic Climate (CRAICC).

References

Arason, T., Rognvaldsson, O., Olafsson, H., 2010. Validation of numerical simulations of precipitation in complex terrain at high temporal resolution. Hydrology Research 41 (3–4), 164–170.
Arnalds, O., 2010. Dust sources and deposition of aeolian materials in Iceland. Icelandic Agricultural Sciences 23, 3–21.
Arnalds, O., Gisladottir, F.O., Orradottir, B., 2012. Determination of aeolian transport rates of volcanic soils in Iceland. Geomorphology 167-168, 4–12.
Arnalds, O., Thorarinsdottir, E.F., Metusalemsson, S., Jonsson, A., Gretarsson, E., Arnason, A., 2001. Soil Erosion in Iceland. Soil Conservation Service and Agricultural Research Institute, Reykjavik, p. 121.
Arnalds, O., Thorarinsdottir, E.F., Thorsson, J., Dagsson-Waldhauserova, P., Agustsdottir, A.M., 2013. An extreme wind erosion event of the fresh Eyjafjallajökull volcanic ash. Nature Scientific Reports 3, 1257.
Bjornsson, H., Jonsson, T., 2003. Climate and climatic variability at Lake Mývatn. Aquatic Ecology 38 (1), 129–144.
Blechschmidt, A.-M., Kristjansson, J.E., Olafsson, H., Burkhart, J.F., Hodnebrog, Ø., 2012. Aircraft-based observations and high-resolution simulations of an Icelandic dust storm. Atmospheric Chemistry and Physics Discussion 12, 7949–7984.
Bullard, J.E., 2013. Contemporary glacigenic inputs to the dust cycle. Earth Surface Processes and Landforms 38, 71–89.
CMA, 1979. Regulations of Surface Meteorological Observation, China. Meteorological Press, Beijing, pp. 21–27.
Crusius, J., Schroth, A.W., Gasso, S., Moy, C.M., Levy, R.C., Gatica, M., 2011. Glacial flour dust storms in the Gulf of Alaska: hydrologic and meteorological controls and their importance as a source of bioavailable iron. Geophysical Research Letters 38, L06602.
D'Almeida, G.A., 1986. A model for Saharan dust transport. Journal of Climate and Applied Meteorology 25, 903–916.
Donarummo, J.J., Ram, M., Stolz, M.R., 2002. Sun/dust correlations and volcanic interference. Geophysical Research Letters 29 (9), 75-1–75-4.
Drab, E., Gaudichet, A., Jaffrezo, J.L., Colin, J.L., 2002. Mineral particles content in recent snow at Summit (Greenland). Atmospheric Environment 36, 5365–5376.
Eldridge, F.R., 1980. Wind Machines, second ed. Van Nostrand Reinhold, New York.
Ekström, M., McTainsh, G.H., Chappell, A., 2004. Australian dust storms: temporal trends and relationships with synoptic pressure distributions (1960–99). International Journal of Climatology 24, 1581–1599.
Formenti, P., Schutz, L., Balkanski, Y., Desboeufs, K., Ebert, M., Kandler, K., Petzold, A., Scheuvens, D., Weinbruch, S., Zhang, D., 2011. Recent progress in understanding physical and chemical properties of African and Asian mineral dust. Atmospheric Chemistry and Physics 11, 8231–8256.
Grousset, F.E., Ginoux, P., Bory, A., Biscaye, P.E., 2003. Case study of a Chinese dust plume reaching the French Alps. Geophysical Research Letters 30 (6), 1277.
Hanna, E., Jonsson, T., Box, J.E., 2004. An analysis of Icelandic climate since the nineteenth century. International Journal of Climatology 24, 1193–1210.
Hugenholtz, C.H., Wolfe, S.A., 2010. Rates and environmental controls of aeolian dust accumulation, Athabasca River Valley, Canadian Rocky Mountains. Geomorphology 121, 274–282.
Husar, B.R., 2004. Transport of Dust: Historical and Recent Observational Evidence. In: The Handbook of Environmental Chemistry 4, pp. 277–294. Part G.
Hyslop, N.P., 2009. Impaired visibility: the air pollution people see. Atmospheric Environment 43, 182–195.
Jamalizadeh, M.R., Moghaddamnia, A., Piri, J., Arbabi, V., Homayounifar, M., Shahryari, A., 2008. Dust storm prediction using ANNs technique (a case study: Zabol city). Proceeding of World Academy of Science, Engineering and Technology 33, 529–537.
Leadbetter, S.J., Hort, M.C., von Löwis, S., Weber, K., Witham, C.S., 2012. Modeling the resuspension of ash deposited during the eruption of Eyjafjallajökull in spring 2010. Journal of Geophysical Research 117, D00U10.
Leys, J.F., Heidenreich, S.K., Strong, C.L., MsTainsh, G.H., Quigley, S., 2011. PM10 concentrations and mass transport during "Red Dawn" Sydney September 2009. Aeolian Research 3, 327–342.
McGowan, H.A., Sturman, A.P., Owens, I.F., 1996. Aeolian dust transport and deposition by foehn winds in alpine environment, Lake Tekapo, New Zealand. Geomorphology 15, 135–146.
Mountney, N.P., Russell, A.J., 2004. Sedimentology of cold climate Aeolian sand sheet deposits in the Askja region of northeast Iceland. Sedimentary Geology 166, 223–244.
N'TchayiMbourou, G., Berrand, J.J., Nicholson, S.E., 1997. The diurnal and seasonal cycles of wind-borne dust over Africa north of the equator. Journal of Applied Meteorology 36, 868–882.
Nace, R.L., Pluhowski, E.J., 1965. Drought of the 1950's with Special Reference to the Midcontinent in U.S. In: Geological Survey Water-Supply Paper No. 1804. United States Government Printing Office, Washington, D.C, p. 88.
Nickling, W.G., 1978. Eolian sediment transport during dust storms: Slims River Valley, Yukon Territory. Canadian Journal of Earth Sciences 15 (7), 1069–1084.
NASA, 2012. http://lance-odis.eosdis.nasa.gov/imagery/subsets/?subset=Iceland2.2008261.aqua.250 m (accessed 19.09.12.).
Natsagdorj, L., Jugder, D., Chung, Y.S., 2003. Analysis of dust storms observed in Mongolia during 1937–1999. Atmospheric Environment 37, 1401–1411.
Olafsson, J., 1999. Connections between oceanic conditions of N Iceland, Lake Mývatn temperature, regional wind direction variability and the North Atlantic Oscillation. Journal of Marine Research 16, 41–57.
Petersen, G.N., Björnsson, H., Arason, T., 2012. The impact of the atmosphere on the Eyjafjallajökull 2010 eruption plume. Journal of Geophysical Research 117, D00U07.
Prospero, J.M., Bullard, J.E., Hodgkins, R., 2012. High-latitude dust over the North, Atlantic: inputs from Icelandic proglacial dust storms. Science 335, 1078.
Qian, W.H., Quan, L., Shi, S., 2002. Variations of the dust storm in China and its climatic control. Journal of Climate 15, 1216–1229.
Qian, W.H., Tang, X., Quan, L.S., 2004. Regional characteristics of dust storm events in China. Atmospheric Environment 38, 4895–4907.
Quinn, P.K., Miller, T.L., Bates, T.S., Ogren, J.A., Andrews, E., 2002. A three-year record of simultaneously measured aerosol chemical and optical properties at Barrow, Alaska. Journal of Geophysical Research 107 (D11), 4130.
Raatz, W.E., 1984. Observations of "Arctic Haze" during the "Ptarmigan" weather reconnaissance flights, 1948–1961. Tellus 36B, 126–136.
Schumann, U., Olafsson, H., et al., 2011. Airborne observations of the Eyjafjalla volcano ash cloud over Europe during air space closure in April and May 2010. Atmospheric Chemistry and Physics 11, 2245–2279.
Steenburgh, W.J., Massey, J.D., Painter, T.H., 2012. Episodic dust events of Utah's Wasatch front and adjoining region. Journal of Applied Meteorology and Climatology. http://journals.ametsoc.org/doi/abs/10.1175/JAMC-D-12-07.1 (accessed 01.08.11.).
Tao, G., Liu, J.T., Yu, X., Kang, L., Fan, Y.D., Hu, Y.H., 2002. Objective pattern discrimination model for dust storm forecasting. Meteorological Applications 9, 55–62.
Tao, G., 2011. Environmental Science, Engineering and Technology: Dust Storms in Northern China. Nova Science Publishers, Inc, New York.
Thorarinsdottir, E.F., Arnalds, O., 2012. Wind erosion of volcanic materials in the Hekla area, South Iceland. Aeolian Research 4, 39–50.
The Icelandic Meteorological Office, 1981. Reglur um veðurskeyti og veðurathuganir, p. 85. [Weather Observer Handbook]. http://www.vedur.is/media/vedurstofan/utgafa/greinargerdir/1995/Reglur1981.pdf (accessed 24.01.13.).
Wang, Y.Q., Zhang, X.Y., Gong, S.L., Zhou, C.H., Hu, X.Q., Liu, H.L., Niu, T., Yang, Y.Q., 2008. Surface observation of sand and dust storm in East Asia and its application in CUACE/Dust. Atmospheric Chemistry and Physics 8, 545–553.
WHO, 2005. WHO Air Quality Guidelines Global Update 2005. Report on a Working, Group meeting, Bonn, Germany 18–20 October 2005.
Wu, Z.Y., Lu, G.H., Wen, L., Lin, C.A., 2011. Reconstructing and analyzing China's fifty-nine year (1951–2009) drought history using hydrological model simulation. Hydrology and Earth System Sciences 8, 1861–1893.

Paper VI

TECHNICAL PAPER

Long-term dust aerosol production from natural sources in Iceland

Pavla Dagsson-Waldhauserova,[1,2,*] Olafur Arnalds,[2] and Haraldur Olafsson[1,3,4]
[1]*University of Iceland, Reykjavik, Iceland*
[2]*Agricultural University of Iceland, Hvanneyri, Borgarnes, Iceland*
[3]*The Icelandic Meteorological Office, Reykjavik, Iceland*
[4]*Bergen School of Meteorology, Geophysical Institute, University of Bergen, Bergen, Norway*
[*]*Please address correspondence to: Pavla Dagsson-Waldhauserova, The University of Iceland, Sæmundargata 2, Reykjavik, IS 101, Iceland; e-mail: pavla@lbhi.is*

Iceland is a volcanic island in the North Atlantic Ocean with maritime climate. In spite of moist climate, large areas are with limited vegetation cover where >40% of Iceland is classified with considerable to very severe erosion and 21% of Iceland is volcanic sandy deserts. Not only do natural emissions from these sources influenced by strong winds affect regional air quality in Iceland ("Reykjavik haze"), but dust particles are transported over the Atlantic ocean and Arctic Ocean >1000 km at times. The aim of this paper is to place Icelandic dust production area into international perspective, present long-term frequency of dust storm events in northeast Iceland, and estimate dust aerosol concentrations during reported dust events.

Meteorological observations with dust presence codes and related visibility were used to identify the frequency and the long-term changes in dust production in northeast Iceland. There were annually 16.4 days on average with reported dust observations on weather stations within the northeastern erosion area, indicating extreme dust plume activity and erosion within the northeastern deserts, even though the area is covered with snow during the major part of winter. During the 2000s the highest occurrence of dust events in six decades was reported. We have measured saltation and Aeolian transport during dust/volcanic ash storms in Iceland, which give some of the most intense wind erosion events ever measured.

Icelandic dust affects the ecosystems over much of Iceland and causes regional haze. It is likely to affect the ecosystems of the oceans around Iceland, and it brings dust that lowers the albedo of the Icelandic glaciers, increasing melt-off due to global warming. The study indicates that Icelandic dust may contribute to the Arctic air pollution.

Implications: Long-term records of meteorological dust observations from Northeast Iceland indicate the frequency of dust events from Icelandic deserts. The research involves a 60-year period and provides a unique perspective of the dust aerosol production from natural sources in the sub-Arctic Iceland. The amounts are staggering, and with this paper, it is clear that Icelandic dust sources need to be considered among major global dust sources. This paper presents the dust events directly affecting the air quality in the Arctic region.

Introduction

Iceland is a volcanic island in the North Atlantic Ocean with maritime climate, mild and moist winters, and cool summers. In spite of its moist climate, large areas are with limited vegetation cover where >40% of Iceland is classified as having considerable to very severe erosion and 21% of Iceland is volcanic sandy deserts (Arnalds et al., 2001). Not only do dust emissions from these natural sources influenced by strong winds affect regional air quality in Iceland ("Reykjavik haze"), but dust particles are transported over Atlantic Ocean more than 1000 km at times (Arnalds, 2010). Dust aerosol causes regional haze during or after dust events. Furthermore, Iceland is located in one of the main atmospheric transport pathways to the Arctic and dust pollution from natural sources is transported over northeast Iceland toward the Arctic Ocean (Rekacewicz, 2005). Globally, fine dust particles may be transported at altitudes of up to 6 km and can be carried distances of up to 6,000 km (Sivakumar, 2005). Dust is considered to contribute to the Arctic haze phenomena (Quinn et al., 2002).

The global dust belt, where most of the dust sources are located, extends from Africa, through the Middle East, into Central Asia (Formenti et al., 2011). In this study, the long-term frequency of dust events in Northeast Iceland is compared with major world arid regions such as in the United States (Steenburgh et al., 2012), Australia (Ekström, McTainsh, and Chappell, 2004), Mongolia (Natsagdorj, Jugder, and Chung, 2003), the northern part of Africa (N'TchayiMbourou et al., 1997), China (Qian, Quan, and Shi,' 2002), and Iran (Jamalizadeh et al., 2008). These papers show that long-term annual means of days with dust are about 150 days per year in the northern part of Africa, about 50 dust storm days in Australia, about 40 dusty days in Mongolia, up to 35 dust days in active regions of China, about 25 dusty days in Iran, and 4.3 dust events per year in Utah in the United States. Long-term dust activity was significantly greater during the 1950s and 1960s except in

Journal of the Air & Waste Management Association, 00(00):1–8, 2013. ISSN: 1096-2247 print
DOI: 10.1080/10962247.2013.805703

Africa and Mongolia. Dust observations were frequent in Mongolia, Africa, and Iran during the 1980s.

The World Health Organization presents annual a $PM_{2.5}$ concentration standard of 10 $\mu g\ m^{-3}$ and an estimated visibility of 67 km to indicate health risk, or daily standard of 35 $\mu g\ m^{-3}$ and visibility range of 31 km (WHO, 2005). In comparison, visual range can be more than 300 km in dry climates and 100 km in humid climates on clear days (Hyslop, 2009).

Meteorological observations in dust-source regions worldwide include continuous atmospheric dust and sand observations. Visibility is a parameter that is used as an important indicator of the severity of dust events where no in situ measurement of aerosol concentration is provided. Long-term visual observations of atmospheric dust are available in Iceland. Many of the manned weather stations are located downwind of major dust sources. These stations record conventional meteorological parameters, including visibility. Many of these stations have been in continuous operation for more than 60 years, and the data acquired at these stations are ideal for studying long-term variability in dust production and severity of historical dust events. The aim of this paper is to place Icelandic dust production areas into an international perspective, present long-term frequency of dust storm events in northeast Iceland, and estimate dust aerosol concentrations during reported dust events.

Methods

A network of eight weather stations in proximity to the dust sources for northeast Iceland was chosen for the study. Many of these stations, which are run by the Icelandic Meteorological Office, have been in continuous operation for more than 60 years. Figure 1 depicts the location of the stations at Akureyri, Egilsstaðir, Grimsstaðir, Raufarhöfn, Staðarholl, Vopnafjörður, Kollaleira, and additionally Hveravellir. Hveravellir is located on the notional border between northeast and southwest Iceland and is the only weather station in central Iceland. The data are stored at the Icelandic Meteorological Office after being submitted to strict quality control.

Meteorological observations with present weather (codes for dust observations) and related visibility were used to identify the frequency and the long-term changes in dust production in Northeast Iceland. Present weather refers to atmospheric phenomena occurring at the time of observation, or which has occurred preceding the time of observation. In this study only atmospheric phenomena such as for "moldrok" (blowing soil/dust), "sandfok" (blowing sand/dust), "sandbylur" (extreme blowing sand/dust), and codes for dust haze, suspended dust, blowing dust, and dust whirls, are used and defined as a "dust observation." The synoptic codes (ww) for present weather that refer to dust observation are 7–9, 30–35, and 4–6 only if the codes for primary or secondary past weather (ww_1, ww_2) are 3 for blowing soil, dust, sand, and dust storm. At all stations, the weather is observed every day of the year three to eight times per day.

The initial data set was built from the occurrence of "dust observations" made at one or more weather stations. Long-term dust activity is expressed in dust days. "Dust day" is defined as a day when at least one station recorded at least one dust observation.

Unfortunately, dust aerosol measurements are not made in northeast Iceland and it is therefore necessary to estimate the concentrations based on visibility observations. Several methods

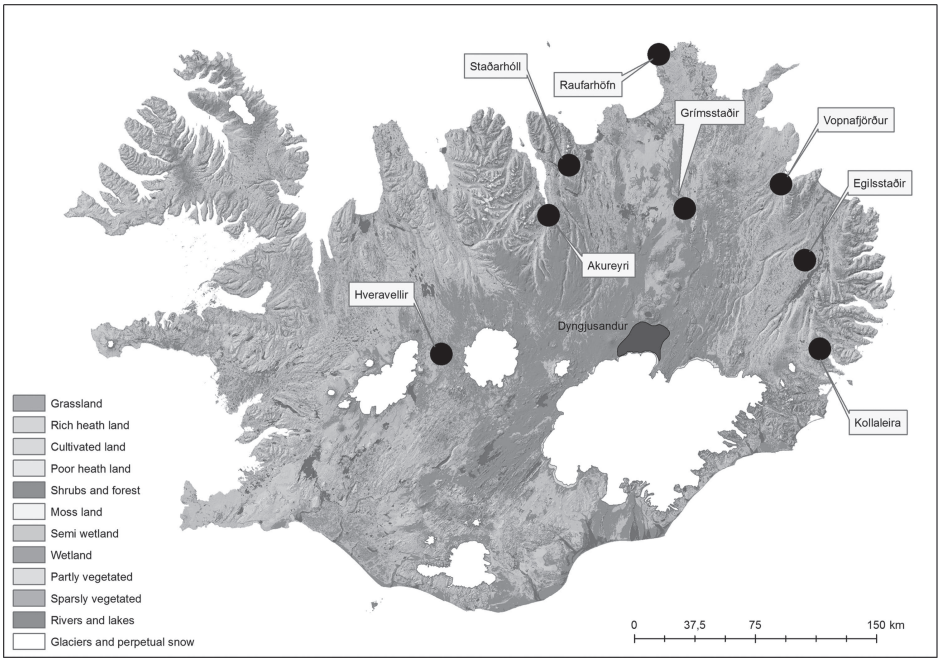

Figure 1. The locations of weather stations in northeast Iceland (Akureyri, Egilsstaðir, Grímsstaðir, Raufarhöfn, Staðarholl,Vopnafjörður, and Kollaleira) and station in central Iceland (Hveravellir). The major dust source for northeast Iceland is Dyngjusandur (marked red).

have been developed to relate visibility with total suspended particle concentration. D'Almeida (1986) found a good correlation ($r^2 = 0.95$) between horizontal visibility and PM_{10} in the 0.2 to 40 km range (shown in eq 1). This relationship was obtained during measurements with the Mainz sun photometer during Saharan sand storms in 1981–1982. In the present study, Aeolian dust concentrations were derived from eq 1 based on conversion between horizontal visibility and suspended particle concentration presented by D'Almeida (1986).

The aerosol dust concentration formula estimated from visibility and PM_{10} concentration is

$$PM_{10} = aV^{-b} + c \quad (1)$$

where PM_{10} is the particulate matter concentration in $\mu g\ m^{-3}$, V is the horizontal visibility in km, and a, b, and c are coefficients (a is set to 914.06, b is set to –0.73, c is 19.03).

Dust events were classified from visibility ranges (Table 1) based on criteria in Leys at al. (2011) and Wang et al. (2008). Dust events with visibility less than 500 m are often classified as "severe dust storms." This classification is used in the present study. Dust events with observed visibility above 10 km have been used in the literature to represent floating dust or suspended dust (Natsagdorj et al., 2003). In this study we classify a dust event in the visibility range 11–30 km as "suspended dust" and for the visibility range above 30 km it is called "moderate suspended dust."

Results and Discussion

Frequency and temporal variability in dust production

There were annually 16.4 days on average with reported dust observations on weather stations in northeast Iceland in 1949–2011. This indicates extreme dust plume activity and erosion within the northeastern deserts, even though the area is covered with snow during the major part of the 6- to 8-month-long winter. Such an annual mean is similar to that found in Iran (Jamalizadeh et al., 2008), and more active than Utah (4.3 dust days/yr; Steenburgh et al., 2012), but much less frequent than in Africa north of the equator (up to 150 dust days/yr; N'TchayiMbourou et al., 1997).

Table 1. Dust event classification based on visibility categories; mean visibility of each dust class is calculated into PM_{10} concentration using the formula in D'Almeida (1986)

Dust event class	Visibility (km)	PM_{10} concentration ($\mu g\ m^3$)
Severe dust storm	≤0.5	19,753
Moderate dust storm	>0.5–1.0	10,062
Severe haze	>1.0–5.0	385
Moderate haze	>5.0–10.0	201
Suspended dust	>10.0–30.0	112
Moderate suspended dust	>30.0–70.0	67

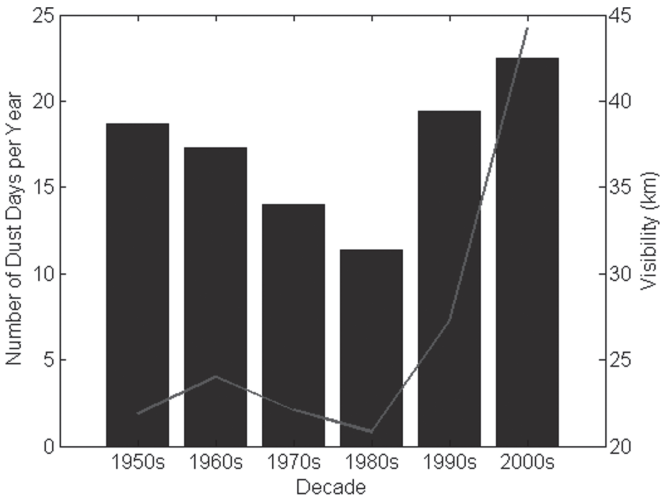

Figure 2. Total number of dust days per year in decade. Solid line represents mean visibility during the dust events.

The number of dust days for each decade from 1950 to 2010 is shown in Figure 2. The first decade of the 2000s had the highest occurrence of dust days in northeast Iceland and also in Iran (Jamalizadeh et al., 2008). Contrarily, the 1980s was the least active decade, which coincides with trends in the United States (Steenburgh et al., 2012), China (Qian et al., 2002), and Australia (Ekström et al., 2004). The most active decade, the first decade in the 2000s, has double the mean frequency compared to the least active decade, the 1980s. The occurrence of total "dust observations" is, however, the highest in the 1990s and during the first decade of the 2000s. In the long term, the most active periods were the 1950s and the period from the early 1990s until 2008. Worldwide peaks in dust production in the 1950s coincide with a period in northeast Iceland with higher temperatures and lower than average precipitation (Bjornsson and Jonsson, 2003). There was a significant drop in temperature in northeast Iceland in the late 1960s continuing through the 1970s. However, the annual temperature at inland stations reached values in the 1990s similar to those observed in the 1950s (Bjornsson and Jonsson, 2003), which correlates well with increased dust event frequency.

The mean visibility during all dust observations was 26.7 km (shown as the solid line in Figure 2). It was lowest during the 1980s, 20.8 km, and highest for dust observations during the 2000s, up to 44 km. Dust event visibility during the 1950s and the 1970s was about 22 km, 24 km in the 1960s, and 27 km in the 1990s. After the year 2000, there is the highest occurrence of dust days but reported dust event visibility is almost double compared to the other decades. Severe dust events occurred less frequently in the 2000s than during the decades 1950 to 1990 (see Figure 6, shown later).

In total, 1033 dust days were reported in Northeast Iceland during the six decades. The annual variability in the number of dust days is shown in Figure 3. The most active year was 1955, with 37 reported dust events with an average visibility of 23.2 km, about 3 km less than mean dust day visibility. The same year had also dust storm peak in the Tarim Basin, China, where 50

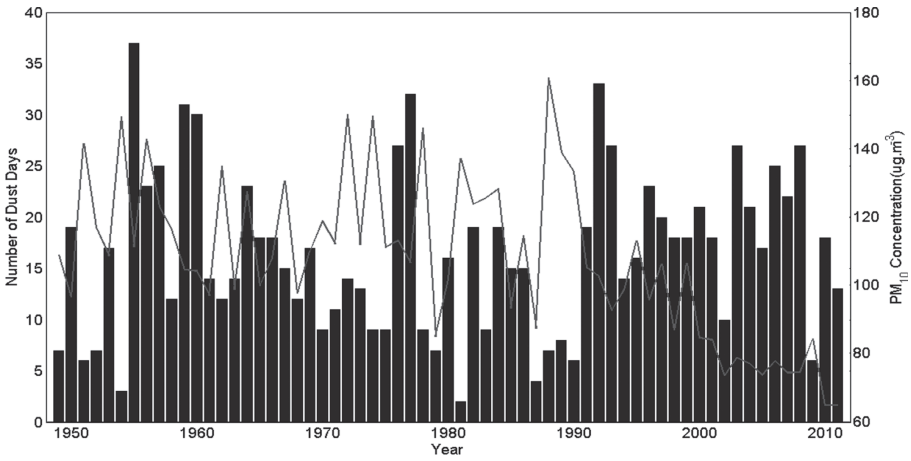

Figure 3. Number of dust days (bars) and calculated mean annual PM_{10} concentration from visibility during dust events (solid line).

dust storms were recorded (Qian, Tang, and Quan, 2004). The year 1955 was calculated with the highest total dust flux in Utah in 1950–2010 by Steenburgh et al. (2012). The mean visibility during dust days varies and is notably low in 1954, 1972, 1974, and 1978. The lowest mean annual visibility during dust observations (12.8 km) was recorded in 1988 when dust events of high severity were observed. There was a severe dust event on June 18, 1988, which has been used to illustrate a severe dust storm, the so-called "June 88 storm" (Arnalds and Gisladottir, 2009). Generally, visibility during dust events increased during the first decade of the 2000s with a maximum in 2010.

Spatial variability in dust production

There is considerable variability between weather stations in the total number of dust observations recorded in northeast Iceland. The Grimsstaðir station has by far the greatest frequency of the eight weather stations, with 70% (1685 dust observations) of the total 2387observations over the 63 recorded years. Egilsstaðir counts 368 dust observations, followed by 132 observations at Hveravellir, and less than 100 observations at each of the other stations. The lowest number of dust days occurred in the 1980s but with more evenly spread observations between the weather stations. The Egilsstaðir station observed the most dust events in the 1980s, and the fewest events in the 1990s, but dust monitoring was discontinued there in 1998. Low occurrence of dust events in the 1980s coincides with low frequency of moderate or strong southerly winds (wind direction 100–280°). Only about 40% of all winds blew from southerly directions, which are the most frequent winds responsible for the majority of the dust events in northeast Iceland.

The highest frequency of dust observations is clearly at the inland stations, which are closer to the inland dust sources than the coastal areas. The Grimsstaðir station is the most active station, with more than 12 dust days reported annually. It is located in the vicinity of a local dust-source area and downwind from the Dyngjusandur dust plume source. The second is the Egilsstaðir station with almost 4 dust days annually. More than half of the stations observe <1 dust day annually. The average dust event visibility at these stations is about 25 km. The lowest dust event visibility was at the Raufarhöfn station. It is located at the open ocean and might be influenced by easier coagulation of dust particles and water (fog) droplets in humid areas.

Aerosol dust concentration

Aerosol dust concentration during dust events was estimated from visibility observation based on conversion between horizontal visibility and suspended particle concentration presented in a paper by D'Almeida (1986). Dust is expected to absorb weakly solar radiation, it scatters light, and it is coarse. However, Icelandic dust is of volcanic origin and the particles are darker than the Saharan dust studied by D'Almeida (1986). The optical properties of Icelandic volcanic dust correspond to stronger absorption and weaker scattering at longer wavelengths than the Saharan mineral dust (Weinzierl et al., 2012). As the optical properties of the volcanic dust in Iceland are not known and may differ considerably from properties of the Saharan dust, the present calculations of the dust loadings are associated with considerable uncertainties. Figure 3 depicts the mean annual PM_{10} dust concentrations during the dust events in northeast Iceland in 1949–2011. The maximum mean annual concentration of 160 μg $m^{-3}$was obtained in 1988 when dust events of high severity with annual mean visibility of 12.8 km were observed. Total median dust concentration of all dust events was calculated as 106 μg m^{-3} with maxima in May and September (122 μg m^{-3}). Mean dust concentration during dust events in northeast Iceland is 199 μg m^{-3}. Maximum mean with 805 μg m^{-3} is in April, the month that represents only 2% of total dust events. Highest frequency of the severe dust storms occurs also in September (37% of all severe dust storms) and May (21% of severe dust storms). Clearly, the highest median dust concentrations are confined to months with high dust event occurrence (Figure 4 and Figure 5).

Generally, visibility during dust events has doubled after 2000, and thus the calculated PM_{10} concentrations of dust events decreased (Figure 3). All the annual dust aerosol means exceeded the European guideline, which determines the limit

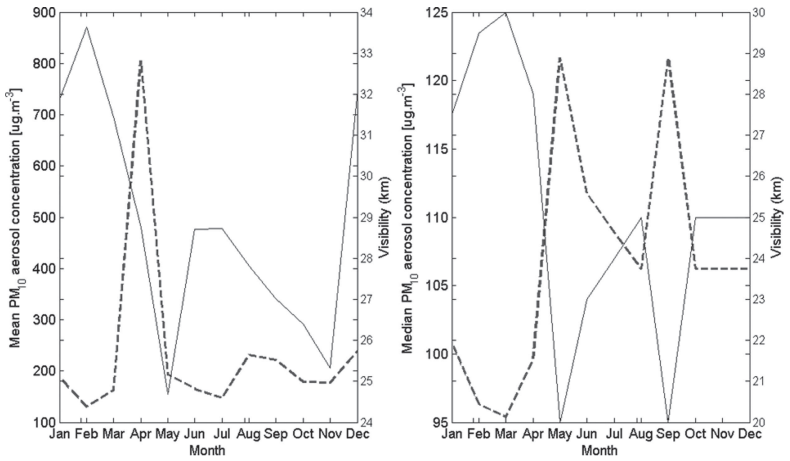

Figure 4. Mean (left) and median (right) dust concentration of dust events. Dashed line represents dust concentration and solid line shows visibility.

value for health protection as 50 μg m^{-3} over 24 hr (http://ec.europa.eu/environment/air/quality/standards.htm).

Dust event classification

Most of the dust events during the study period were classified within the "suspended dust" class (46%) with visibility 10–30 km (Table 2). There were annually 10 events of suspended dust on average, 7 events of moderate suspended dust, and less than 3 events of higher severity (Table 2). Of all the dust events, about 13% (192 dust days) had visibility less than 5 km. The two dust storm classes (visibility 0–1 km) were most often recorded in the 1950s and the 1990s but only once observed in the 2000s (Figure 6). About 50% of dust events had visibility <10 km in the 1950s. In total, there were 14 severe dust storms from 1949 to 2011 (about 1% of dust events). Severe events are less frequent in northeast Iceland compared to Australia (20%; Ekström et al., 2004), but more often than in Utah where no severe dust storm was observed (Steenburgh et al., 2012). About 37 % of severe dust storms occurred in September, which is the month of highest median dust concentration during dust events (Figure 4).

Duration of dust events in northeast Iceland ranges from 1 day up to 7 days of continuous dust observations. About 70% of dust observations lasted 1 day or less, about 15% lasted 2 days, and 7% lasted for 3 days. More 2- and 3-day dust events were observed during the 1950s, but 7-day observations of moderately suspended dust were reported in the 2000s.

The Moderate Resolution Imaging Spectroradiometer (MODIS) flying on NASA's Terra satellite has captured many images of dust plumes blowing off the northern and northeastern coast of Iceland over the Arctic Ocean. Unfortunately, there are no clean pictures of severe or moderate dust storms without the cloud cover available. The most severe event captured by MODIS was the severe haze on September 17, 2008, which caused reduced visibility at the Grimsstaðir station for 7 days (Figure 7). The lowest visibility was observed as 1.5 km and mean wind velocity was about 19 m sec^{-1}. The visible part of the plume extended 350 km (solid line). For this event, the 3-day forward trajectory was calculated using the National Oceanic and Atmospheric Administration (NOAA) Hybrid Single Particle Lagrangian Integrated Trajectory model (HYSPLIT), showing that air parcels originating in northeast Iceland moved northward and reached 1800 km in distance within 24 hr (NOAA, 2012). Fine dust particles could have been uplifted

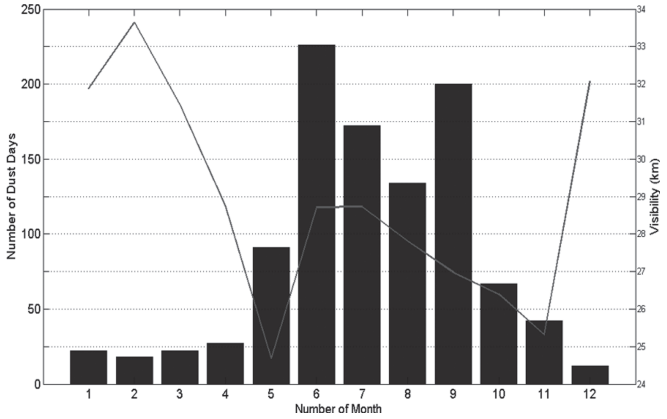

Figure 5. Number of dust days per month (bars) and monthly means of dust visibility (solid line) for the period 1949–2011.

Table 2. Dust event classification based on visibility ranges; frequency and annual number of dust days are included

Dust event class	Visibility (km)	Frequency (%)	Number of dust days/yr
Severe dust storm	≤0.5	<1	0.2
Moderate dust storm	>0.5–1.0	2	0.5
Severe haze	>1.0–5.0	10	2
Moderate haze	>5.0–10.0	13	3
Suspended dust	>10.0–30.0	46	10
Moderatd suspended dust	>30.0–70.0	27	7

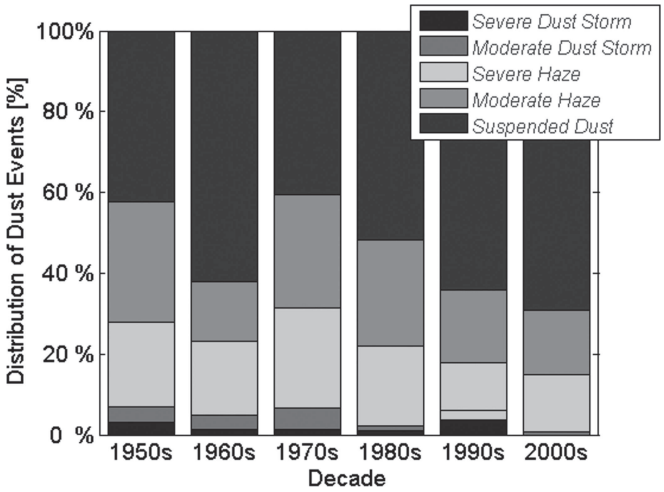

Figure 6. Distribution of dust event classes during decades in 1950–2010.

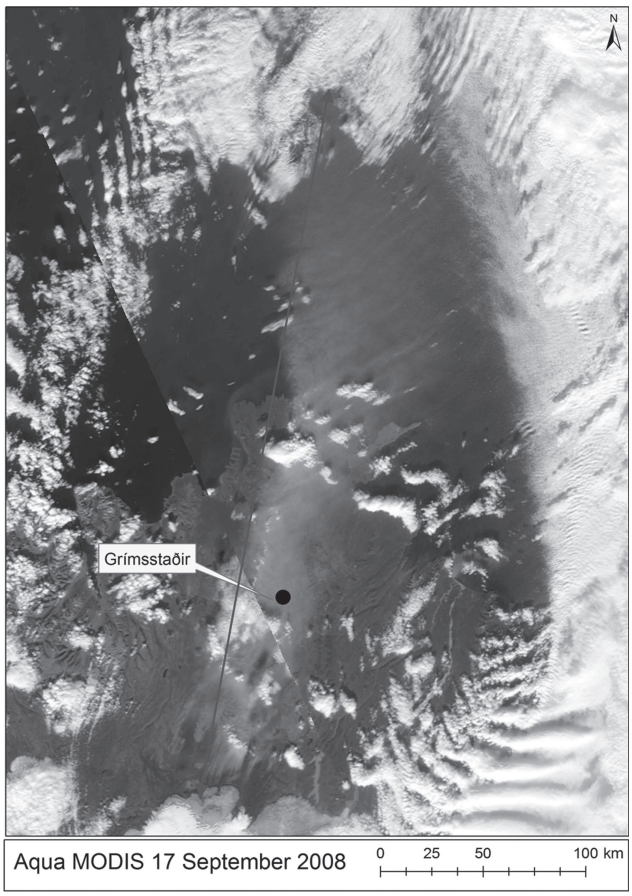

Figure 7. Severe haze blowing from Dyngjusandur and off the northern coast of Iceland over the Arctic Ocean on September 17, 2008 (NASA, 2012).

above the Greenland's ice sheet during the first day and travelled about 3,500 km through the Ellesmere Island to the Somerset Island within 3 days (Figure 8). Unfortunately, in situ measurements at Greenland's station Alert are not available for these dates.

Icelandic dust has been identified in ice-core samples in central Greenland (Drab et al., 2002). The prevailing winds of dust events in northeast Iceland are southerly (wind directions 130–250°). The major deposition area is over the Greenland Sea, and several trajectories of severe dust events were traced over Greenland and further into the Arctic. Dust deposition on snow or sea ice may affect the snow albedo and melting rate, while deposition over the sea may increase the ocean productivity. Chemical composition of Icelandic dust differs depending on the local dust sources. The Dyngjusandur source mainly corresponds to basaltic volcanic glasses formed below Vatnajökull glacier during subglacial eruptions (Baratoux et al., 2011). The major elements are SiO_2, Al_2O_3, Fe_2O_3, and CaO. The Dyngjusandur sediment has little of quartz-rich materials but contains of more Al_2O_3, Fe_2O_3, and CaO than crustal dust. The higher iron content of the Dyngjusandur re-suspended sediments may be an essential micronutrient in marine biota in the Arctic Ocean. Frequent dust events in September may increase the ocean productivity, as the bloom ends in summer and productivity is known to be iron-limited (Prospero, Bullard, and Hodgkins, 2012).

Recent changes in dust production

High severity and low visibility of dust events in the 1990s but the highest dust day frequency and high dust event visibility in the 2000s indicate changes in the environment of northeast Iceland. Such a trend could indicate that a large amount of material was transported during the 1990s but less material during the 2000s even though the frequency of dust days was higher. However, this could reflect lower availability of fine materials susceptible to dust production due to changes in the flow rate of the Jokulsa a Fjollum river in the 1990s and the 2000s, but the reason remains unclear. We found no significant correlation between high dust seasons and global climate drivers or any link to the local meteorological conditions. It is interesting to note that a volcanic ash deposited during the 2010 Eyjafjallajokull and 2011 Grimsvotn eruptions did not increase dust activity in Northeast Iceland (Figure 3). This shows that freshly deposited volcanic material is not the main source for dust mobilization in northeast Iceland during this period.

Conclusions

Dust affects the ecosystems over much of Iceland. The severity and frequency of dust events in northeast Iceland are comparable to many of the major dust areas of the world (Arnalds et al., 2013). There is great variability in the frequency of the dust events both within year and when measured by decade. The most active periods were the 1950s and the period from the early 1990s until 2008. The study indicates that Icelandic dust is not only a substantial source for regional air pollution, but may contribute to Arctic air pollution.

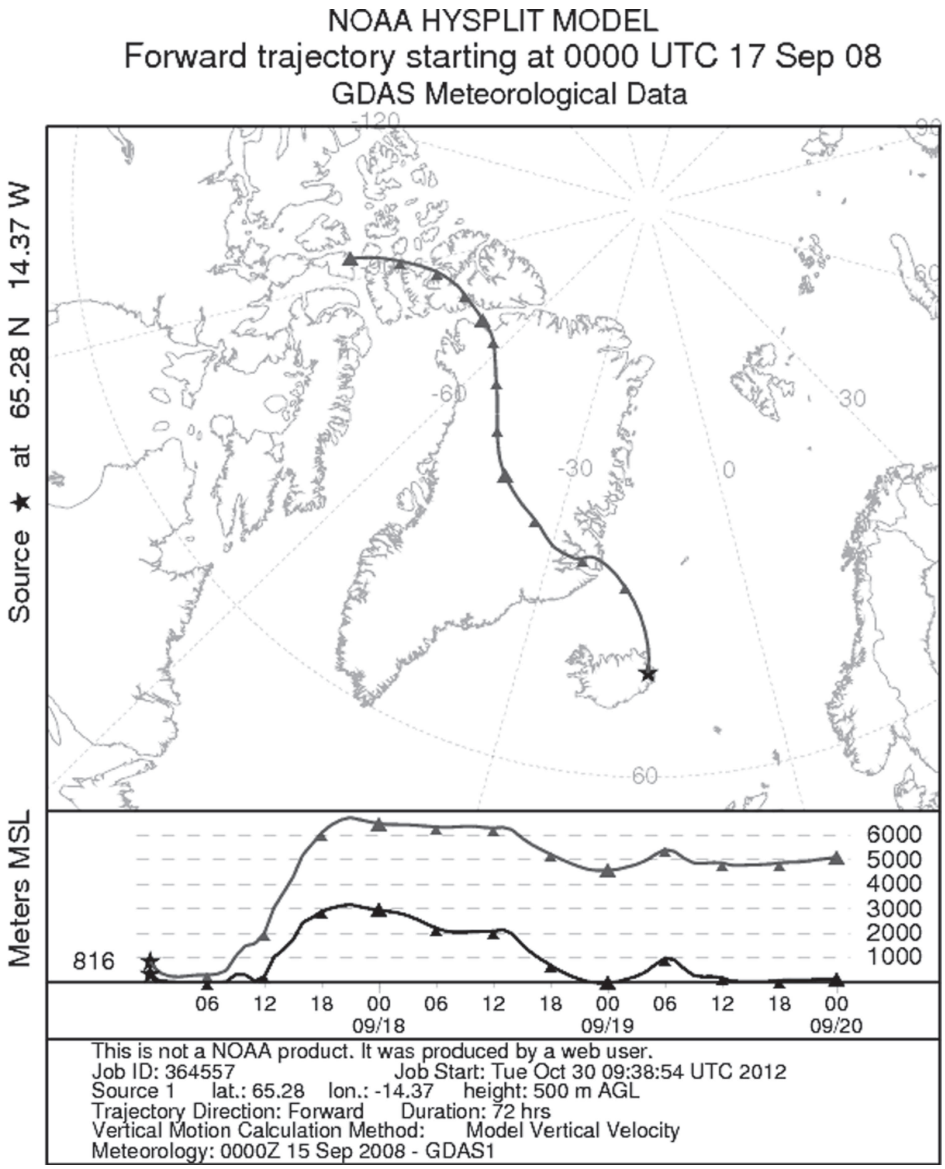

Figure 8. NOAA HYSPLIT 72-hr forward trajectory for air parcels released in northeast Icleand during the severe haze on September 17, 2008 (NOAA, 2012).

References

Arnalds, O. 2010. Dust sources and deposition of aeolian materials in Iceland. *Icelandic Agricultural Sciences* 23: 3–21.

Arnalds, O., E.F. Thorarinsdottir, S. Metusalemsson, A. Jonsson, E. Gretarsson, and A. Arnason. 2001. *Soil Erosion in Iceland*. Reykjavik, Iceland: Gutenberg.

Arnalds, O., and F.O. Gisladottir. 2009. Erosion measurements at Holsfjoll, NE Iceland. Agricultural University of Iceland, Hvanneyri. LBHI Report No. 25.

Arnalds, O., E.F. Thorarinsdottir, J. Thorsson, P. Dagsson-Waldhauserova, and A.M. Agustsdottir. 2013. An extreme wind erosion event of the fresh Eyjafjallajökull volcanic ash. *Nature Scientific Reports* 3: 1257. doi:10.1038/srep01257

Baratoux, D., N. Mangold, O Arnalds, J.-M. Bardintzeff, B. Platevoet, M. Grégorie, and P. Pinet. 2011. Volcanic sands of Iceland—Diverse origins of Aeolian sand deposits revealed at Dyngjusandur and Lambahraun. *Earth Surf. Proc. Land.* 36: 1789–1808.doi:10.1002/esp.2201

Bjornsson, H., and T. Jonsson. 2003. Climate and climatic variability at Lake Mývatn. *Aquat. Ecol.* 38(1): 129–144.

D'Almeida, G.A. 1986. A model for Saharan dust transport. *J. Climate Appl. Meteorol.* 25: 903–916. doi:10.1175/1520-0450(1986)025<0903:AMFSDT>2.0.CO;2

Drab, E., A. Gaudichet, J.L. Jaffrezo, and J.L. Colin. 2002. Mineral particles content in recent snow at Summit (Greenland). *Atmos. Environ.* 36: 5365–5376. doi:10.1016/S1352-2310(02)00470-3

Ekström, M., G. McTainsh, and A. Chappell. 2004. Australian dust storms: temporal trends and relationships with synoptic pressure distributions (1960–99). *Int. J. Climatol*. 24: 1581–1599. doi:10.1002/joc.1072

Formenti, P., L. Schutz, Y. Balkanski, K. Desboeufs, M. Ebert, K. Kandler, A. Petzold, D. Scheuvens, S. Weinbruch, and D. Zhang. 2011. Recent progress in understanding physical and chemical properties of African and Asian mineral dust. *Atmos. Chem. Phys*. 11:8231–8256. doi:10.5194/acp-11-8231-2011

Hyslop, N.P. 2009. Impaired visibility: the air pollution people see. *Atmos. Environ.*43: 182–195. doi:10.1016/j.atmosenv.2008.09.067

Jamalizadeh, M.R., A. Moghaddamnia, J. Piri, V. Arbabi, M. Homayounifar, and A. Shahryari. 2008. Dust storm prediction using ANNs technique (A case study: Zabol City). *Proceeding of World Academy of Science,Engineering and Technology* 33: 529–537.

Leys, J.F., S.K. Heidenreich, C.L.Strong, G.H. McTainsh, and S. Quigley. 2011. PM10 concentrations and mass transport during "Red Dawn" Sydney September 2009. *Aeol. Res.*3: 327–342. doi:10.1016/j.aeolia.2011.06.003

NASA, 2012. http://lance-odis.eosdis.nasa.gov/imagery/subsets/?subset=Iceland2.2008261. aqua.250m (accessed September 19, 2012).

Natsagdorj, L., D. Jugder, and Y.S. Chung. 2003. Analysis of dust storms observed in Mongolia during 1937–1999. *Atmos. Environ*. 37: 1401–1411. doi:10.1016/S1352-2310(02)01023-3

NOAA, 2012. http://ready.arl.noaa.gov/hysplit-bin/trajresults.pl?jobidno=324664 (accessed Oct 30, 2012).

N'TchayiMbourou, G., J.J. Berrand, and S.E. Nicholson. 1997. The diurnal and seasonal cycles of wind-borne dust over Africa north of the Equator. *J. Appl. Meteorol.* 36: 868–882. doi:10.1175/1520-0450(1997)036<0868:TDASCO>2.0.CO;2

Prospero, J.M., J.E. Bullard, and R. Hodgkins. 2012. High-latitude dust over the North Atlantic: Inputs from Icelandic proglacial dust storms. *Science* 335: 1078. doi:10.1126/science.1217447

Rekacewicz, P., 2005.Long range transport of air pollutants to the Arctic. UNEP/GRID-Arendal. http://www.grida.no/graphicslib/detail/long-range-transport-of-air-pollutants-to-the-arctic_bfc6 (accessed February 21, 2013).

Qian, W.H., L. Quan, and S. Shi. 2002. Variations of the dust storm in China and its climatic control. *J. Climate* 15: 1216–1229. doi:10.1175/1520-0442(2002)015<1216:VOTDSI>2.0.CO;2

Qian, W.H., X. Tang, and L.S. Quan. 2004. Regional characteristics of dust storm events in China. *Atmos. Environ.*38: 4895–4907.doi:10.1016/j.atmosenv.2004.05.038

Quinn, P.K., T.L. Miller, T.S. Bates, J.A. Ogren, and E. Andrews. 2002. A three-year record of simultaneously measured aerosol chemical and optical properties at Barrow, Alaska. *J. Geophys. Res*. 107(D11). doi:10.1029/2001JD001248.

Sivakumar, M.V.K. 2005. *Natural Disasters and Extreme Events in Agriculture*. Meppel, The Netherlands: Krips BV. doi:10.1007/3-540-28307-2

Steenburgh, W.J. 2012. Episodic dust events of Utah's Wasatch Front and adjoining region. *J. Appl. Meteorol. Clim.*http://journals.ametsoc.org/doi/abs/10.1175/JAMC-D-12-07.1 (accessed August 1, 2012). doi:10.1175/JAMC-D-12-07.1

Wang, Y.Q., X.Y. Zhang, S.L. Gong, C.H. Zhou, X.Q. Hu, H.L. Liu, T. Niu, and Y.Q. Yang. 2008. Surface observation of sand and dust storm in East Asia and its application in CUACE/Dust. *Atmos. Chem. Phys*. 8:545–553. doi:10.5194/acp-8-545-2008

Weinzierl, B., D. Sauer, A. Minikin, O. Reitebuch, F. Dahlkötter, B. Mayer, C. Emde, I. Tegen, J. Gasteiger, A. Petzold, A. Veira, U. Kueppers, and U. Schumann. 2012. On the visibility of airborne volcanic ash and mineral dust from the pilot's perspective in flight. *Phys. Chem. Earth Parts A/B/C* 45–46:87–102. doi:10.1016/j.pce.2012.04.003

World Health Organization. 2005. WHO air quality guidelines global update 2005. Report on a Working Group meeting, Bonn, Germany, October 18–20.

About the Authors

Pavla Dagsson-Waldhauserova is an assistant teacher and Ph.D. student at the University of Iceland and the Agricultural University of Iceland, in Reykjavik, Iceland; e-mail pavla@lbhi.is.

Olafur Arnalds is a professor at the Agricultural University of Iceland, Hvanneyri, Borgarnes, Iceland.

Haraldur Olafsson is a professor in atmospheric sciences at the University of Iceland, Reykjavik, Iceland, and the Bergen School of Meteorology, University of Bergen, Bergen, Norway.

Paper VII

SCIENTIFIC REPORTS

OPEN

SUBJECT AREAS:
ENVIRONMENTAL SCIENCES
VOLCANOLOGY
GEOLOGY
CONSERVATION

Received
3 October 2012

Accepted
25 January 2013

Published
13 February 2013

Correspondence and requests for materials should be addressed to O.A. (oa@lbhi.is)

An extreme wind erosion event of the fresh Eyjafjallajökull 2010 volcanic ash

Olafur Arnalds[1], Elin Fjola Thorarinsdottir[2], Johann Thorsson[2], Pavla Dagsson Waldhauserova[1,2] & Anna Maria Agustsdottir[2]

[1]Agricultural University of Iceland, Hvanneyri, 311 Borgarnes, Iceland, [2]Soil Conservation Service of Iceland, Gunnarsholt, 851 Hella, Iceland.

Volcanic eruptions can generate widespread deposits of ash that are subsequently subjected to erosive forces which causes detrimental effects on ecosystems. We measured wind erosion of the freshly deposited Eyjafjallajökull ash at a field site the first summer after the 2010 eruption. Over 30 wind erosion events occurred (June-October) at wind speeds $>$ 10 m s^{-1} in each storm with gusts up to 38.7 m s^{-1}. Surface transport over one m wide transect (surface to 150 cm height) reached $>$ 11,800 kg m^{-1} during the most intense storm event with a rate of 1,440 kg m^{-1} hr^{-1} for about 6½ hrs. This storm is among the most extreme wind erosion events recorded on Earth. The Eyjafjallajökull wind erosion storms caused dust emissions extending several hundred km from the volcano affecting both air quality and ecosystems showing how wind erosion of freshly deposited ash prolongs impacts of volcanic eruptions.

Wind erosion has been extensively studied in arid environments, coastal areas and within agricultural fields[1,2]. It can have a direct negative impact on ecosystems by burial of vegetation[3], and by causing loss of fertile topsoil, with immense impact on agriculture[4]. Fine, airborne dust particles generated by wind erosion affect ecosystems, often far away (up to 1000s of km), but the nature of the impact depends on factors such as distance from the source, the amount transported, grain size and chemistry of the dust materials[5]. Most large active dust sources are associated with arid environments[6] with major sources traced to depressions with relatively fine materials (fine silt and clay)[7,8], but the contribution of agriculture to dust production is also important[4]. Aeolian deposition can have positive benefits for vegetation and soils if deposition is moderate (e.g., in mm) by adding nutrients to the ecosystem[9]. Dust can, however, have adverse effects on humans such as on respiratory systems[5,10]. In addition, dust in the atmosphere can have substantial influence on climate, including solar radiation and precipitation[11].

Volcanic eruptions can bury landscapes with tephra (a collective term for airborne volcanic materials) and create extensive areas with unstable surfaces[12]. Water erosion of fresh volcanic deposits can produce extreme sediment yields of $>$ 100 000 tons km^{-2} yr^{-1}, as was measured following the 1991 Mt. Pinatubo (Philippines) eruption[13]. Wind erosion of unstable newly deposited volcanic ash (tephra $<$ 2 mm) has been reported to cause a range of problems such as burial of vegetation and agricultural land, and impact on livestock and humans[14]. Volcanoes are often found in mountainous regions where higher wind speeds and more turbulent winds can be expected than on relatively flat land surfaces, thus increasing the probability of wind erosion events near volcanoes. Low density of some of the tephra can lower the threshold velocity required to move the materials and increase sediment transport[14,15]. Dust emissions of volcanic materials from Iceland have recently received considerable attention[16,17], especially after the recent volcanic eruption in Eyjafjallajökull[18,19]. Catastrophic floods (jökulhlaups) that are caused by volcanic eruptions under glacier, with subsequent deposition of volcanic materials over large areas have also been identified as major sources of dust materials in Iceland[16,17]. However, knowledge of field conditions and wind erosion rates of fresh volcanic deposits under severe wind conditions is limited. Furthermore, wind erosion of fresh volcanic deposits are believed to have caused rapid and large scale ecosystem destruction during historic times in Iceland, with volcanic sand materials encroaching on fully vegetated agricultural areas, leaving sandy deserts behind[20]. Yet surface conditions during such events are poorly understood.

The Eyjafjallajökull volcano in Iceland erupted Mars - May 2010 with an ash plume reaching 3–10 km height[21–23]. The eruption produced about 0.27 km^3 of tephra with about ½ being deposited on Iceland[23]. The tephra was relatively fine, with a high proportion of 0.25–1 mm ash at 10 km from the crater[23]. The ash was commonly 1–15 cm thick at 5–20 km downwind from the volcano during the main ash deposition episodes[23]. This deposition caused severe damage to areas with sparse vegetation, while more resistant systems, such as

woodlands, stabilised the ash without causing permanent damage. Dust storms were frequent in the years following the eruption. We monitored wind erosion the first seasons after the eruption employing collectors and automatic sensors in an area that received 2–5 cm tephra, about 12 km SE of the crater (Figure 1) (see Methods for site selection and characteristics). The purpose of the research was to quantify wind erosion of freshly deposited ash under field conditions. Such measurements are fundamental for understanding the remobilisation of volcanic ash by wind, dust production of such areas, the large scale ecosystem destruction, and for predicting negative impacts of volcanic ash deposition on ecosystems and society.

Results

There were > 30 wind erosion events recoded at the Eyjafjallajökull wind erosion research site during the period June – October 2010. In September 2010, an extreme storm event was recorded. It lasted from 13:46 on September 14th with the main episode ending at about 06:00 the following day. However, erosion recorded by the saltation sensor lasted until 23:08 on September 15th. The storm was divided into 7 episodes defined by saltation intensity determined by the automated saltation sensor (Figure 2). The temperature ranged between 5 and 9.3°C during the storm with relative humidity ranging between 67 and 74%. Wind was blowing from the NNE, hence carrying materials downwind from the volcano towards the instruments. The BSNE sediment samplers placed at 10, 30 and 60 cm filled up during the storm with 1,100 – 1,600 g collected in the samplers. As a result, only the sampling set with a sampler placed at 90 and 120 cm height gave us a reasonable estimate of the total transport during the storm that is discussed in this paper (see Methods).

The total transport during the storm was calculated as 11,802 kg m^{-1} based on materials collected in the BSNE samplers and average height distribution curves. Our results do not consider surface creep movement, which could add 10–30% to this value[24]. Saltation pulse counts at 10 cm height give a detailed description of the progress of the storm (Figure 2). Each pulse of the saltation sensor was assigned weight (see Methods), based on calculated total transport to obtain an estimate of the transport in kg m^{-1} for each of the storm episodes (Table 1). Average 1 minute wind speed for each episode ranged between 14.1 and 22.5 m s^{-1} with gusts reaching 38.7 m s^{-1} (one minute average) which were reached during episode V. During the 6½ hr long episode V, about 9,500 kg of material was transported over a one m wide transect, with an average flux rate of 1,440 kg m^{-1} hr^{-1}.

Discussion

The transport during the storm of 11 800 kg m^{-1} and the maximum rate of transport reaching about 38 kg m^{-1} min^{-1} (corresponds to about 2300 kg m^{-1} hr^{-1}). We have not been able to find such high measured transportation rates in the published literature.

The measured transport is considerably greater than previously measured in Iceland but storms of > 500 kg m^{-1} hr^{-1} have been predicted based on field measurements and up to > 5,000 kg m^{-1} in single storms based on modelling of the measurements[25]. In comparison, the maximum recorded transport of volcanic material in the Hekla area reached about 3,000 kg m^{-1} over one relatively calm summer season[15]. The largest previously measured amount in Iceland in one storm was about 4,200 kg m^{-1} at Landeyjasandur, South Iceland, in 2004[26]. During the period from the ash deposition

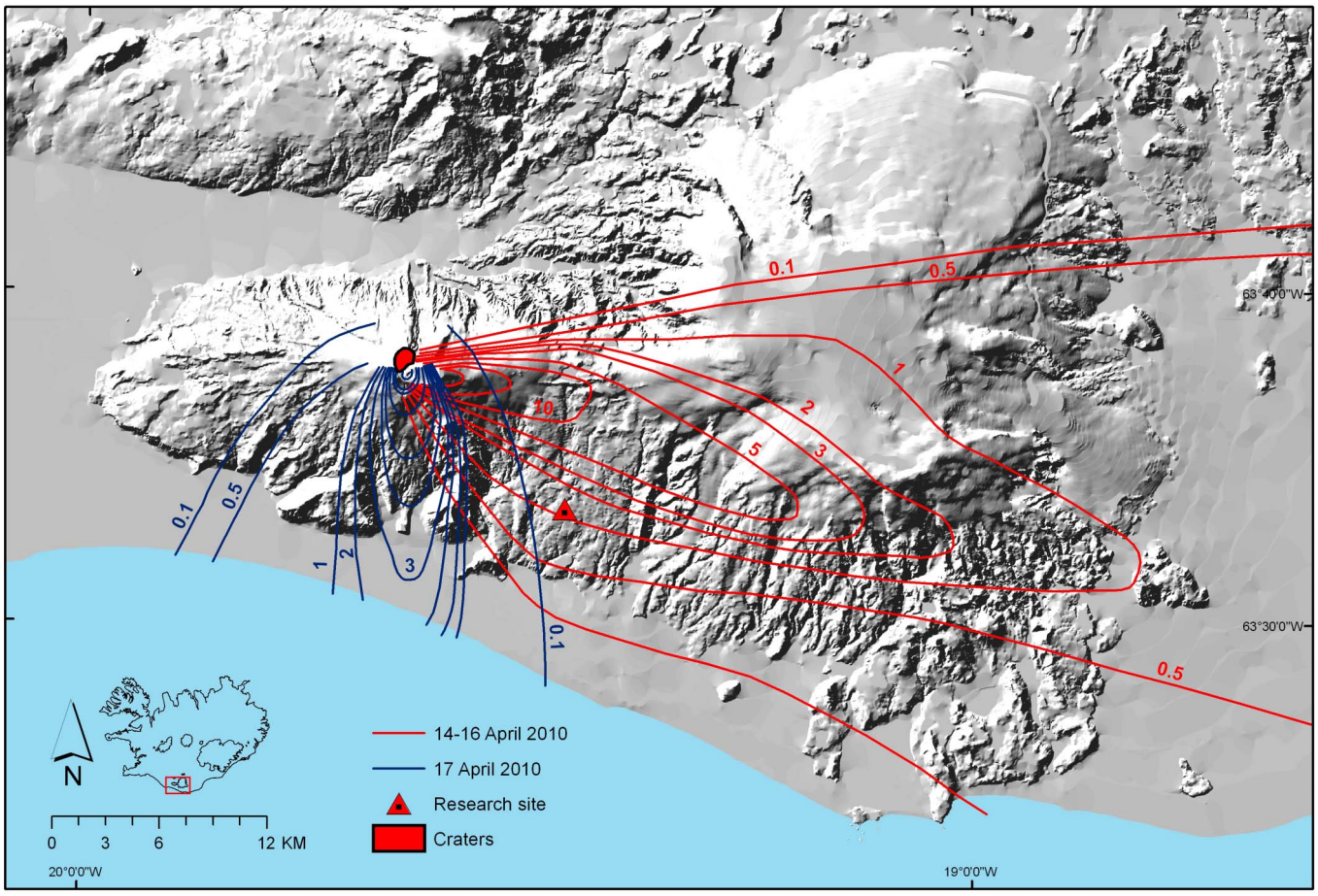

Figure 1 | Hill shade map of Eyjafjallajökull and the surrounding areas showing location of the research site and isopach data indicating the main distribution of the 2010 tephra. The distance from the crater to the research site is about 12 km. Isopach data from Gudmundsson *et al.*[23].

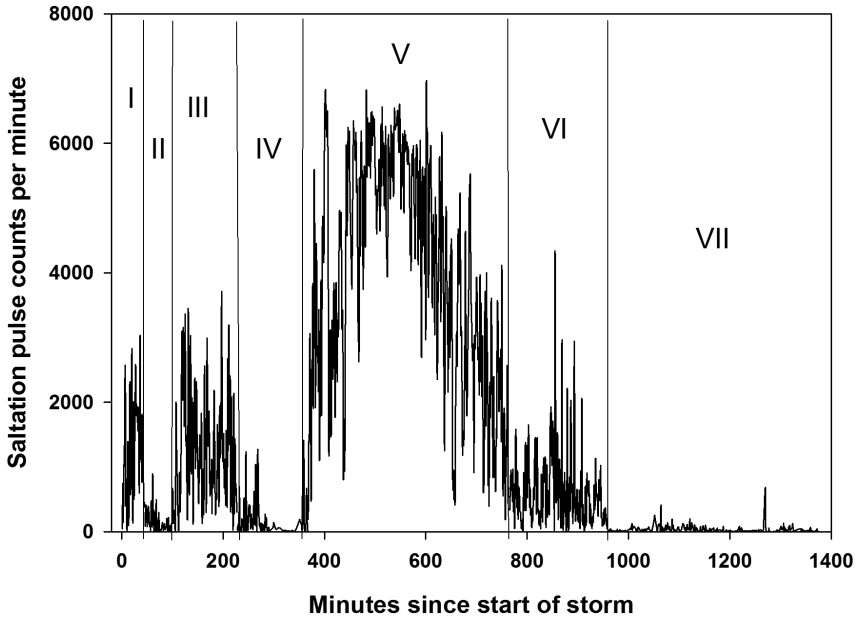

Figure 2 | Sediment transport measured with automated saltation sensor during the storm September 14 (13:46 hr) – September 15 (23:08); 2010. The storm is divided into 7 episodes labelled I-VII on the graph with the most intense sediment transport during episode V.

until the end of this storm, much of the 2–5 cm thick tephra had been removed from the barren exposed sites, with materials deposited in depressions such as gullies or blown away from the area, resulting in sediment yields of $>$ 10 000 metric tons km^{-2} yr^{-1}. After such events, water erosion will eventually become more dominant in redistribution of the tephra materials, as was witnessed after the 1943–1990 Paricutin (Mexico) eruption[27]. We have noted evidence of water erosion starting to cause damage of previously stable surfaces in depressions at the experimental site. Wind-blown ash remained as a severe problem for more than 6 months after the 1991 Hudson (Chile) eruption[14]. However, more materials continued to be blown towards our research site from areas receiving thicker tephra deposition with continued wind erosion activity in 2012, indicating that dust events can be maintained for many years under Icelandic conditions.

We have found that the BSNE samplers give a good overview of total sediment movement, while the data generated by the automatic sensors are ideal to study the characteristics of each storm, which is consistent with conclusions made by Brachyn *et al.*[28]. The relationship between wind speed and saltation pulse counts over the entire storm period and during episode V of the storm is presented in Figure 3. The logarithmic relationship is evident with the average wind speed showing relatively narrow distribution considering the length of the storm, indicating relatively steady climatic and surface conditions during the storm. The most intensive part of the storm (episode V; Figure 3B) shows clear signs of transport saturation at the higher end of the curve at about 28 m s^{-1} wind speed at sediment flux of about 2,300 kg m^{-1} hr^{-1}.

Mean grain size of the particles sampled in BSNE erosion samplers range from 0.1 to 0.7 mm, and grains $>$ 2 mm were moved during the most intense storms during the first summer after the eruption. During the intense storm discussed here, about 78% of materials sampled in the 10 cm BSNE trap were 0.25 – 1 mm, and the proportion of this coarse ash remained similar all the way up to 120 cm (76% 0.25 – 1 mm) (Figure 4). This is coarser than reported for wind erosion within other active aeolian areas[29]. Our results show that the height of the saltation layer extends above 120 cm height, with relatively coarse materials saltating at such height during this storm, which is considerably higher than the 20–40 cm height often reported elsewhere[30,31]. Furthermore, grains $>$ 2 mm are found in the 120 cm traps, which we have also experienced elsewhere in Iceland during major storms. The density of the material ranges from about 1.5 (porous tephra) to 2.8 g cm^{-3} (dense glass)[20], which in part explains how high the materials are lifted, but the coarse grain size and high wind speeds also favour high saltation heights[32].

Icelandic land surfaces are unique in that they are subjected to long term continuous aeolian deposition of reworked volcanic materials originating from the desert areas. The deposition rates range from 15 to $>$ 800 g m^{-2} yr^{-1} in all of Iceland[16]. Our results suggest that average sediment deposition rates for Iceland are influenced by such

Table 1 | Wind and sediment transport characteristics during each of seven storm episodes

Episode	Length	Wind speed m s^{-1}			Calculated transport	
	min	Average$	Max$	No of saltation pulses	kg m^{-1}	kg m^{-1} hr^{-1}
I	45	15.5	21.7	55,293	331	442
II	62	15.3	19.1	10,225	61	59
III	122	17.8	23.8	160,949	964	474
IV	148	14.4	21.5	19,023	114	46
V	397	22.5	38.7	1,589,559	9528	1440
VI	192	17.4	24.3	124,073	743	232
VII	405	14.1	20.1	9832	59	9

$: 1 minute averages, measured at 2.2 m height.

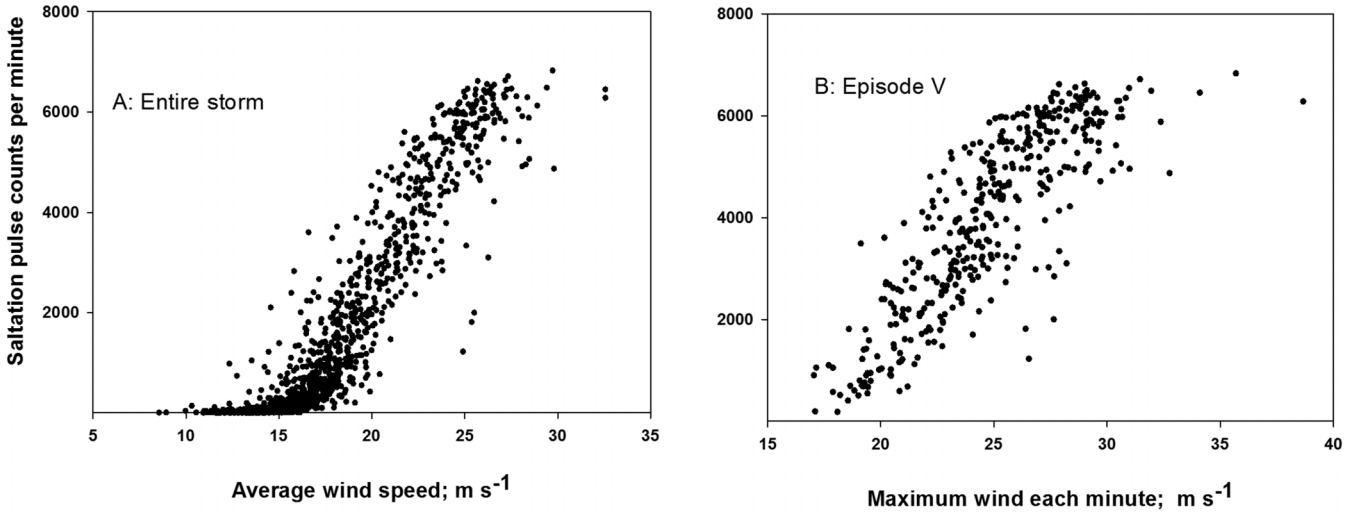

Figure 3 | Wind erosion of Eyjafjallajökull volcanic ash presented as saltation pulse counts at 10 cm height. Figure 3A shows data for the entire storm period while Figure 3B shows saltation as a function of maximum wind speed per minute for the most intense episode of the storm. Note different scale for the x-axis. Evidence of grain saturation is evident at maximum wind speeds above 28 m s^{-1}.

intense sediment production pulses. Icelandic dust storms are of regional scale, producing dust that reaches far over the North Atlantic[16,17], and they occur continuously, regardless of volcanic activity[16]. Eruptions of this kind seem to create temporary pulses which cause substantial inputs of fine ash into the atmosphere. The year following the eruption was characterized by many intense wind erosion events that greatly affected air quality over much of the South and Southwest Iceland and plumes of wind-born ash was seen far into the ocean on NOVA satellite images. As an example, the PM_{10} (particulate matter $<$ 10 μm) reached concentrations of $>$ 10,000 μg m^{-3} in the vicinity of the volcano during the major storms and the PM_{10} value occasionally exceeded 2000 μg m^{-3} in Reykjavik, 125 km from the volcano the first summer after the eruption[18]. Our measurements within the source areas during the storm give a good indication of the surface conditions during such immense dust events.

Volcanic eruptions are considered to be major contributors of nutrient renewal in ecosystems on a global scale[33]. Volcanic ash has furthermore been suggested to have a significant impact on ocean surface waters, releasing bio-available materials that benefit primary production[34,35]. Icelandic ocean areas have been reported to be nutrient limited, mainly by iron[36], which is among materials released by the ash[34]. Although there will be a higher nutrient availability with freshly deposited ash during eruptions compared to older ash the

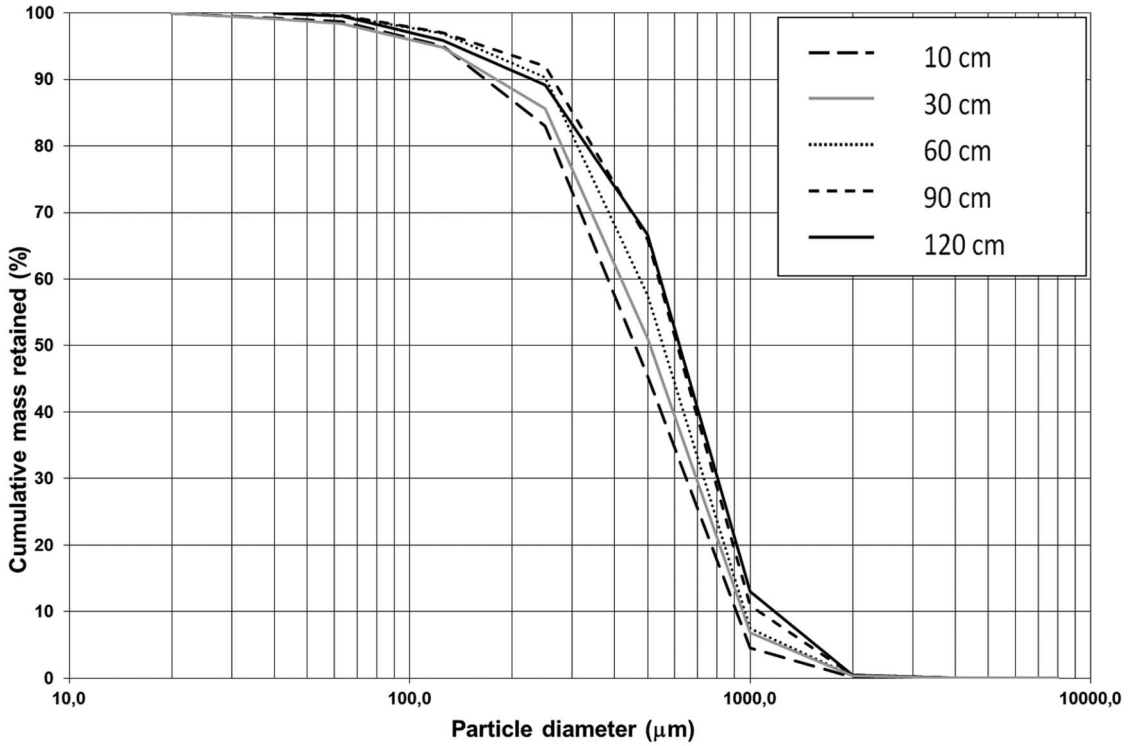

Figure 4 | Cumulative grain size for materials trapped by the BSNE samplers during the storm. The difference in grain size is notably small.

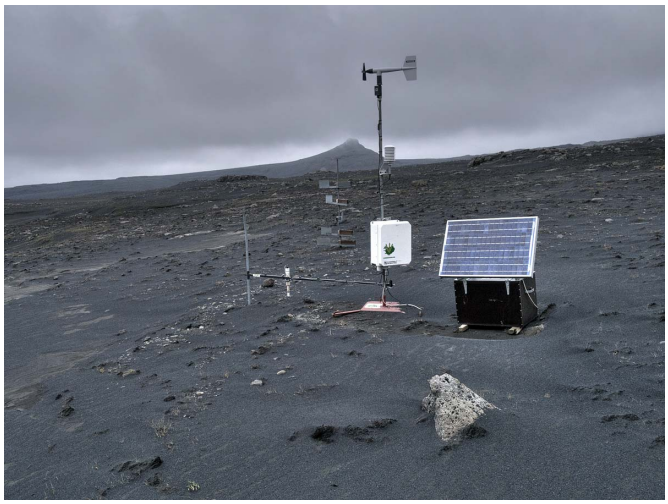

Figure 5 | Instrumentation at site. A Senist saltation sensor (white) together with equipment to measure wind speed and relative humidity. The instruments are solar powered and data is stored in a datalogger hosed in the white box, and can be accessed by a telephone link. BSNE samplers mounted on a pole in the background. The photo is taken after the occurrence of one major storm and ash has eroded from exposed sites while depressions have accumulated ash (photo: JT, June 23, 2010).

high intensity and the long duration of the dust storms related to volcanic activity may contribute to the fertility of surface waters around Iceland. This merits further research.

The erosion of the Eyjafjallajökull volcanic ash provides insight into possible scenarios for the severe soil erosion that took place in Iceland during the Middle Ages and up to the 19th century, causing large scale desertification and sand advancing over vegetated systems forming sandy areas. There are indications that when heavy land use had caused severe ecosystem degradation, some of the most severe soil erosion episodes occurred following volcanic eruptions and glacial river flooding[37]. Furthermore, the fate of the volcanic ash after deposition also highlights the importance of maintaining resistant vegetation cover such as woodlands closest to the most active

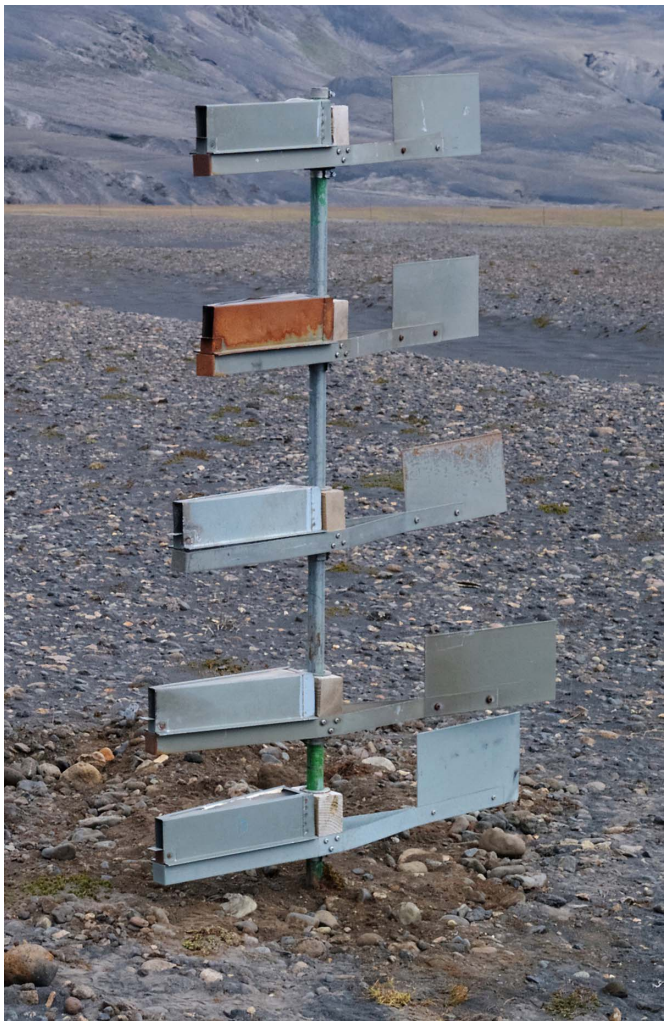

Figure 6 | A pole with five BSNE samplers placed at 10, 30, 60, 90, and 120 cm height. The opening is always directed upwind (photo: JT).

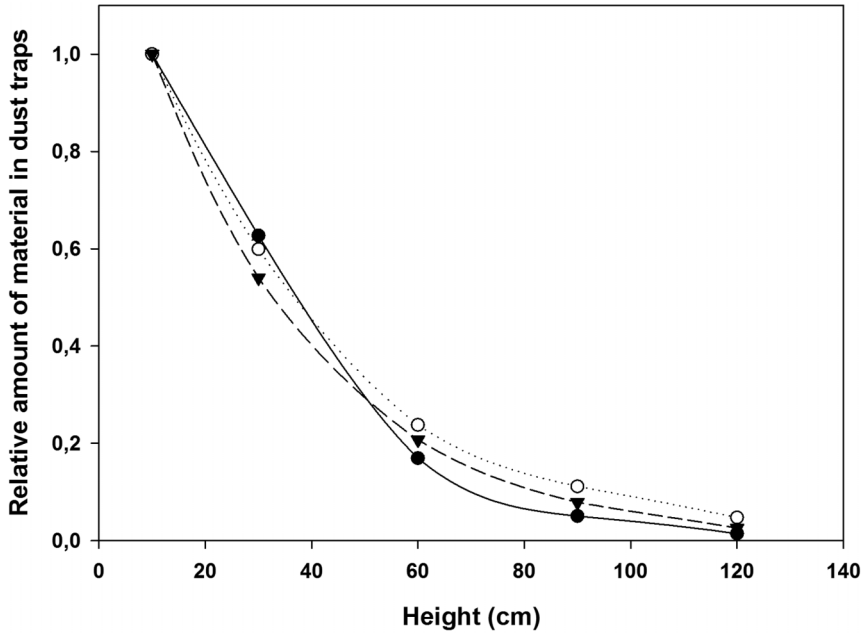

Figure 7 | Height distribution of materials collected at 10, 30, 60, 80, and 120 cm height during three storms prior to the main storm discussed in the paper. Materials collected in the 10 cm sampler is given the value of 1, others proportional to the amount in the 10 cm trap.

volcanoes in order to stabilise the tephra and prevent harmful intense dust storms.

Methods

Wind erosion was monitored on a 1,200 m long transect at 402 to 482 m elevation perpendicularly across the main ash deposition lobe about 10 km from the crater (Figure 1). The site was chosen because of relatively easy access by all-terrain vehicles along a rough track. The area received 2-5 cm of volcanic ash during the eruption. Vegetation cover was sparse prior to the ash deposition, consisting predominantly of mosses (*Racomitrium* spp. 1–2 cm high), but herbs and grasses were also common, including *Dryas octopetala, Silene acaulis*, *Armeria maritima* and *Festuca* spp.). Most of the surface, however, was barren, forming large patches of gravelly surface.

The amount of windblown material was estimated at 5 locations on the transect. We employed two methods to determine aeolian sediment transport rates: sediment accumulation in dust traps and an electronic saltation sensor (Figure 5). The dust traps were 'Big Spring number eight' (BSNE) samplers[38]. This sampler is a passive device, reliant on ambient wind conditions, to measure horizontal sand movement[39]. The sampler is placed on a pole and turns to place the opening into the wind (Figure 6). Dust-laden air passes through the sampler opening (about 9 cm^2) and the dust settles out in a collection pan. We placed a "cluster" pole at the middle of the sampling transect, with five BSNE collectors[38], mounted at heights of 10, 30, 60, 90 and 120 cm (Figure 6); and at 4 other locations a set of two samplers were employed (30 and 60 cm). Samples were dry sieved using the mesh sizes of 2, 1, 0.5, 0.25, 0.125, 0.063 and 0.040 mm, with grain size characteristics analysed and cumulative graphs made using Graditat software (v.8).

Response values used in wind erosion research varies considerably in the literature, but includes deflation (e.g., tons ha^{-1} yr^{-1}), sedimentation yield (e.g., tons km^{-2} yr^{-1}) and transport (e.g., kg m^{-1} hr^{-1} or kg m^{-2} hr^{-1}). Icelandic wind erosion research has commonly employed measurements of transport over a one m wide line or transect (kg m^{-1}) over a given time[15,25]. This unit relates well to practical situations working in the field in Iceland[25]. Previous research in Iceland suggests that height distribution curves tend to be relatively stable at the same site between storm events[25]. Average height distribution curve was constructed for available data from 2010 from the 5 sampler data sets, however excluding data when any of the traps filled up or when little was blown into the traps, a total of 3 storms (Figure 7). The average height distribution was used to calculate the transport over 1 m wide transect (kg m^{-1}) up to 150 cm height for each storm, with kg m^{-1} hr^{-1} as a flux unit, employing methods outlined in detail previously[15,25]. We assume that limited amounts of materials are saltated above 150 cm height. When the lower BSNE filled up during the most intensive storms, such as during the storm reported here, the average height distribution curve was employed, and total transport calculated based on the amount in the top samplers (90 and 120 cm). A piezoelectric transducer (Sensit) saltation sensor was used to detect the movement of wind-blown particles at 10 cm height, which has previously been found ideal height for measurements of wind erosion of volcanic materials in Iceland[15,25]. Simultaneous measurements were made of wind speed (2.2 m height), wind direction, air temperature and relative humidity. The total number of saltation counts were divided into the total amount of transported material measured by the BSNE traps to arrive at transport in g per each saltation pulse (1.97 million counts; 11,802 kg; about 6 g m^{-1} per saltation pulse).

1. Okin, G. S., Gillette, D. A. & Herrick, J. E. Multi-scale controls on and consequences of aeolian processes in landscape change in arid and semi-arid environments. *J. Arid Environ.* **65**, 253–275 (2006).
2. Skidmore, E. L. in *Soil Erosion Research Methods, 2nd ed.* : Wind erosion (ed Lal, R.) 265–293 (Soil and Water Conservation Society, Ankeny, Iowa,1994).
3. Maun, M. A. Adaptations of plants to burial in coastal sand dunes. *Can. J. Botany* **76**, 713–738 (1998).
4. Pimentel, D. & Harvey, C. in *Ecosystems of Disturbed Ground. Ecosystems of the World:Ecological effects of erosion* (ed Walker, L. R.) 123–135 (Elsevier Publ., Amsterdam, 1999).
5. Buzea, C., Pacheco, I. I. & Robbie, K. Nanomaterials and nanoparticles: Sources and toxicity. *Biointerphases* **2**, 17–71 (2009).
6. Lawrence, C. R. & Neff, J. C. The contemporary physical and chemical flux of aeolian dust: A synthesis of direct measurements of dust deposition. *Chem. Geol.* **267**, 46–63 (2009).
7. Prospero, J. M., Ginoux, P., Torres, O., Nicholson, S. E. & Gill, T. E. Environmental characterization of global sources of atmospheric soil dust identified with the NIMBUS 7 Total Ozone Mapping Spectrometer (TOMS) absorbing aerosol product. *Rev. Geophys.* **40**, 1002 (2002).
8. Washington, R. *et al.* Links between topography, wind deflation, lakes and dust: The case of Bodélé Depression, Chad. *Geophys. Res. Lett.* **33**, L09401 (2006).
9. Poortinga, A., Visser, S. M., Riksen, M. J. P. M. & Stroosnijder, L. Beneficial effects of wind erosion: Concepts, measurements and modelling. *Aeolian Res.* **3**, 81–86 (2011).
10. Gudmundsson, G. Respiratory health effects of volcanic ash with special reference to Iceland. A review. *Clin. Resp. J.* **5**, 2–9 (2011).
11. CCSP. *Atmospheric Aerosol Properties and Climate Impacts*, A Report by the U.S. Climate Change Science Program and the Subcommittee on Global Change Research. (NASA, Washington, D.C., USA, 128 pp, 2009).
12. del Moral, R. & Grishin, S. Y. in *Ecosystems of Disturbed Ground. Ecosystems of the World: Volcanic disturbances and ecosystem recovery* (ed Walker, L. R.)137–160 (Elsevier Publ., Amsterdam, 1999).
13. Hayes, S. K., Montgomery, D. R. & Newhall, C. G. Fluvial sediment transport and deposition following the 1991 eruption of Mount Pinatubo. *Geomorphology* **45**, 211–224 (2002).
14. Wilson, T. M., Cole, J. W., Stewart, C., Cronin, S. J. & Johnston, D. M. Ash storms: impacts of wind-remobilised volcanic ash on rural communities and agriculture following the 1991 Hudson eruption, southern Patagonia, Chile. *B. Volcanol.* **73**, 223–239 (2011).
15. Thorarinsdottir, E. F. & Arnalds, O. Wind erosion of volcanic materials in the Hekla area, South Iceland. *Aeolian Research* **4**, 39–50 (2012).
16. Arnalds, O. Dust sources and deposition of aeolian materials in Iceland. *Icel. Agric. Sci.* **23**, 3–21 (2010).
17. Prospero, J. M., Bullard, J. E. & Hopkins, R. High-latitude dust over the North Atlantic: inputs from Icelandic proglacial dust storms. *Science* **335**, 1078–1082 (2012).
18. Thorsteinsson, T., Johannesson, T., Stohl, A. & Kristiansen, N. J. High levels of particulate matter in Iceland due to direct ash emissions by the Eyjafjallajökull eruption and resuspension of deposited ash. *J. Geophys. Res.* **117**, B00C05 (2012).
19. Leadbetter, S. J., Hort, M. C., von Löwis, S., Weber, K. & Witham, C. S. Modeling the resuspension of ash deposited during the eruption of Eyjafjallajökull in spring 2010. *J. Geophys. Res.* **117**, D00U10 (2012).
20. Arnalds, O., Gisladottir, F. O. & Sigurjonsson, H. Sandy deserts of Iceland: an overview. *J. Arid Environ.* **47**, 359–371 (2001).
21. Arason, P., Petersen, G. N. & Bjornsson, H. Observations of the altitude of the volcanic plume during the eruption of Eyjafjallajökull, April-May 2010. *Earth Sys. Sci. Data* **4**, 1–25 (2011).
22. Sigmundsson, F. *et al.* Intrusion triggering of the 2010 Eyjafjallajökull explosive eruption. *Nature* **468**, 462–430 (2010).
23. Guðmundsson, M. T. *et al.* Ash generation and distribution from the April-May 2010 eruption of Eyjafjallajökull, Iceland. *Sci. Rep.* **2**, 572 (2012).
24. Dong, Z. & Qian, G. Characterizing the height profile of the flux of wind-eroded sediment. *Environ. Geol.* **51**, 835–845 (2007).
25. Arnalds, O., Gisladottir, F. O. & Orradottir, B. Determination of aeolian transport rates of volcanic soils in Iceland. *Geomorphology* **167–168**, 4–12 (2012).
26. Agustsdottir, A. M. Research on the effects of wind barriers - Fences for wind erosion control at Halslon, the water storage reservoir for the Karahnjukar Hydropower Project, in Eastern Iceland [In Icelandic]: Landsvirkjun LV - 2007/111. Reykjavik, Iceland (2007).
27. Inbar, M., Hubp, J. L. & Ruiz, L. V. The geomorphological evolution of the Paricutin cone and lava flows, Mexico, 1943–1990. *Geomorphology* **9**, 57–76 (1994).
28. Barchyn, T. E., Hugenholtz, C. H. & Ellis, J. T. A call for standardization of aeolian process measurements: moving beyond relative case studies. *Earth Surf. Proc. Land.* **36**, 702–705 (2011).
29. Pye, K. & Tsoar, H. *Aeolian Sand and Sand Dunes.* Unwin Hyman Ltd, London (1990).
30. van Donk, S. J. & Skidmore, E. L. Field experiments for evaluating wind erosion models. *Ann. Arid Zone* **40**, 283–302 (2001).
31. Zobeck, T. M. *et al.* Measurement and data analysis methods for field-scale wind erosion studies and model validation. *Earth Surf. Proc. Land.* **28**, 1163–1188 (2003).
32. Dong, Z., Liu, X., Wang, H., Zaho, A. & Wang, X. The flux profile of a blowing sand cloud: a wind tunnel investigation. *Geomorphology* **49**, 219–230 (2003).
33. Vitousek, P., Chadwick, O., Matson, P., Allison, S., Derry, L., Kettley, L., Luers, A., Mecking, E., Monastra, V. & Porder, S. Erosion and rejuvenation of weathering-derived nutrient supply in an old tropical landscape. *Ecosystems* **6**, 762–772 (2003).
34. Frogner, P., Gislason, S. R. & Oskarsson, N. Fertilizing potential of volcanic ash in ocean surface water. *Geology* **29**, 487–490 (2001).
35. Duggen, S., Olgun, N., Croot, P., Hoffmann, L., Dietze, H., Delmelle, P. & Teschner, C. The role of airborne volcanic ash for the surface ocean biogeochemical iron-cycle: a review. *Biogeosciences* **7**, 827–844 (2010).
36. Nielsdottir, M. C., Moore, C. M., Sanders, R., Hinz, D. J. & Achterberg, E. P. Iron limitation of the postbloom phytoplankton communities in the Iceland Basin. *Glob. Biochem. Cycl.* **23**, GB3001 (2009).
37. Arnalds, O. *et al. Soil Erosion in Iceland.* Soil Conservation Service and Agricultural Research Institute, Reykjavik, Iceland (2001).
38. Fryrear, D. W. A field dust sampler. *J. Soil Water Conserv.* **41**, 117–121 (1986).
39. Goossens, D. & Offer, Z. Y. Wind tunnel and field calibration of six aeolian dust samplers. *Atmos. Environ.* **34**, 1043–1057.

Acknowledgements

This research was funded by the Soil Conservation Service of Iceland and the Agricultural University of Iceland. We greatly acknowledge the help of Odinn Burkni Helgason at the Soil Conservation Service of Iceland for technical support with electronic equipment at the site.

Author contribution

O.A. coordinated the writing of the paper. A.M.A., E.F.T., J.T. and O.A. made original plans for the project. All authors took part in data collection while analysis of sediment transport was made by E.F.T., P.D.W. and O.A. O.A., E.F.T., J.T., P.D.W. and A.M.A. commented and discussed the results during the writing.

Additional information

Competing financial interests: The authors declare no competing financial interests.

How to cite this article: Arnalds, O., Thorarinsdottir, E.F., Thorsson, J., Waldhauserova, P.D. & Agustsdottir, A.M. An extreme wind erosion event of the fresh Eyjafjallajökull 2010 volcanic ash. *Sci. Rep.* **3**, 1257; DOI:10.1038/srep01257 (2013).

Paper VIII

Snow-Dust Storm: A case study from Iceland, March 6-7, 2013

Pavla Dagsson-Waldhauserova[a,b], Olafur Arnalds[a], Haraldur Olafsson[b, c, d], Jindrich Hladil[e], Roman Skala[e], Tomas Navratil[e], Leona Chadimova[e], Outi Meinander[f]

[a]Agricultural University of Iceland, Hvanneyri, Borgarnes, Iceland

[b]University of Iceland, Department of Physics, Reykjavík, Iceland

[c]Icelandic Meteorological Office, Bústaðavegi 9, Reykjavík, Iceland

[d]Bergen School of Meteorology, Geophysical Institute, University of Bergen, Norway

[e]Institute of Geology AS CR, v.v.i., Prague, Czech Republic

[f]Finnish Meteorological Institute, Helsinki, Finland

Corresponding author at: Agricultural University of Iceland, Keldnaholt, 112 Reykjavík, Iceland. Tel.: +354 4335267; Fax: +354 4335201; E-mail address: pavla@lbhi.is (P. Dagsson-Waldhauserova).

Abstract

Iceland is an active dust source in the high-latitude and cold region. About 50 % of the annual dust events in the southern part of Iceland take place at sub-zero temperatures or in winter, when dust is being mixed with snow. We investigated one winter dust event that occurred in March 2013. It resulted in a several mm thick dark layer of dust deposited on snow. Dust was transported over 250 km causing impurities on snow in the capital of Iceland, Reykjavik. One-minute PM_{10} concentration measured in Kirkjubæjarklaustur (20-50 km from the dust source) exceeded 6500 µg m^{-3} while the mean (median) PM_{10} concentration during 24-hour storm was 1,281 (1,170) µg m^{-3}. Dust concentrations before the dust deposition in Reykjavik were only about 100 µg m^{-3}, suggesting a rapid removal of the dust particles by snow during the transport. Dust sample taken from the snow top layer in Reykjavik after the storm showed that about 75 % of the dust deposit was a volcanic glass with SiO_2~ 45 %, FeO~14.5 %, and TiO_2~3.5. A significant proportion of organic matter and diatoms was also found. This case study shows that severe dust storms are related also to meteorological conditions, such as

winter snow storms, and moist conditions. Small volcanic dust particles deposited on snow tend to form larger particles ("clumping mechanism") resulting in stronger light absorbance. The deposition of Icelandic dust on snow, glaciers and sea ice may accelerate the thaw and contribute to the Arctic warming.

1. Introduction

Dust emissions have pronounced influences on Earth's ecosystems (Field et al., 2010), originated from deserts occurring in a variety of climatic conditions. Cold climate regions have less extensive dust sources than warmer areas; yet cold desert dust is an important input to the dust cycle (Bullard, 2013). Iceland is likely the largest and most active high-latitude dust source, where dust deposition is expected to influence an area of > 500,000 km^2 (Arnalds et al., 2014; Dagsson-Waldhauserova et al., 2014a). The frequency of > 34 dust days per year in Iceland is comparable to that found in Mongolia and Iran (Dagsson-Waldhauserova et al., 2014a). Including synoptic codes for "Visibility reduced by volcanic ashes" and "Dust haze" into the criteria for dust observations increases the frequency to > 135 dust days annually, which is comparable to the major deserts of the world. Suspended dust was detected during moist and low wind conditions in Iceland in summer (Dagsson-Waldhauserova et al., 2014b). However, almost half of all dust events in southern part of Iceland occurred during winter or at sub-zero temperatures (Dagsson-Waldhauserova et al., 2014a).

Winter dust deposition on snow has been studied in Colorado and Utah, USA, where dust in snow accelerated snowmelt by direct reduction of snow albedo and indirect reduction of albedo by accelerating the growth of snow grain size (Painter et al., 2012; Steenburgh et al., 2012). Recently, several winter dust events caused a closure of the skiing areas in Colorado mountain areas while avalanche danger was triggered by the dust deposition (Summit County, 2014). A historical dust deposition on snow and "snow dust storm" was described in Central Europe (Czech Republic) on April 19, 1903, when the Saharan yellowish-red dust mixed with snow and rain was deposited on snow (Ankert, 1903).

Darker snow surface after dust deposition lowers snow albedo, increases melt, and can also reduce snow density (Meinander et al., 2014). Icelandic volcanic dust is dark in colour and the optical properties are similar to black carbon (Dagsson-Waldhauserova et al., 2014c). Direct radiative forcing of mineral dust was calculated as negative in the IPCC report (IPCC, 2013), but indirect forcing of dust deposited on snow needs to be investigated in a greater detail. The

first dust-on-snow studies showed that the average spring dust radiative forcing ranged from 45 to 75 W m^{-2}, reducing snow cover duration by 21 to 51 days (Painter et al., 2012).

Icelandic dust differs from dust originating from continental dust sources, such as the Saharan, Asian or American dust. The dust is volcanogenic in origin and of basaltic composition (SiO_2 <50%, high Al_2O_3, and Fe_2O_3 contents). Volcanic dust made of glass can be sharp and porous allowing particles as large as 50 µm to travel long distances (Navratil et al. 2013). Suspended glacial dust can, however, contain a high number of close-to-ultrafine particles (Dagsson-Waldhauserova et al., 2014b).

The purpose of this study was to investigate a special weather phenomenon, which we term "Snow-Dust storm", in a cold climate region. The main characteristics of severe Snow-Dust storm were investigated: i) the source region, ii) horizontal extent, iii) suspended dust concentrations, iv) chemical and mineralogical composition of transported material, and v) dust-on-snow deposition mechanisms in natural conditions.

2. Methods

The snow-dust storm (SDS) and dust deposition on snow occurred in S and SW Iceland on March 6-7 2013. The impurities on snow were visible on March 6 and 7 in Reykjavik (SW) and Kirkjubæejarklaustur (S), which is about 200 km from Reykjavik. Particulate matter (PM) mass concentration data were obtained from Reykjavik (Thermo EMS Andersen FH 62 I-R instrument) and Kirkjubæjarklaustur (Grimm EDM 365) by the Environmental Agency of Iceland. A snow sample with deposited dust was taken in Reykjavik (Keldnaholt) on March 7 at 10:00. The compositions of the tephra glass and mineral grains were studied using backscattered electrons and quantitative x-ray analysis (EDX SEM) on samples fixed in resin and polished to planar cross-sectional surfaces. Major mineral compositions were also checked by x-ray powder diffraction (XRD).

3. Results and Discussion

Two peaks of increased PM_{10} concentrations of about 75-154 µg m^{-3} (thirty-min mean) were reported in Reykjavik on March 6 (first at 0:00-3:00, second at 17:00-20:00) as depicted in Figure 1. A severe dust storm with the PM_{10} concentrations up to 6500 µg m^{-3} (one-min mean) passed Kirkjubæjarklaustur on March 6-7. Mean (median) PM concentrations during

the SDS in Kirkjubæjarklaustur was 1,281 (1,170) µg m^{-3}. The snow was first found covered with dust on March 6 around 10:00. A new dust layer was found in Reykjavik on March 7, when the sample was taken (Figure 2).

The HYSPLIT back trajectory analysis showed that the dust peak 1 (0:00-3:00) observed in Reykjavik consisted of dust from a NE direction and the dust peak 2 (17:00-20:00) contained dust arriving from a SE direction, and is the same dust storm as observed in Kirkjubæjarklaustur (Figure 1). The dust source Skeidararsandur is located about 20 km east of Kirkjubæjarklaustur, while Reykjavik is about 250 km downwind (WNW) of Skeidararsandur. Relatively low PM concentrations in Reykjavik during the storm are likely the result of the rapid removal of the dust particles by snow during the transport.

Mineralogical and geochemical composition of a dust sample, taken from the top layer of the snow in Reykjavik on March 7, was investigated to determine the source of the dust transported to Reykjavik. The XRD combined with the optical microscopy identified about 75 % of the dust deposit as a volcanic glass with grains 1–250 µm in diameter (average 17 µm). However, about 70 % of the particles were <10 µm and 20% were in range 10-50 µm. High PM_{10} mass concentrations detected during the SDS in Kirkjubæjarklaustur measured only the particles <10 µm, but about 30 % of transported material found in Reykjavik was >10 µm. Including large particles would increase the suspended dust mass substantially.

Most of the volcanic glass particles (about 70%) showed chemical compositions of: SiO_2~ 45 %, FeO~14.5 %, TiO_2~3.5%, Al_2O_3~14.5 %, CaO~12 %, MgO~6.25 %, and Na_2O+K_2O~ 4 %. This composition corresponds closely to the composition of the Grimsvotn tephra materials (see Oladottir et al., 2011a), suggesting the Skeidararsandur origin of the dust. Small number of glass shards corresponded to alkalic transitional tephra and materials from the alkalic Holocene eruptions of the S, SW Iceland (Oladottir et al., 2011b), which could originate from the Hagavatn dust source (northern trajectory in Figure 1), but also, alternatively from the 2010 Eyjafjallajökull deposits (southern trajectory in Figure 1). The Hagavatn dust analysed by Baratoux et al. (2011) also shows similarities in major element composition with our sample. The PM_{10} concentrations measured in Reykjavik and chemical analysis of the snow-dust sample indicate that the majority of the dust was deposited on snow during the peak 1 on March 6 (0-3h). Consequently, volcanic glass from the Grimsvotn volcanic system was transported towards Reykjavik (dust peak 2).

The most common glass morphologies were characterized by numerous ~10–20 μm gas bubbles. Low frequency of bubbles corresponded to massive shards, while high frequency was in bubble-wall shards. Rare alkali- and silica-rich glasses showed different, very fine pipe-vesicular structures (Figure 3, top-right). Such elongated shapes are more similar to asbestos particles or black carbon than mineral dust, and may pose health risks (Donaldson et al., 2006). The individual mineral grains and crystals embedded in the glass were mostly plagioclases (labradorite and andesine), pyroxenes (augite), olivines (fayalite) and amphiboles (ferrohornblende), whereas Na–K feldspars were rare. Titanium and iron were often concentrated to ulvospinel (Figure 3), magnetite-titanomagnetite and ilmenite. Such mineralogical contribution along with the chemical compositions indicates that the sample was a mixture of material originating in Skeidararsandur (southern trajectory, peak 2) and Hagavatn dust (northern trajectory, dust peak 1).

Transported dust contained various clay minerals, chlorites, zeolites and many minerals revealing a wide spectrum of altered, heterogeneous tephras and primitive soils. We identified hydrated palagonites with imperfect lattices of ferrihydrite and smectites (possibly also allophane, imogolite, zeolites and carbonates) in several glass fragments. Detritus of decayed organic matter (from algae to vascular plants, ~0.25 vol. %) and scattered *Bacillariophyceae* opal frustrules were also found (Figure 3). Presence of diatoms and organic matter in transported dust indicates that the dust originated in area of lakes or river beds. However, the identification of exact location from the 49 examined lakes and 139 diatom taxa found in Iceland is complicated (Karst-Riddoch et al., 2009). Identified diatoms are benthic and may be present in shallow pools or waters around the edges of lakes and rivers. Figure 3 shows the *Rhopalodia* and *Epithemia* diatom species (likely epiphytic).

Dust deposition on snow affects climate by reducing snow albedo and increasing snow-melt due to light-absorbing particles (Painter et al., 2012). The melting rates of snow influenced by Icelandic volcanic dust were similar to snow with a black carbon layer (Meinander et al., 2014). Small volcanic dust particles tend to form larger particles resulting in stronger absorbing effects (Dagsson-Waldhauserova et al., 2014c). This clumping mechanism has been linked to artificially deposited impurities on snow (Brandt et al. 2011). Here we observed the same mechanism in natural conditions (Figure 2). There are strong indications that Icelandic dust is a positive radiative forcing agent, both directly and indirectly, which is contrary to mineral dust effects reported by the IPCC (IPCC, 2013). Dust deposition on Icelandic glaciers

was calculated as 4.5 million t per year with the mean deposition of 400 $gm^{-2}yr^{-1}$ (Arnalds et al., 2014). We suggest that Icelandic volcanic dust events not only affect Iceland but have the potential to reach the Arctic glaciers and sea ice and accelerate the Arctic warming.

Acknowledgements

The work was supported by the Eimskip Fund of The University of Iceland, the Nordic Center of Excellence (NCoE), Nordic Top Research Initiative "Cryosphere-atmosphere interactions in a changing Arctic climate" (CRAICC) and the AS CR RVO:67985831 support. We would like to thank Tammy Karst-Riddoch from the Hutchinson Environmental Sciences Ltd. for the advices on diatoms and Thorsteinn Johannsson from the Environment Agency of Iceland for providing the PM data.

References

Ankert H., 1903. Der Staubfall am 19. April 1903. Mitteilungen des Nordböhmischen Exkursions-Klubs 26 (1903), 373-374.

Arnalds O., Olafsson H., Dagsson-Waldhauserova P., 2014. Quantification of iron rich volcanogenic dust emissions and ocean deposition from Icelandic dust sources. Biogeosciences Discussions 11, 5941–5967.

Arnalds O., Thorarinsdottir E.F., Thorsson J., Dagsson-Waldhauserova P., Agustsdottir A.M., 2013. An extreme wind erosion event of the fresh Eyjafjallajokull 2010 volcanic ash. Nature Scientific Reports 3, 1257.

Baratoux D., Mangold N., Arnalds O., Bardintzeff J.-M., Platevoet B., Grégorie M., Pinet P., 2011. Volcanic sands of Iceland—Diverse origins of Aeolian sand deposits revealed at Dyngjusandur and Lambahraun. Earth Surface Processes and Landforms 36, 1789–1808.

Brandt R.E., Warren S.G, Clarke A.D., 2011. A controlled snowmaking experiment testing the relation between black carbon content and reduction of snow albedo. Journal of Geophysical Research 116, D08109. doi:10.1029/2010JD015330.

Bullard J.E., 2013. Contemporary glacigenic inputs to the dust cycle. Earth Surface Processes and Landforms 38, 71–89.

Dagsson-Waldhauserova P., Arnalds O., Olafsson H., 2014a. Long-term variability of dust events in Iceland. Atmospheric Chemistry and Physics Discussions 14, 17331-17358. doi:10.5194/acpd-14-17331-2014

Dagsson-Waldhauserova P., Arnalds O., Olafsson H., Skrabalova L., Sigurdardottir G. M., Branis M., Hladil J., Skala R., Navratil T., Chadimova L., Menar S., Thorsteinsson T., Carlsen H.K., Jonsdottir I., 2014b. Physical properties of suspended dust during moist and low-wind conditions in Iceland. Icelandic Agricultural Sciences 27, 25-39.

Dagsson-Waldhauserova P., Arnalds O., Olafsson H., Hladil H., Skala R., Navratil T., Chadimova L., Gritsevich M., Peltoniemi J., Hakala T., 2014c. Optical properties and climate forcing of Icelandic dust. Geophysical Research Abstracts 16, EGU2014-8640.

Dagsson-Waldhauserova P., Arnalds O., Olafsson H., 2013. Long-term frequency and characteristics of dust storm events in Northeast Iceland (1949-2011). Atmospheric Environment 77, 117-127.

Donaldson K., Stone V., Faux S., MacNee W., 2006. Testing New Particles. In: Ayres J., Maynard R., Richards R. (eds.) The Impact of Air Pollution on Respiratory Health. Imperial College Press, London, pp. 163–195.

Fields J.P., Belnap J., Breshears D.D., Neff J.C., Okin G.S., Whicker J.J., Painter T.H., Ravi S., Reheis M.C., Reynolds R.L., 2010. The ecology of dust. Frontiers in Ecology and the Environment 8, 423–430.

IPCC, 2013. "Climate Change 2013: The Physical Science Basis. Working Group I Contribution to the IPCC 5th Assessment Report – Changes to the Underlying Scientific/Technical Assessment" (IPCC-XXVI/Doc.4). URL: http://www.ipcc.ch/report/ar5/wg1/#.UlvUNVPfShM (accessed Apr 14, 2014).

Karst-Riddoch T., Malmquist H.J., Smol J.P., 2009. Relationships between freshwater sedimentary diatoms and environmental variables in Subarctic Icelandic lakes. Fundamental and Applied Limnology (Archiev fur Hydrobiologie) 175, 1–28.

Meinander O., Kontu A., Virkkula A., Arola A., Backman L., Dagsson-Waldhauserová P., Järvinen O., Manninen T., Svensson J., de Leeuw G., Leppäranta M., 2014. Brief Communication: Light-absorbing impurities can reduce the density of melting snow. The Cryosphere 8, 991-995.

Navratil T., Hladil J., Strnad L., Koptikova L., Skala R., 2013. Volcanic ash particulate matter from the 2010 Eyjafjallajokull eruption in dust deposition at Prague, central Europe. Aeolian Research 9, 191-202.

Oladottir B.A., Larsen G., Sigmarsson, O., 2011a. Holocene volcanic activity at Grímsvötn, Bárdarbunga and Kverkfjöll subglacial centres beneath Vatnajökull, Iceland. Bulletin of Volcanology. doi:10.1007/s00445-011-0461-4.

Oladottir B.A., Sigmarsson O., Larsen G., Devidal J.L., 2011b. Provenance of basaltic tephra from Vatnajökull subglacial volcanoes, Iceland, as determined by major- and trace-element analyses. The Holocene 21/7, 1037–1048.

Painter T.H., Skiles S.M., Deems J.S., Bryant A.C., Landry C., 2012. Dust radiative forcing in snow of the Upper Colorado River Basin: Part I. A 6 year record of energy balance, radiation, and dust concentrations. Water Resources Research. doi:10.1029/2012WR011985.

Summit County, 2014. http://www.summitdaily.com/news/10886504-113/dust-snow-avalanche-colorado (accessed June 20, 2014).

Steenburgh W.J., Massey J. D., Painter T.H., 2012. Episodic dust events of Utah's Wasatch Front and adjoining region. Journal of Applied Meteorology and Climatology 51, 1654-1669.

Figure 1. PM_{10} concentrations during the Snow-Dust storm in Reykjavik (upper graph) and Kirkjubaejarklaustur (lower graph) on March 6-7, 2013. The HYSPLIT backward trajectories calculated for the dust peak 1 (00:00-03:00) and the peak 2 (17:00-20:00) in Reykjavik.

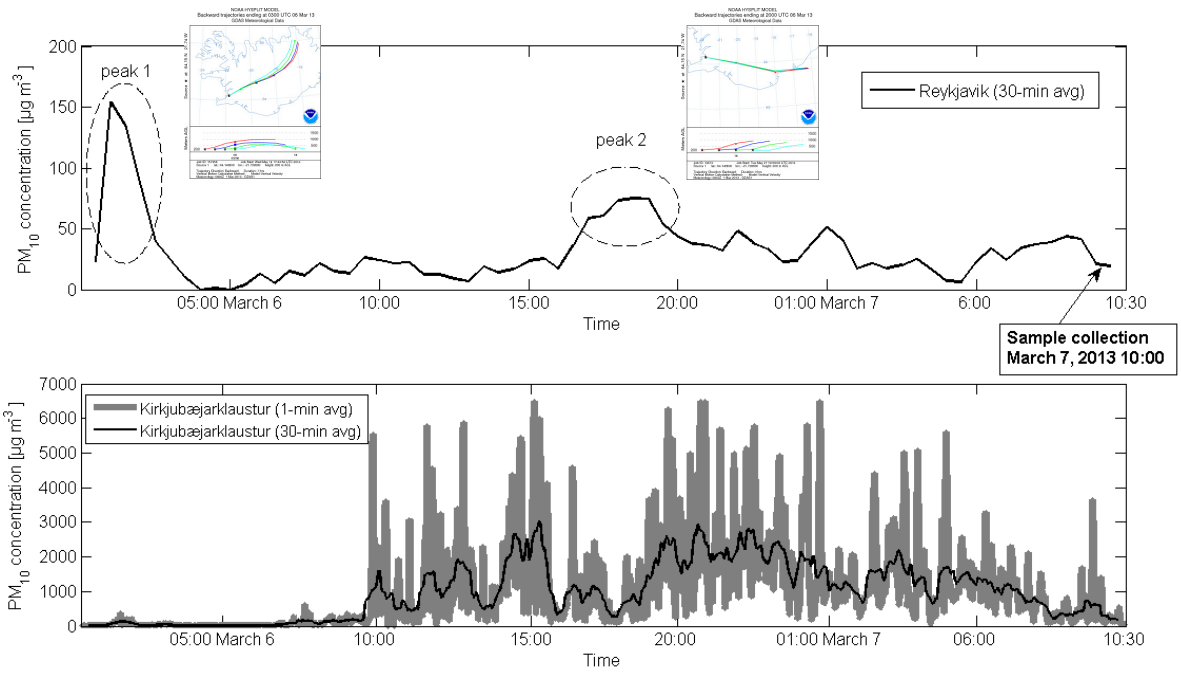

Figure 2. The Icelandic Snow-Dust storm on March 6 2013, in Kirkjubaejarklaustur (left), caused a significant volcanic dust deposition on snow (see also the car). The impurities on snow were visible in Reykjavik, 250 km from the dust source (right) on March 6 and 7, 2013. On the snow surface, the impurities were observed to form larger particles ("clumping mechanism") and accelerate snow melt. Such high-latitude winter and cold Icelandic dust events (> 9 annually) have the potential to contribute to Arctic warming. The Icelandic dust deposition is estimated to influence an area of > 500,000 km^2. Left photo - courtesy of Ingveldur Gudny Sveinsdottir from Kirkjubaejarklaustur. Right photos – ©Pavla Dagsson-Waldhauserova.

Figure 3. Microscopic images of the dust material. Upper row: Examples of backscattered electron images of planar-polished sections of the dust particles; the analyzed and interpreted minerals and glasses are marked by symbols: An – andesine, Aug – augite, Fe2-Hbl – ferrohornblende, Lrt – labradorite, Ol – olivine, Px – pyroxene, Usp – ulvospinel; Gl-t – volcanic glass of tholeitic series, Gl-a – volcanic glass of alkalic series; palgnt – palagonitic material. Lower row: The fine particle distributions are illustrated in the figure on the left (optical microscope, dark field). Examples of diatoms - *Rhopalodia sp*., poss. *R. gibba (upper), Epithemia sp*., poss. *E. adnata (lower)*